

Winter 2007

Drug loading and release from polypeptide multilayer nanofilms

Yang Zhong
Louisiana Tech University

Follow this and additional works at: <https://digitalcommons.latech.edu/dissertations>



Part of the [Biomedical Engineering and Bioengineering Commons](#), and the [Pharmacology Commons](#)

Recommended Citation

Zhong, Yang, "" (2007). *Dissertation*. 552.
<https://digitalcommons.latech.edu/dissertations/552>

This Dissertation is brought to you for free and open access by the Graduate School at Louisiana Tech Digital Commons. It has been accepted for inclusion in Doctoral Dissertations by an authorized administrator of Louisiana Tech Digital Commons. For more information, please contact digitalcommons@latech.edu.

DRUG LOADING AND RELEASE FROM POLYPEPTIDE
MULTILAYER NANOFILMS

by

Yang Zhong, M.S.

A Dissertation Presented in Partial Fulfillment of the
Requirement for the Degree of
Doctor of Philosophy

COLLEGE OF ENGINEERING AND SCIENCE
LOUISIANA TECH UNIVERSITY

March 2007

UMI Number: 3264699

INFORMATION TO USERS

The quality of this reproduction is dependent upon the quality of the copy submitted. Broken or indistinct print, colored or poor quality illustrations and photographs, print bleed-through, substandard margins, and improper alignment can adversely affect reproduction.

In the unlikely event that the author did not send a complete manuscript and there are missing pages, these will be noted. Also, if unauthorized copyright material had to be removed, a note will indicate the deletion.

UMI[®]

UMI Microform 3264699

Copyright 2007 by ProQuest Information and Learning Company.

All rights reserved. This microform edition is protected against unauthorized copying under Title 17, United States Code.

ProQuest Information and Learning Company
300 North Zeeb Road
P.O. Box 1346
Ann Arbor, MI 48106-1346

LOUISIANA TECH UNIVERSITY

THE GRADUATE SCHOOL

February 23, 2007

Date

We hereby recommend that the dissertation prepared under our supervision
by Yang Zhong

entitled Drug Loading and Release from Polypeptide Multilayer Nanofilms

be accepted in partial fulfillment of the requirements for the Degree of
PhD in Engineering

Donald J. Haynie
Supervisor of Dissertation Research
[Signature]
Head of Department
Engineering
Department

Recommendation concurred in:

[Signature]
[Signature]
[Signature]
[Signature]

Advisory Committee

Approved: [Signature]
Director of Graduate Studies

Approved: [Signature]
Dean of the Graduate School

[Signature]
Dean of the College

ABSTRACT

Polypeptides, linear macromolecules, are formed from amino acid residues by linkage of peptide bonds. Proteins are polypeptides too, with more complex conformations contributing to specific functionalities. Disulfide bonds are very important to maintain the structure and functions of proteins, which will form between two cysteine (Cys) residues under oxidizing circumstance.

Cys containing polypeptides are designed and synthesized by F-moc (9-Fluorenylmethyloxycarbonyl) chemistry. The number and position of Cys residues can be controlled by amino acid sequences design and following peptide synthesis, which is important to gain insights on the nature of polyelectrolyte multilayer film assembly and stability.

Both commercial and designed polypeptides have been used to fabricate multilayer nanofilms by Layer-by-layer self-assembly (LBL). The thickness, refractive index, and surface morphology of Cys containing polypeptide multilayer films can be controlled by adjusting assembly pHs over a small range, because these are affected by the deprotonation of Cys side chains and rearrangement of charge distributions. The number of Cys residues in the polypeptide chain can influence the number of disulfide bonds formed under an oxidizing environment, and furthermore affect the stability of multilayer films. The 2-D or 3-D disulfide crosslinkings can fortify the polypeptide multilayer film stabilities.

Multilayer polypeptide films made from poly-L-lysine (PLL), poly-glutamic acid (PLGA), and designed peptides have been used in methylene blue (MB) dye loading and release. The amount of MB loaded can be finely controlled by adjusting assembly pHs and architecture of polypeptide multilayers. The controlled release of MB from nanofilms could be influenced by various factors such as pH and salt concentrations of the release medium.

The side chains of Cys residues can form mixed disulfides with drugs containing thiol groups. The reversible disulfide bond can act as a switch for the redox-stimulated drug loading and release. 5,5'-dithiobis-(2-nitrobenzoic acid) (DTNB) has been used as a drug indicator to bind to Cys containing polypeptides covalently. Controlled release of 2-nitro-5-thiobenzoate anions (TNB^{2-}) from labeled polypeptides has been tested both in solution phase and solid phase—multilayer films. The new drug loading and release mechanism, the change of redox potential, provides a promising possibility for future targeted drug delivery.

APPROVAL FOR SCHOLARLY DISSEMINATION

The author grants to the Prescott Memorial Library of Louisiana Tech University the right to reproduce, by appropriate methods, upon request, any or all portions of this Dissertation. It is understood that "proper request" consists of the agreement, on the part of the requesting party, that said reproduction is for his personal use and that subsequent reproduction will not occur without written approval of the author of this Dissertation. Further, any portions of the Dissertation used in books, papers, and other works must be appropriately referenced to this Dissertation.

Finally, the author of this Dissertation reserves the right to publish freely, in the literature, at any time, any or all portions of this Dissertation.

Author Kang Zhou

Date Feb. 23rd, 2007

TABLE OF CONTENTS

ABSTRACT.....	iii
LIST OF TABLES.....	viii
LIST OF FIGURES	ix
ACKNOWLEDGEMENTS.....	xvi
CHAPTER ONE INTRODUCTION.....	1
1.1 Protein Engineering	1
1.1.1 Protein Structure	2
1.1.2 Protein Functionality.....	4
1.2 Polypeptide Multilayer Film.....	5
1.3 Polypeptide Synthesis	5
1.4 Dissertation Objectives	7
1.5 Dissertation Organization	8
CHAPTER TWO THEORETICAL BACKGROUND	11
2.1 Properties and Functions of Polypeptide Multilayer Films	12
2.2 Layer-by-Layer Self Assembly (LBL).....	14
2.3 Crosslinking by Disulfide Bonds	16
2.4 Drug Loading and Release of Polyelectrolyte Multilayer Films	17
CHAPTER THREE METHODOLOGY	19
3.1 Quartz Crystal Microbalance (QCM)	19
3.2 UV-Vis Spectroscopy (UVS).....	21
3.3 Circular Dichroism Spectroscopy (CD).....	23
3.4 Ellipsometry.....	24
3.5 Surface Profilometry.....	26
3.6 Atomic Force Microscope (AFM)	27
CHAPTER FOUR FINE TUNING OF PHYSICAL PROPERTIES OF DESIGNED POLYPEPTIDE MULTILAYER FILMS BY CONTROL OF PH.....	30
4.1 Introduction.....	30
4.2 Experiments	31
4.3 Results.....	32
4.4 Discussion	37
4.5 Conclusion	41

4.6 Supplementary Information	42
CHAPTER FIVE CONTROL OF STABILITY OF POLYPEPTIDE MULTILAYER NANOFILMS BY QUANTITATIVE CONTROL OF DISULFIDE BOND FORMATION.....	45
5.1 Introduction.....	45
5.2 Experiments	46
5.3 Results.....	48
5.4 Discussion	54
5.5 Conclusion	60
5.6 Supplementary Information	61
CHAPTER SIX CONTROLLED LOADING AND RELEASE OF A MODEL DRUG FROM POLYPEPTIDE MULTILAYER NANOFILMS	62
6.1 Introduction.....	62
6.2 Experiments	63
6.3 Results.....	66
6.4 Discussion	75
6.5 Conclusion	80
CHAPTER SEVEN REDOX-STIMULATED RELEASE OF SMALL MOLECULES FROM POLYPEPTIDE MULTILAYER NANOCOATINGS.....	81
7.1 Introduction.....	81
7.2 Experiments	82
7.3 Results and Discussion	85
7.4 Conclusion	90
CHAPTER EIGHT CONCLUSIONS	91
8.1 Conclusions.....	91
8.2 Future Work	93
REFERENCES	95

LIST OF TABLES

Table 4-1	Thickness in nm, measured by surface profilometry and ellipsometry, of 20- and 40-layer peptide films produced at different pH values34
Table 5-1	Hydrophobicity/hydrophilicity* of polypeptides.....57
Table 6-1	Assembly and loading comparison of polypeptide multilayer films68

LIST OF FIGURES

Figure 1-1	Protein structure. (a) Primary structure. (b) Secondary structure. Left: α -helix; right: β -sheet. (c) Tertiary structure (hexokinase). (d) Quaternary structure (hemoglobin) [2]4	4
Figure 2-1	Position of polypeptide multilayer films in the broader scheme [3].....13	13
Figure 2-2	Polypeptide multilayer film fabrication. Bottom: schematic diagram of LBL. Top: corresponding experimental data. Oppositely charged polypeptides in solution (bottom left) are adsorbed consecutively onto a solid support (bottom center), for example quartz slide, yielding a multilayer film (bottom right). Loosely bound material is rinsed off in water or buffer. The film could be dried after each adsorption step for measurement. The deposition process results in short peptides going from a random coil conformation in solution (top left) to a β sheet in the film (top right). Some α helix might be present, depending on peptide sequence and solution conditions. Generally, 20 min is sufficient for most binding sites on the film to become saturated with the oppositely charge polypeptide (top center), when the linear density of charge is above 0.5, the concentration of material in solution is on the order of 1 mg/mL, and the temperature is about 25 °C. Evidently, the amount of material on the resonator did not change much during deposition of the negative peptide, but deposition was none the less important for reversing the surface charge density of the film and enabling subsequent adsorption of the positive peptide [3].....15	15
Figure 2-3	Proposed disulfide locking of polypeptide microcapsules. Polycations are represented by green/solid lines and polyanions by blue/dashed lines. The polypeptides contain Cys which can form a disulfide bond represented as a crosslink between layers under oxidizing conditions. The scheme is idealized, as oxidation did not result in complete oxidation under the conditions discussed here. In principle, it should be possible to optimize the locking process for a particular harsh environment, maximizing the yield of capsules of desired longevity [30]..17	17
Figure 3-1	QCM quartz resonator.....21	21
Figure 3-2	Single-beam UV/vis spectrophotometer [75]22	22

Figure 3-3	CD mechanism. Chiral or asymmetric molecules produce a CD spectrum because they absorb left and right handed polarized light to different extents [77].....	23
Figure 3-4	Far UV CD spectra associated with various types of secondary structure. Solid line, α -helix; long dashed line, anti-parallel β -sheet; dotted line, type I β -turn; cross dashed line, extended 3_1 -helix or poly (Pro) II helix; short dashed line, irregular structure [81].....	24
Figure 3-5	Mechanism of ellipsometry [84].....	25
Figure 3-6	Comparison of measurements for polypeptide films by ellipsometry and surface profilometry.....	26
Figure 3-7	Atomic force microscopy block diagram [94].....	27
Figure 3-8	AFM cantilevel force <i>versus</i> distance. (a) Original piezomovement (cantilevel tip movement) vs. cantilevel force. (b) Indentation vs. cantilevel force (Plot from raw experimental data, comparable to [90]).....	28
Figure 4-1	Calculated net charge <i>versus</i> pH. Shaded region indicates range of values discussed here. Solid symbols: Triangles: P1. Squares: N1. Solid symbols: as studied here. Open symbols: P1 and N1 with Cys replaced by serine.....	31
Figure 4-2	pH dependence of peptide multilayer film preparation. (a) UV-vis. The numbers of layers are 3, 6, 9, 12, and 15, respectively, as the absorbance increases. (b) Comparison of UV-vis and CD (inset) for 15-layer films. (c) QCM.....	33
Figure 4-3	Bulk film properties. (a) Film thickness versus adsorption step, measured by ellipsometry. (b) Typical surface profilometry scanning profile over a gently prepared scratch on a peptide sample. The thickness measurements were performed on at least three sections for each scratch. The inset shows the scratch on the film. (c) RI of peptide multilayer films determined by ellipsometry.....	35
Figure 4-4	AFM micrographs of 40-layer peptide films deposited at different pH values, $20\ \mu\text{m} \times 20\ \mu\text{m}$ and $1\ \mu\text{m} \times 1\ \mu\text{m}$ (insets). (a) pH 8.9, (b) pH 7.8, (c) pH 7.4, and (d) Si wafer. Vertical scales, for $20\ \mu\text{m} \times 20\ \mu\text{m}$, are 194 nm, 150 nm, 84 nm, 36 nm, respectively; and for $1\ \mu\text{m} \times 1\ \mu\text{m}$, are 34 nm, 29 nm, 27 nm, 15 nm, respectively.....	36

Figure 4-5	Schematic representation of the adsorbed layer at (a) pH 7.4 and (b) pH 8.9. The heterogeneity and surface roughness is much higher for pH 8.9 than 7.4, while the density for pH 8.9 is much smaller than for pH 7.4.....	38
Figure 4-S1	Film deposition, monitored by QCM, at various pH values for two 32 mer peptides (sequences as follows). The inset is the LBL of polylysine (MW 13.6 kDa) and polyglutamic acid (MW 14.6 kDa). In both cases, no obvious influence of pH on assembly behavior was observed	43
Figure 4-S2	The AFM micrographs, $20\ \mu\text{m} \times 20\ \mu\text{m}$, and roughness profiles, of 20-layer peptide films deposited at different pH values. (a) pH 8.9, (b) pH 7.8, (c) pH 7.4, and (d) Si wafer. It is clear that films prepared at higher pH have rougher surface than those at lower pH in the range of pH 7.4 to 8.9	44
Figure 5-1	Estimated peptide net charge <i>versus</i> pH [1]. Peptides P0, P1, P2, N0, N1, and N2 all have about the same linear charge density at pH 7.4	47
Figure 5-2	Film thickness. (a) Peptide bond absorbance at 190 nm during the assembly process. The inset shows the ratio of absorbance P0/N0 to absorbance of P1/N1. The ratio is approximately 2 for 0-10 layers. The molecular weights of P0, N0, P1 and N1 are 3719, 3733, 3567 and 3581 Da, respectively. The ratio of molecular weights of P0/N0 and P1/N1 is 2.1. (b) Ellipsometric film thickness during the assembly process. P1/N1 and P2/N2 behave similarly with regard to absorbance and thickness.....	49
Figure 5-3	CD spectra of 10-bilayer films. The amplitudes of CD spectra follow the trend: P0/N0 > P1/N1 > P2/N2. In P0/N0 the negative Cotton effect amplitude is about 240 % larger than the positive one. On the contrary, the asymmetry of the positive and negative Cotton effect amplitudes of P1/N1 and P2/N2 is much smaller, with the negative amplitudes 39 % and 25 % larger than positive ones, respectively. The inset illustrates the correlation between CD and UVS data for P0/N0, P1/N1 and P2/N2. $ \text{CD}^+/\text{CD}^- $ is the absolute ratio of the positive Cotton effect amplitude to negative Cotton effect amplitude for 10-bilayer films. Absorbance was at 190 nm. CD spectra are sensitive to the secondary structure of the films, which will depend on different amino acid sequences of designed polypeptides	50

- Figure 5-4 Polypeptide film disassembly in pH 2.0 KCl buffer. (a) Absorbance at 190 nm during film disassembly. Film P0/N0 loses almost all of its absorbance within 0.5 h, P1/N1 loses about 45 % of its absorbance within 0.5 h but only an additional 5 % within 2 h. P2/N2 loses practically no material on the same time scale. (b) Ellipsometric thickness during film disassembly. After 4.5 h of disassembly, P2/N2 has retained almost all its thickness and P1/N1 has lost 30 % of its thickness. P0/N0 loses all its thickness in 15 min.....51
- Figure 5-5 Film disassembly in pH 3.0 glycine-HCl buffer. After 40 min of disassembly, P1/N1 has almost the same mass; P1/PLGA has lost 5 % of its mass while PLL/N1 has lost about 10 %. PLL/PLGA has lost 45 % of its mass within the first 5 min of disassembly, and after 40 min, it has lost about 55 %. Time constants of film disassembly were determined by fitting the data with a first-order exponential decay model. P1/PLGA, PLL/N1 and PLL/PLGA have time constants of 5.8 min, 3.7 min, and 3.2 min, respectively. The inset shows the assembly behavior of the same four pairs of peptides. P1/N1 assembles the most material; PLL/PLGA, the least52
- Figure 5-6 AFM images of P1/N1 during disassembly at pH 2.0. (a) After assembly, (b) After oxidation, (c) After 30 min disassembly, (d) After 1 h disassembly, (e) After 2 h disassembly, (f) After 3 h disassembly. Image dimensions are $1 \times 1 \mu\text{m}^2$, and the z-axis scales for (a)~(f) are all 24 nm. Surface roughness (from section profiles) is about 6 nm, 6 nm, 7 nm, 10 nm, 6 nm, and 8 nm, respectively.....53
- Figure 5-7 LBL assembly mechanism. (a) The main driving force in LBL is coulombic attraction, and effectively one peptide layer only is formed during each adsorption step. (b) Assembly of peptide molecules with alternating charged and hydrophobic side chains. In aqueous solvent, two peptide layers will form in each deposition step [62]56
- Figure 5-8 Model of disassembly Cys containing peptide PEMs. (a) LBL multilayer peptide film assembled on substrate. After oxidation, disulfide bonds form between and inside layers. (b) Film is immersed in acidic solution. The solution etches the film, firstly protuberant parts. The film becomes smoother. (c) Regions with few or no disulfide bonds are etched away. The film surface becomes rougher, but the grains become smaller as compared to (a). (d) Acidic disassembly solution etches the protuberant parts. The surface becomes smooth again60

- Figure 5-S1 AFM images for 20-layer polypeptide films. (a)-(c) marked with $20 \times 20 \mu\text{m}^2$ AFM images for 20-layer P0/N0, P1/N1, P2/N2 peptide films on wafer substrate with vertical scale 50 nm, 110 nm, 100 nm respectively. The insets are $1 \times 1 \mu\text{m}^2$ images with vertical scale 18 nm, 15 nm, 16 nm respectively. (d) is $20 \times 20 \mu\text{m}^2$ AFM image for clean wafer substrate with vertical scale 25 nm. The inset is $1 \times 1 \mu\text{m}^2$ image with vertical scale 7 nm. (e) is $20 \times 20 \mu\text{m}^2$ AFM image for clean quartz slide with vertical scale 30 nm. The inset is $1 \times 1 \mu\text{m}^2$ image with vertical scale 10 nm61
- Figure 6-1 Comparison of calculated net charge of polypeptides in solution. The net charge of PLL-S and of PLGA-S is comparatively large at pH 4.0, 5.0, 5.5 and 7.4. The charge density will be somewhat different in a multilayer film: the increased presence of oppositely charged groups results in a shift of pK_a 64
- Figure 6-2 Loading with MB at pH 7.4 of PLL/PLGA assembled at pH 4.0. Inset, UVS spectra of PLL/PLGA during loading process. The peak at 572 nm is attributable to MB. The film is loaded to 90 % of capacity within 15 min. MB loading is saturated by 30 min. The time constant for MB loading at ambient temperature, 5.3 ± 1.0 min, was determined by fitting experimental data with a first order exponential decay model67
- Figure 6-3 Absorbance spectra of PLL/PLGA before loading with MB. PLL/PLGA assembled at pH 4.0, pH 5.5, and pH 7.4, respectively. Absorbance at 190 nm follows the trend: pH 4.0 > pH 5.5 > pH 7.4. Inset, absorbance spectra of the films after MB loading. A typical MB absorbance peak is visible at about 570 nm in the pH 4.0 film. By contrast, the films assembled at pH 5.5 and pH 7.4 show no MB peak67
- Figure 6-4 Absorbance spectra of 10.5-bilayer films of PLL/PLGA, PLL-S/PLGA-S, P1/N1, P3/N3 and P3/PLGA after loading of MB. See Table 1 for pH of assembly. The absorbance peak at 572 nm indicates the amount of MB loaded, while absorbance at 190 nm indicates the amount of polypeptide deposited. Table 6-1 presents details of the spectra68
- Figure 6-5 AFM images of 10.5-bilayer polypeptide films. (a) PLL/PLGA assembled at pH 4.0. (b) PLL/PLGA assembled at pH 5.5. (c) PLL/PLGA assembled at pH 7.4. (d) PLL-S/PLGA-S assembled at pH 4.0. (e) P1/N1 assembled at pH 5.5. Surface roughness (from section profiles) from (a) ~ (e) is about 20 nm, 12 nm, 8 nm, 6 nm, and 4 nm, respectively70

- Figure 6-6 Absorbance spectra of polypeptide films with different numbers of capping layers. (a) Absorbance spectra before loading. (b) Absorbance spectra after 1 h of MB loading. (PLL/PLGA)_{5.5} represents a 5.5-bilayer base film assembled at pH 4.0. All capping layers were assembled at pH 7.4. +PLL represents one PLL capping layer. +(PLL/PLGA)_{2.5} and +(PLL/PLGA)_{4.5} represent 2.5 and 4.5 capping bilayers, respectively.....71
- Figure 6-7 MB release in pH 5.5 deionized water from PLL/PLGA assembled at pH 4.0. (a) MB in film as a function of time. (b) Kinetics of release of MB into pH 5.5 deionized water. Insets, spectra of film and release medium after 30 min of release, respectively. The time constants for MB loss from film and MB increase in pH 5.5 deionized water were 0.80 ± 0.10 h and 0.71 ± 0.02 h, respectively, as determined by fitting experimental data with a first-order exponential decay model. Agreement is good. The difference in MB spectra may reflect differences in electronic environment between film and aqueous solution.....72
- Figure 6-8 Release of MB into different media from PLL/PLGA assembled at pH 4.0. (a) Release into pH 4.0, pH 5.5 and pH 7.4 assembly buffer (timescale of min). The release rate follows the trend: pH 4.0 buffer > pH 5.5 buffer > pH 7.4 buffer. The time constants are 0.41 ± 0.11 min, 0.88 ± 0.06 min, and 1.63 ± 0.05 min, respectively. (b) Release into pH 5.5 and pH 7.4 deionized water (timescale of h). The time constants are 0.89 ± 0.12 h and 8.63 ± 2.52 h, respectively. Insets, apparent disassembly of film during MB release process as assessed by absorbance at 190 nm73
- Figure 6-9 PLL/PLGA spectra before and after capping. “After reloading” represents the same film after capping and after attempted reloading with MB. The last two spectra are virtually identical.....74
- Figure 7-1 Loading of the model drug onto peptide N1 for subsequent multilayer film assembly. (a) DTNB reacts with Cys side chains in N1. A TNB group becomes attached to a peptide thiol group by formation of a disulfide bond. (b) Absorbance spectrum of LN1 solution after extensive dialysis to remove unreacted DTNB but before (0 h) and 1.5 h after adding DTT: The peak at 412 nm in the 1.5 h spectrum is due to TNB dianions, while that at 328 nm (0 h) is due to TNB-thiol mixed disulfide [131]. The sharp increase in absorbance below 300 nm is due to DTT. The shoulder evident around 275 nm in later time points (not shown) is due to oxidized DTT84
- Figure 7-2 Multilayer film absorbance at 190 nm *versus* number of layers. Assembly behavior falls into three categories: P1/N1; PLL/N1, P1/LN1, and P1/PLGA; and PLL/PLGA.....86

Figure 7-3 Release of TNB from multilayer nanocoatings. (a) TNB dissociates from peptide LN1 on the inward diffusion of DTT. (b) Absorbance spectra of liquid medium surrounding of 10 P1/LN1 nanocoatings, recorded 0, 5, 30, or 60 min after immersion in 0.1 mM DTT solution. TNB absorbance increases with time. (c) Absorbance at 412 nm of release media for 10 P1/LN1 films v. incubation time. “Capped” films had (P1/N1)₂ on the outer surface (see panel d). TNB release kinetics depends on redox potential and the physical behavior presented by the capping layers. (d) Schematic diagram of redox-stimulated release of TNB from polypeptide multilayer nanocoatings. DTT molecules are omitted for simplicity. ΔE signifies the change in reducing potential, Δt is time89

ACKNOWLEDGEMENTS

I am very grateful to my dissertation advisor, Dr. Don T. Haynie, for his kindness, insightful guidance and support in my research work throughout the last three years.

I also want to thank my advisory committees: Dr. B. Ramu Ramachandran, Dr. Daniela Mainardi, Dr. James Palmer, and Dr. Cheng Luo, for their support and constructive directions in my dissertation study.

I want to give thanks to Dr. Bingyun Li for his great help and guidance in my research work. I am indebted to Karen Xu and Deborah Wood at the Institute for Micromanufacturing for their warm-hearted help and technical supports.

I would like to give my special thanks to Ling Zhang and Wanhua Zhao, for their mental and emotional support in my life, and for helpful discussion in research work. I would also like to thank Tom and Laura Malone, Naveen Palath, Sujay Bhad, and Jai Rudra in Artificial Cell Technologies, Inc., for their support in my research work.

I am blessed that I have such a wonderful family, thanks to my parents and parents-in-law, for their unreserved support and unending love in my life and study. I give my deepest appreciation to my husband for sharing every moment in our lives, and going through the happiness and bitterness together. In the past three years of my PhD study, I got pregnant and gave birth to my lovely daughter- Anna Guan. For a quite long time, she was doing the research together with me. Thank God to give me such a precious creature, making my life happier and more meaningful.

CHAPTER ONE

INTRODUCTION

1.1 Protein Engineering

Protein, a complex biomacromolecule, consists of amino acids joined by peptide bonds. Together with carbohydrates (or polysaccharides), lipids, and nucleic acids, peptides and proteins constitute one of four basic classes of biological macromolecules. These extraordinary polyelectrolytes, alone or in aggregate form, serve as nanoscale machines in the synthesis of organic molecules, building blocks of tissue, vehicles for gas transport, and chemical effectors of development and growth in living organisms. Muscles, hairs, enzymes and hemoglobin, are composed of proteins. Proteins are essential to the structure and function of all living cells and viruses.

The amino acids components in nature peptide chain follow specific sequence, for which information is stored in the code of a gene. A cell can use the genetic information to construct corresponding proteins through processes of transcription and translation.

Proteins play important roles on organism conformation and metabolism, but how they can form such complex structures and have specific functions are not completely understood yet. Protein engineering contains the application of science, mathematics, and economics to the process of developing useful or valuable proteins. In current stage, the main researches of protein engineering focus on protein folding, protein recognition, and

protein design principles. Computer-aided simulation is also an important tool to analyze protein structure and functionalities.

Polypeptide design is the first stage of protein design. Polypeptide chain, or the amino acid sequence, can be synthesized through biological or chemical methods, according to genetic information or *de novo* design. But some technique difficulties limit the length and order of the amino acid chain for the polypeptides synthesized by chemical methods. For example, the coupling efficiency decreases with the increase of chain length. At the same time, it is very difficult to purify the polypeptides synthesized from biology methods without disturbing or damaging their structures and biofunctions. The design of proteins is more complicated than polypeptides. Only certain amino acid sequences can fold reliably to a native state of protein. Currently, the protein folding process is not completely understood.

Pioneering research about the application of polypeptide design, especially the Cys containing polypeptides, and the investigation on properties of multilayer nanofilms, have been done in this thesis work. Polypeptides with different amino acid sequences have been designed and synthesized. Multilayer nanofilms have been fabricated from these polypeptides, and the assembly properties, the nanofilm stability, application for model drug loading, and release have been investigated in detail.

1.1.1 Protein Structure

Peptides or proteins are polymers of amino acids. An amino acid is any molecule which contains both amine and carboxylic acid functional groups. There are 20 essential amino acids that the human body needs to take from food since they cannot be synthesized from other compounds through chemical reactions. The 20 amino acids vary

from each other by their distinct side chains, which are used to differentiate amino acids into various categories, e.g., polar or nonpolar, hydrophobic or hydrophilic, acidic or basic. The amino group of one amino acid can react with the carboxyl group of another amino acid through dehydration synthesis. The resulting CO-NH bond is called a peptide bond. The amino acids link one after another by peptide bonds, which forms the backbone of a polypeptide molecule (Figure 1-1a). The rigidity and planarity of a peptide bond limit the degrees of freedom of the polypeptide backbone [1]. This is crucial for the secondary structure formation of the protein molecules.

There are four secondary structures of proteins, α -helix, β -sheet (Figure 1-1b), β -turn, and random coil. The hydrogen bond is the main interaction to stabilize secondary structures of proteins. Tertiary structure is the full three dimensional folded structure of entirely one polypeptide chain, which determines the function and activity of a protein (Figure 1-1c). A protein in its native state is often described as folded, and is considered denatured while it is not in its native state. If the tertiary structure gets disturbed, the protein molecule is denatured and loses its activity. Quaternary structure is considered the interconnections and organizations of more than one polypeptide chains. For example, hemoglobin is composed of four subgroups: two α -globins and two β -globins, with each globin having one entire polypeptide chain (Figure 1-1d).

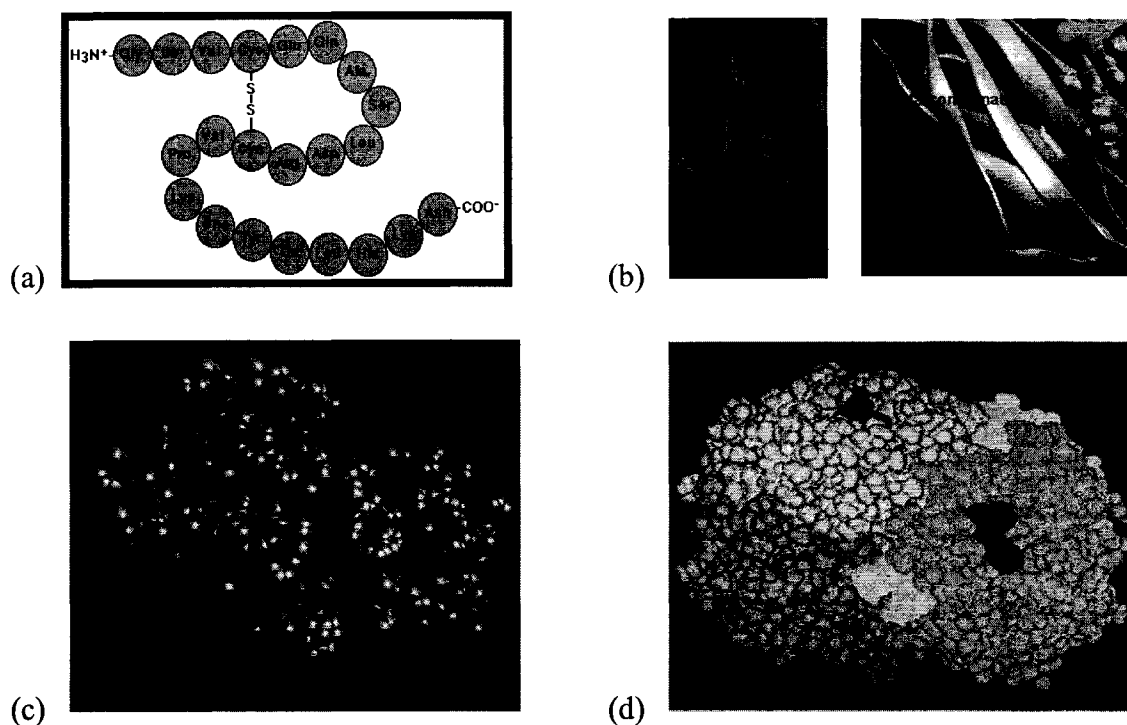


Figure 1-1. Protein structure. (a) Primary structure. (b) Secondary structure. Left: α -helix; right: β -sheet. (c) Tertiary structure (hexokinase). (d) Quaternary structure (hemoglobin) [2].

1.1.2 Protein Functionality

Proteins comprise 70 % of the dry mass of human body. Protein intakes need to be broken down by digestion, and then to be adsorbed in the form of smaller polypeptides. Polypeptide can finally turn to be amino acids to be used to construct new protein *in vivo*. Proteins are involved in almost every function performed by a cell. According to the wide variety of biological functions, proteins can be divided into different categories: biological catalysts (e.g., enzymes), structural protein (e.g., tubulin), regulatory proteins (e.g., cyclins), signaling molecules (e.g., hormones), and defensive proteins (e.g., antibodies). Life, as far as we know, cannot exist without proteins.

1.2 Polypeptide Multilayer Film

A polypeptide multilayer film is defined as a multilayer film made of polypeptides [3]. Polypeptide films are very useful in many areas of biology, for instance, surface modification, device fabrication. They have been used to change the biofunctions and or surface specificities. They have many desirable applications because of their features of biodegradability, biocompatibility, biosensibility, environmental benignity, etc. The biofunctions and chemical properties of polypeptide multilayer films can be controlled in polypeptide synthesis, film assembly and post-fabrication treatment processes. For example, Cys residues can be introduced into polypeptides chain by amino acid sequence design and followed polypeptide synthesis; after film fabrication, disulfide bonds can form between two Cys residues under oxidation circumstance, both intra- and inter- layers; the disulfide crosslinking can increase the stability of polypeptide multilayer films. The physical properties of polypeptide multilayer films, e.g., thickness, refractive index, surface morphology, can be controlled by various methods [4-6]. LBL is a convenient method to fabricate polypeptide multilayer films with thickness control over nano-scale, which is a crucial technique of this thesis work and will be stated in details in Chapter Two.

1.3 Polypeptide Synthesis

In general, there are two ways to design polypeptide productions: biotic synthesis and abiotic synthesis [3]. Biotic synthesis uses host cells, for instance, *E. Coli*, to synthesize polypeptides *in vivo* according to designed genetic coding. A specific gene can be introduced in an expression vector in the host cell, and then a protein encoded by this gene can be produced by cellular transcription and translation. Biotic synthesis can

produce a high yield of polypeptides without limitation in peptide chain length or amino acid order. But it is very difficult to purify desired polypeptide from bacterial contaminations. Abiotic synthesis is the chemical method widely used in laboratories to synthesize polypeptides of designed sequences. These can be classified into two categories: solution phase synthesis and solid phase synthesis. Most of the commercial homopolypeptides, for example PLL and PLGA, are synthesized by solution phase synthesis, for which the chain length of polypeptides can not be defined.

In this thesis work, 24 mers (mer: counter number for amino acids) and 32 mer designed polypeptides are prepared by solid phase peptide synthesis (SSPS), which was pioneered by Bruce Merrifield (an American biochemist who won the Nobel Prize in Chemistry in 1984) in 1959. The polypeptides synthesized by SSPS contain less contamination than by biotic methods. They can include unnatural amino acids, and even have peptide/protein backbone modification. But the chain length of polypeptide is limited and can not be longer than 75 mers because amino acids coupling efficiency decreases with the increase of chain length. Wang resin is used as insoluble substrate and linked with the first amino acid, normally Tyrosine, by a cleavable polyethylene glycol (PEG) linker. Amino acids couple onto the polypeptide chain on the insoluble resin one by one through the formation of peptide bonds, with coupling direction from C terminal to N terminal for each amino acid. F-moc chemistry (introduced by Sheppard, R.C. in 1971) is used in N- α group protection for the amino acids. The N- α protection group for the previous amino acid in the chain is removed before the next amino acid (also with N- α protected) coupling. Side chains of amino acid residues can react with other chemicals under various conditions, for example, the carboxyl groups of side chains of

aspartic and glutamic acids, the phenol of tyrosine, the guanidine of arginine, the thiol of cysteine. In the coupling procedure, all the side chains of amino acids are protected to prevent from acylation, alkylation, etc. After all the coupling and rinsing processes, all the protection groups for side chains are cleaved and then the polypeptides are cleaved from the resins. The final products are purified with High Performance Liquid Chromatography (HPLC) and analyzed by mass spectrometry.

The designed polypeptides used in this thesis work are listed as:

P0: (KVKV)₇ KVKY

N0: (EVEV)₇ EVEY

P1: (KVKGKCKV)₃ KVKGKCKY

N1: (EVEGECEV)₃ EVEGECEY

P2: (KCKGKCKV)₃ KCKGKCKY

N2: (ECEGECEV)₃ ECEGECEY

P3: (KV)₁₁ KY

N3: (EV)₁₁EY

where K, E, V, G, C, and Y represent the amino acids lysine, glutamic acid, valine, glycine, cysteine, and tyrosine, respectively. P1N1, P2N2 contain 4, 8 cysteine residues in their amino acid sequences respectively.

1.4 Dissertation Objectives

The objective of this thesis work is to investigate the properties of polypeptide multilayer nanofilms, especially those assembled from designed polypeptides containing Cys residues. The pH influence on assembly behaviors of Cys containing polypeptide is investigated, as well as the thickness, refractive index, density, surface morphology of the multilayer nanofilms. The stability of Cys containing polypeptide multilayer films is controlled by 2-D or 3-D disulfide crosslinkings and compared with no-crosslinked films.

Furthermore, commercial and designed polypeptide multilayer nanofilms have been used in model drug release. Small molecular weight cationic MB is used as drug indicator for the investigation of loading and release behaviors from above films. Redox-based drug loading and release by usage of DTNB has been tested in Cys containing polypeptide multilayer nanofilms.

1.5 Dissertation Organization

Chapter One introduces the concepts of protein and polypeptide. The structural hierarchy and biofunctions of protein have been stated. Polypeptide multilayer film, the main object of this project, has been defined. The features and applications of polypeptide films have been stated briefly. SSPS based on F-moc chemistry, the peptide synthesis method, has been introduced. The designed polypeptides used in this work are listed in this part. Finally, the objectives and organization of the research work are described.

Chapter Two covers the theoretical background of this work. It also introduces the object—polypeptide multilayer nanofilm, the main film fabrication method—LBL technique, and the emphasis of this research work—Cys containing polypeptide multilayer films. The properties of polypeptide multilayer nanofilm can be controlled by changing the assembly parameters, such as, assembly solution species, pHs, salt concentration, or assembly time per deposition step, etc. LBL is the method of assembling polyelectrolyte films from oppositely charged molecules from liquid solutions, by which nano-meter thickness films or capsules can be fabricated. Cys containing polypeptide films can have controlled stability and are suitable for redox-based drug loading and release.

Chapter Three introduces the methodologies used in this research work. Combining the various approaches can provide a relatively comprehensive and reliable view of polypeptide LBL. Several label-free techniques, *viz*, quartz crystal microbalance, UV-vis spectroscopy, circular dichroism spectroscopy, ellipsometry, surface profilometry, and atomic force microscope, which are used to measure and record the experimental results, bring out complementary and fairly complete analysis.

Chapter Four focuses on the influence of pH on the properties of the 32 mer polypeptide multilayer films containing 4 Cys residues in the polypeptide chains. While the assembly pH varies from pH 7.4 to pH 8.9, the film assembly behaviors and film properties change a lot, because of the deprotonation of Cys residues.

Chapter Five discusses the influence of disulfide crosslinking network on the polypeptide multilayer film stability. Designed 32 mer polypeptides containing 0, 4, 8 Cys residues in their peptide chains and commercial polypeptides PLL and PLGA have been used to fabricate multilayer films. Then a disulfide crosslink forms between two Cys residues of these films under mild oxidation condition. Film disassembly has been monitored under strong acidic circumstance and modeled. It is proved that the disulfide crosslinking can increase the stability of polypeptide multilayer films.

In Chapter Six, polypeptide multilayer nanofilms have been used as carriers for the cationic drug indicator—MB. By design of polypeptide sequences and choice of polypeptides assembly combination, the amount of loaded MB can be adjusted. The controlled release has been tested in different release media at different pHs.

Redox-based drug release from liquid phase (aqueous polypeptide solution) and solid phase (polypeptide multilayer films) is demonstrated in Chapter Seven. DTNB is a

model drug which can bind to the free thiol group of Cys residue. The mixture disulfide between the TNB and side chain of Cys residue can be cleaved under reducing circumstance, which will be a simulation for the drug delivering *in vivo*.

Chapter Eight is the conclusion for all the research work done in this dissertation and possible future work.

CHAPTER TWO

THEORETICAL BACKGROUND

Polypeptide, a weak polyelectrolyte, has both essential properties of weak polyelectrolytes and the specificities of proteins. This will affect its assembly behavior while forming multilayer films and the after-fabrication characteristics [3]. The characteristics, functions, and assembly properties of polypeptide multilayer films will be briefly introduced in this chapter.

All of the polypeptide multilayer films discussed in this research work were prepared by LBL technique. LBL is a convenient method of fabricating nanometer-scale multilayer films by alternate deposition of oppositely charged chemical species (e.g. polypeptides, polymers) on suitably charged substrates (e.g., QCM resonators, quartz slides, silicon wafers, electrodes, cores of capsule) [7-10]. The adsorbing surface both attracts oppositely charged particles in the adsorbing layer and repels like-charged particles. LBL is self-limited and can be controlled by a variety of parameters, such as peptide chain length, linear charge density, pH values, polypeptide species, number of deposition layers [4,11], which will be reviewed in Section 2.2.

This research work focuses on the investigation of Cys containing polypeptide multilayer nanofilms. The existence of Cys in peptide chain can influence film assembly behavior [6], and the disulfide bonds formed between two Cys residues will influence

film stability [12]. Furthermore, Cys containing polypeptide film can be used for redox-stimulated drug loading and release [13]. The research articles relating to Cys residue, thiol group, disulfide bond, crosslinking, drug loading and release will be summarized in Sections 2.3 and 2.4.

2.1 Properties and Functions of Polypeptide Multilayer Films

In biotechnology, surface modification with proteins or peptides is of considerable interest for different applications. Membranes, biosensors, and implants [14-16] are all examples of these applications. The interaction of biomolecules and cells with an implant depends on not only topology and roughness of the surface but also chemical composition [17]. Self-assembled peptide scaffolds have imaginatively been proposed for the development of three-dimensional cell culture and tissue engineering [18].

Multilayer nanofilms have been investigated by numerous researchers for use in applications ranging from micro-devices to biomaterials. Examples include polymeric electronic micro-devices [19], ion-transport selective membranes [20], redox-active polyelectrolyte multilayer films [21], and biofunctional microcapsules [22].

The hierarchy of thin films in surface and interface science has been described in Figure 2-1. Significant research on weak polyelectrolyte films have been done by Rubner and the colleagues [23]. The pK_a of ionizable groups in a weak polyelectrolyte is sensitive to the local electronic environment. Thus, the surface charge density is tunable by adjustment of pH values. The conformation of weak electrolyte in solution phase or solid phase can also be controlled by pH values, which will influence assembly behavior

and film surface morphologies [24]. Researches on non-peptide polymers and weak polyelectrolyte informed a basis for predicting the physical, chemical, and, most importantly, biological properties of polypeptide multilayer films [3]. For example, the assembly behavior of weak polyelectrolyte and polypeptide are comparable, since both can be fitted with linear or exponential modes [25-27].

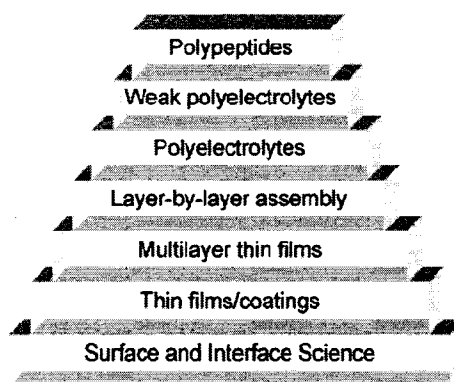


Figure 2-1. Position of polypeptide multilayer films in the broader scheme[3].

Despite extensive work on weak polyelectrolyte (PE) multilayers, further study should be devoted to polypeptide films. One reason is that the properties of a film and therefore its suitability for an application, particularly in a biological context, could depend essentially on chemical properties of peptides versus some other type of weak PE. The other reason is that it should not be assumed that all polypeptides, particularly designed peptides, will behave in ways that can be predicted from the known properties of a handful of well-studied weak PEs or even the known properties of PLL and PLGA.

Research work in our group has characterized self-assembly of polypeptides and various properties of the resulting multilayer nanofilms: pH can be used to the control assembly of PLL and PLGA in the range pH 4-10 and the secondary structure content of

PLL/PLGA films following fabrication at neutral pH [4,28]. Peptides designed according to a few basic principles can be suitable for LBL, even when the molecular weight is as low as ~3500 Da [29,30]. The Cys containing polypeptide multilayer films have increased resistance to degradation at acidic pH on formation of reversible disulfide bonds [11,12,30].

2.2 Layer-by-Layer Self Assembly (LBL)

Different approaches are taken in the self-assembly of molecules into films and related structures. Examples include Langmuir-Blodgett deposition [31,32], sol-gel entrapment [33], covalent binding [34], spontaneous adsorption from solution [35], and polyelectrolyte (PE) LBL. The last of these is attractive to biotechnology for several reasons. LBL is simple—one can make a film from PEs in aqueous solution—and it is versatile with respect to incorporation of specific chemical functionalities [8,9]. The process of LBL was schematically described in Figure 2-2. Moreover, films prepared by LBL can feature nanometer-scale organization, controlled thickness, and designed supramolecular architecture. The ability to build a "nanofilm" from peptides in a predetermined way therefore seems promising for the development of applications in biotechnology, medicine, and other fields. In polyelectrolyte multilayer film (PEM) assembly, control over such variables as the chemical structure of the polyelectrolyte, pH, ionic strength, temperature, immersion and rinsing times, and post-preparation treatment make it possible to obtain a wide variety of film architectures [3,36-40].

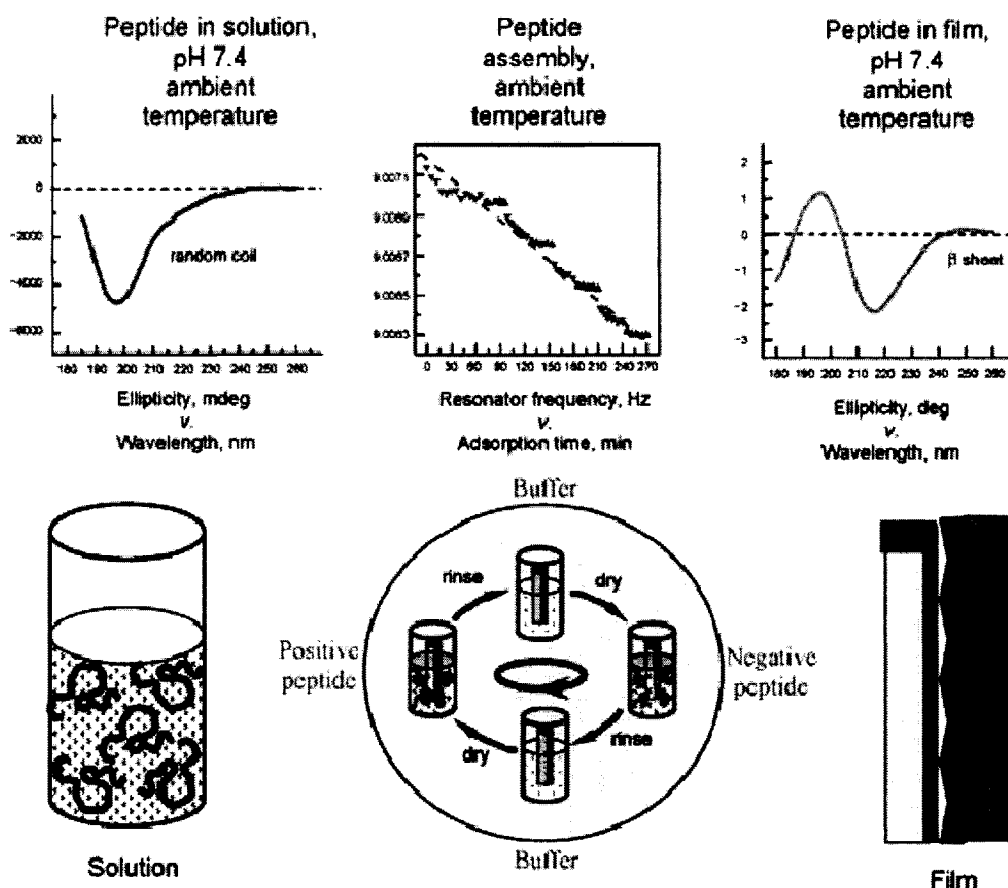


Figure 2-2. Polypeptide multilayer film fabrication. Bottom: schematic diagram of LBL. Top: corresponding experimental data. Oppositely charged polypeptides in solution (bottom left) are adsorbed consecutively onto a solid support (bottom center), for example quartz slide, yielding a multilayer film (bottom right). Loosely bound material is rinsed off in water or buffer. The film could be dried after each adsorption step for measurement. The deposition process results in short peptides going from a random coil conformation in solution (top left) to a β sheet in the film (top right). Some α helix might be present, depending on peptide sequence and solution conditions. Generally, 20 min is sufficient for most binding sites on the film to become saturated with the oppositely charge polypeptide (top center), when the linear density of charge is above 0.5, the concentration of material in solution is on the order of 1 mg/mL, and the temperature is about 25 °C. Evidently, the amount of material on the resonator did not change much during deposition of the negative peptide, but deposition was none the less important for reversing the surface charge density of the film and enabling subsequent adsorption of the positive peptide [3].

2.3 Crosslinking by Disulfide Bonds

Control over the stability of polyelectrolyte multilayers (PEMs) under different conditions is difficult to obtain. Change of the solvent, pH, ionic strength, or layer architecture can affect PEM structural integrity [5,6,11,30,41-43]. Covalent crosslinking of polymers is one means of stabilizing PEMs [30,44-47]. Crosslinking could potentially result in enhanced physical, chemical, and biological properties of PEMs [48,49]. In addition to enhancing PEM stability, crosslinking could influence film permeability and conductivity [50,51]. There are some potential drawbacks to crosslinking. Certain linker molecules, for example glutaraldehyde, will not only modify PEM structure in an uncontrolled manner but also affect biocompatibility [43]; glutaraldehyde is toxic [52]. In general, the effects of particular approach to crosslinking will vary with film architecture.

A disulfide bond is a kind of intermolecular crosslink that forms between free thiol groups under oxidizing conditions. Such bonds, being covalent, are much stronger than hydrogen bonds, van der Waals interactions, and electrostatic interactions. The hydrogen bonds and van der Waals interactions help to stabilize the folded protein structure. Disulfide bonds play an important role in increasing the stability of many folded proteins, e.g., hen egg white lysozyme (HEWL) [53], where they are formed between two Cys side chains. The free thiol groups of Cys side chains can form disulfide bonds in the 2-D or 3-D structure of a polypeptide multilayer film or capsule under mild oxidizing conditions. Figure 2-3 shows a theoretical model on how disulfide bonds in capsule layers can enforce capsule stability even under strong acidic conditions. Disulfide crosslinking is reversed in a sufficiently reducing environment. Cys containing peptides have been with polypeptide LBL to form “naturally” crosslinked polypeptide PEMs

[6,11,30,47] and polypeptide multilayer microcapsules [54]. Disulfide bond-stabilized polypeptide PEMs could be useful for microencapsulation, cellculture coatings, or sensitizing PEMs or microcapsules to the redox potential of the surrounding environment [3,54].

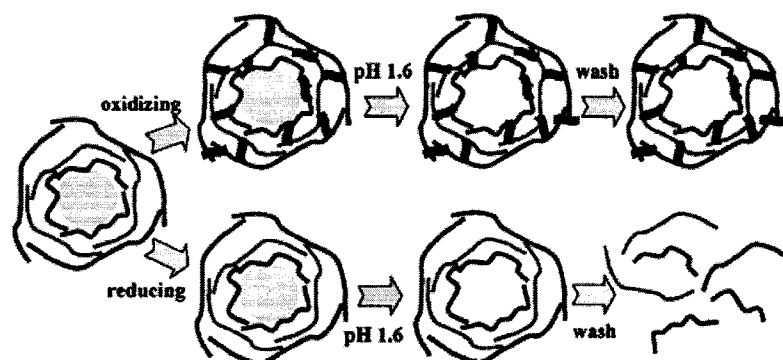


Figure 2-3. Proposed disulfide locking of polypeptide microcapsules. Polycations are represented by green/solid lines and polyanions by blue/dashed lines. The polypeptides contain Cys which can form a disulfide bond represented as a crosslink between layers under oxidizing conditions. The scheme is idealized, as oxidation did not result in complete oxidation under the conditions discussed here. In principle, it should be possible to optimize the locking process for a particular harsh environment, maximizing the yield of capsules of desired longevity [30].

2.4 Drug Loading and Release of Polyelectrolyte Multilayer Films

Multilayer films could work as carriers for drug loading. Generally, the drug models, for example, methylene blue [55], rhodamine B [56], carboxyfluorescein [57], could load into films after film fabrication. And those releases were normally based on concentration-dependent diffusion. As to hydrophobic drug indicator, pyrene, covered with charged micelles, could LBL assemble with oppositely charged polymers to make films and get released [58]. DNA and RNA, the negatively charged molecules, could also be used to fabricate multilayer films and also act as drug models to be released from films

[59-61]. Redox-sensitive multilayer films can be made from Poly(anilineboronic acid) (PABA) and ribonucleic acid (RNA) by the formation of boronate ester as well as electrostatic interactions [61]. When the covalent bonds were broken, RNA was released.

A number of researches in our group have been investigating the role the reversible disulfide bonds on polypeptide multilayer nanofilms or microcapsules [6,11,12,30,62]. In this research work, the role of thiol groups—side chains of Cys residues of designed polypeptides on the redox-stimulated drug loading and release will be investigated.

The drug indicator, DTNB, was covalently loaded onto the Cys containing designed polypeptides. DTNB, known as Ellman reagent [63], are normally used to quantitatively determine peptides by sulfhydryl (-SH) groups, disulfide in peptides, and determine total sulfhydryl groups, protein-bound sulfhydryl groups, and free sulfhydryl groups in biological samples [30,64-67]. DTNB molecules can react with protein molecules with free thiols groups, in other words, be covalently loaded onto designed polypeptides. The labeled polypeptide will be used to fabricate multilayer films. And TNB can release from these films under the change of redox potential.

CHAPTER THREE

METHODOLOGY

Nanotechnology is developing together with the development of more and more precise instruments, from micrometer to nanometer, even to an angstrom [68,69]. It is necessary to measure and analyze polypeptide multilayer films by instruments with nanoscale resolution. Among the instruments used in this work were Quartz crystal microbalance (QCM), UV-vis spectroscopy (UVS), circular dichroism spectroscopy (CD), atomic force microscope (AFM), surface profilometry, and ellipsometry. These instruments were used to determine properties, such as absorbance, thickness, refractive index, roughness, surface morphology. This provided a comprehensive picture to analyze the properties of multilayer films.

3.1 Quartz Crystal Microbalance (QCM)

Quartz crystal microbalance (QCM) utilizes the converse piezoelectric effect to provide information on mass change by real-time measurement of the change in resonant frequency of a piezoelectric quartz crystal, namely, a QCM resonator (Figure 3-1). The most common QCM crystal applications include chemical reaction monitors, biomedical sensors, metal deposition monitors, and environmental monitoring applications, for example, specific recognition of protein ligands by immobilized receptors, adhesion of cells, liposomes and proteins, surfactant interactions with surfaces, etc. [70-72]. It is

useful to determine the properties of polymers and adhesion of proteins to the resonator, and the kinetics of polyelectrolyte adsorption [4,6,30]. When polymers or peptides are coated onto the crystal resonator, they lower the crystal frequency. This frequency lowering directly relates to the mass assembled on the resonator. A QCM is an extremely sensitive mass sensor because the mass change can be detected in the nanogram range [30].

Correlation between mass and frequency is achieved by means of the Sauerbrey equation [73]:

$$\Delta f = -2\Delta m f_0^2 / A \sqrt{\rho_q \mu_q}, \quad (3.1)$$

where f_0 is the resonant frequency of the crystal, A is the active area of the crystal (between electrodes), ρ_q is the density of quartz, and μ_q is the shear modulus of quartz. By using the default values for f_0 (9000 kHz [4]), ρ_q and μ_q , a direct relationship between the frequency shift Δf (Hz) and mass change Δm (g) is given by $\Delta f = -1.832 \times 10^8 \Delta m / A$, where $A = 0.16 \pm 0.01 (cm^2)$, the surface area of the resonator [14]. This formula can be used to calculate the mass of polypeptides firmly and evenly deposited on the resonators. Polypeptide multilayer film formation and perturbation were monitored by a QCM by use of an Agilent 53131A 225 MHz universal counter (USA) and silver-coated resonators (Sanwa Tsusho Co., Ltd., Japan) [5]. If the measurement is in liquid phase, the Sauerbrey equation needs to be modified by liquid density and viscosity.

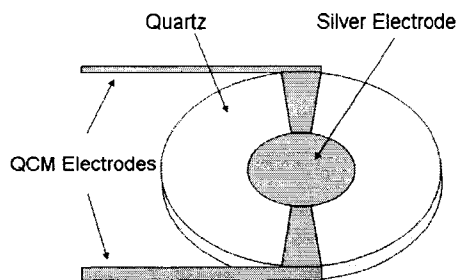


Figure 3-1. QCM quartz resonator.

3.2 UV-Vis Spectroscopy (UVS)

Ultraviolet-visible spectroscopy (UV-1650 PC UV-Vis or UV mini 1240 spectrophotometer, Shimadzu, Japan) uses light in the visible and adjacent near ultraviolet (UV) and near infrared (NIR) ranges, the energy space range where molecules undergo electronic transitions, for quantitative determination of solutions of transition metal ions and highly conjugated organic compounds (Figure 3-2). For example, UVS can measure the optical mass of assembled polypeptides in terms of film absorbance change [6,28]. The peptide bond, the smallest of the three chromophores occurring in proteins (the other two are amino acid side chains and prosthetic groups, e.g., the heme group), has the absorption maximum at 190 nm [74], because visible light that hits the chromophore can thus be absorbed by exciting an electron from its ground state into an excited state.

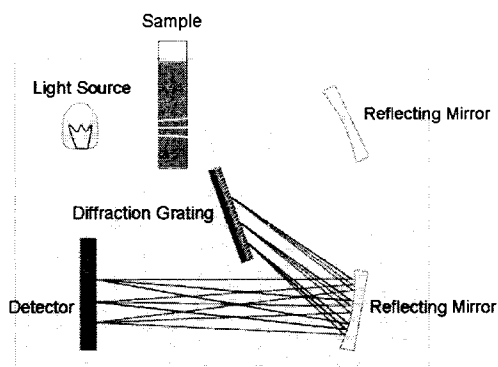


Figure 3-2. Single-beam UV/vis spectrophotometer [75].

Some amino acids or chemical groups have specific absorbance peaks in the UVS spectra, for example, amino acids Tryptophan (Trp), Tyrosine (Tyr) and Cys contributing to absorbance peak at 280 nm [76], MB contributing to ~ 665 nm absorbance peaks in aqueous media and ~572 nm absorbance peaks in polyelectrolyte films [55]. These absorbance peaks together with molar extinction coefficients of the solutes can be used to calculate solution concentration by Beer-Lambert Law. This law states the relation of absorbance and diluted solution concentration, normally 10^{-5} ~ 10^{-6} M [55]:

$$A = -\log(I / I_0) = \epsilon \cdot C \cdot l, \quad (3.2)$$

where A is the measured absorbance, I_0 is the intensity of the incident light at a given wavelength, I is the transmitted intensity, l is the path length through the sample, normally 1 cm for cuvette, and C is the concentration of the absorbing species. For each species and wavelength, ϵ is a constant known as the molar absorptivity or extinction coefficient.

3.3 Circular Dichroism Spectroscopy (CD)

The circular dichroism measurements were recorded with a Jasco model J-810 spectropolarimeter, Japan. Circular dichroism spectroscopy is a method for determining the extent of secondary structures of polypeptides conformation, e.g., random coil, α -helix and β -sheet [1]. Circular dichroism is observed when optically active matter, for example polypeptide, absorbs left and right hand circular polarized light slightly differently (Figure 3-3).

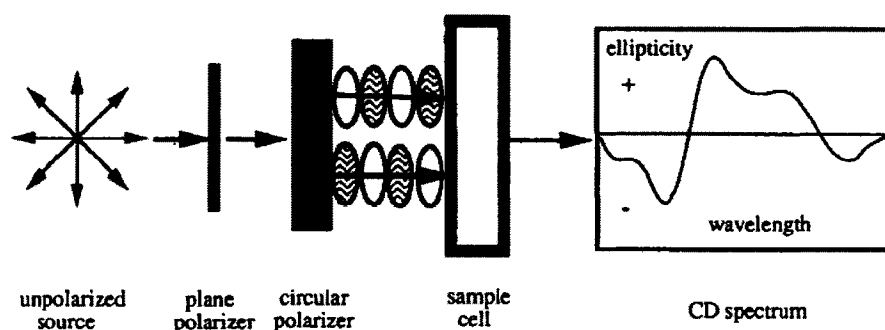


Figure 3-3. CD mechanism. Chiral or asymmetric molecules produce a CD spectrum because they absorb left and right handed polarized light to different extents [77].

Figure 3-4 shows the typical CD spectra for protein secondary structures. For example, a strong, positive band near 190 nm and negative bands at 208 and 220-222 nm are diagnostic of α -helical conformation [1,78]. The dominant feature of random coil peptides is a strong negative band below 200 nm [79,80]. The kinds of polypeptide secondary structures coexist in solid or liquid phase. Thus the CD spectra of polypeptide films or solutions are generally the combination of typical curves as shown in Figure 3-4 [5,6,28]. The deconvolution of CD spectra can provide information on the content of polypeptide secondary structures [28].

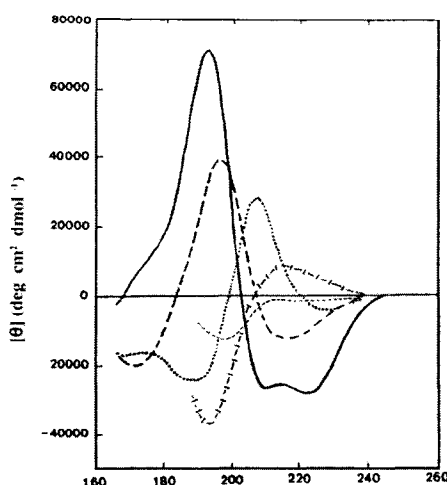


Figure 3-4. Far UV CD spectra associated with various types of secondary structure. Solid line, α -helix; long dashed line, anti-parallel β -sheet; dotted line, type I β -turn; cross dashed line, extended 3_1 -helix or poly (Pro) II helix; short dashed line, irregular structure [81].

3.4 Ellipsometry

Ellipsometry is a non-contacting, nondestructive technique for the measurement of surfaces and very thin films on surfaces using elliptically polarized light (Figure 3-5) [82]. This can even yield information about layers that are thinner than the wavelength of the light itself, down to a single atomic layer or less. Thus, quality ellipsometers can detect film and surface conditions of under an angstrom thick. Ellipsometry is widely used in nanotechnology and biology areas, e.g., measurements of silicon wafers in the semiconductor industry, monitoring vapor deposition of organic and inorganic films, protein growth, polymer adsorption, etc. [6,28,83].

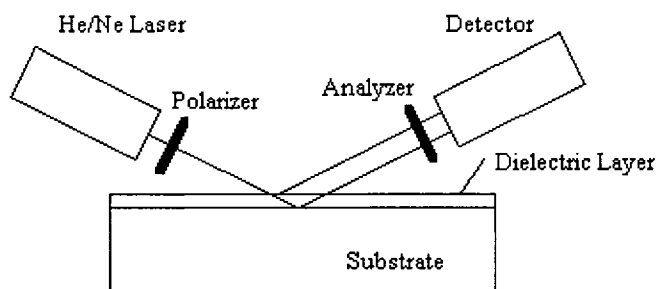


Figure 3-5. Mechanism of ellipsometry [84].

The exact nature of the polarization change is determined by the properties of samples, e.g., film thickness and refractive index (RI). Ellipsometry allows both the thickness and the RI of the adsorbate to be measured at an interface [85,86]. Detailed discussion of this non-contact method and the underlying theory can be found in various places [87-89]. A measurement is made by determining the change in state of polarization of a light probe reflected by the substrate on protein adsorption. In this research work, optical layer models were used to determine mean RI and average thickness of adsorbed layers from measured ellipsometric angles, ψ and Δ . The instrument was a Sentech SE 850 (Germany). This UV-Vis-NIR spectroscopic ellipsometer involves diode array detection (UV-Vis) or interferometric-modulated detection (NIR). The angle of incidence was 70° . Measurements were made at room temperature. A four-layer model, Si substrate/SiO₂/peptide film/ambient air, was used to determine film thickness and RI. The substrate was N-type <100> silicon wafer (Montco Silicon Technologies Inc., USA), with naturally formed ~ 1.5 nm SiO₂ layer on the surface.

3.5 Surface Profilometry

Surface profilometry is a contacting technique with a diamond stylus touching the sample surface, which is commonly used to measure film thickness and surface textures, for example surface profiles and roughness. In this thesis work, polypeptide film thickness was also determined in contact mode using an Alpha-Step IQ surface profiler (KLA Tencor Corporation, USA). A gentle scratch was made on the peptide multilayer nanofilm. Profiling the scratch with a diamond stylus tip at a stylus force of 16.2 mg enabled measurement of its depth. Scan length was 400 μm , speed 5 $\mu\text{m/s}$, sampling rate 50 Hz, and sensor range 20 $\mu\text{m}/1.19 \text{ nm}$

The measurement results of ellipsometry and surface profilometry are comparable, with the results getting from surface profilometry slightly smaller (Figure 3-6) because of its stylus-sample contacting mechanism.

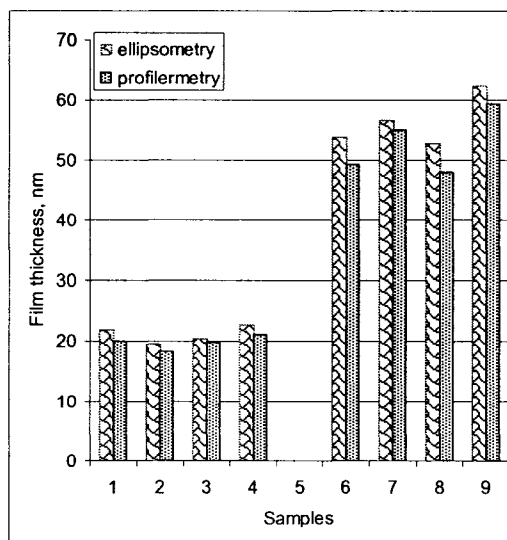


Figure 3-6. Comparison of measurements for polypeptide films by ellipsometry and surface profilometry.

3.6 Atomic Force Microscope (AFM)

An AFM is an important tool for study of surface structure on the nanometer scale (Figure 3-7). A sensitive microscale cantilever with a sharp silicon or silicon nitride tip (probe) at its end scans the specimen surface. The contacting forces between the tip and the sample lead to a deflection of the cantilever according to Hooke's law:

$$F = kd = k(z - \delta), \quad (3.3)$$

in which the loading force, F , is related to the deflection d through the cantilever force constant k . z is the z -position of the piezo, δ is the indentation distance of tip into the film surface, in case the sample is sufficiently soft [90]. The cantilever is sensitive enough to be influenced by all kinds of interactions between the tip and sample surface, for instance, mechanical contact forces, electrostatic forces, hydrophobic interactions, Van der Waals force, chemical bonding, etc.[91-93]. A laser is cast onto the cantilever and gets reflected, to report the deflection information to the detector through a photodiode (Figure 3-7).

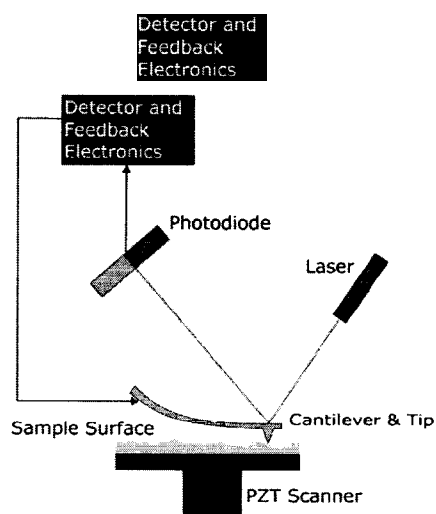


Figure 3-7. Atomic force microscopy block diagram [94].

The general relations of cantilever force and deflection or indentation distance can be described in Figure 3-8. A nonlinear relationship exists between the cantilever force F and the indentation distance δ [90]:

$$F = \frac{4E\sqrt{r}}{3(1-\sigma^2)}\delta^{3/2}, \quad (3.4)$$

where the multilayer polymer film is assumed to behave as an elastic rubber and thus imposed a Poisson ratio of $\sigma = 0.5$. E is Young's modulus. r is a constant representing the average specified tip radius. It is difficult to calculate the Young's modulus for very thin polypeptide multilayer films (tens of nanometers) by this method. Since a series of indentations of different depths are required.

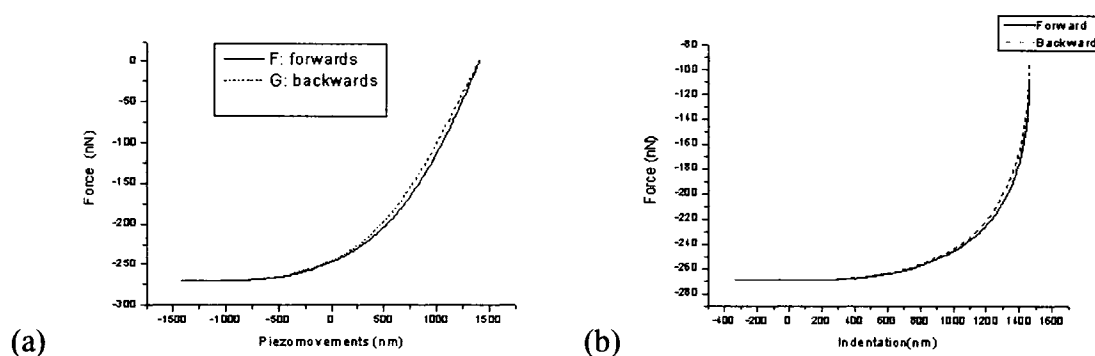


Figure 3-8. AFM cantilever force *versus* distance. (a) Original piezomovement (cantilever tip movement) vs. cantilever force. (b) Indentation vs. cantilever force (Plot from raw experimental data, comparable to [90]).

There are two types of modes for a cantilever to contact sample surface: contacting (static) and tapping (dynamic) modes. The contacting mode is avoided in fairly soft polypeptide multilayer films scanning because of the risk of getting the cantilever tip contaminated or damaged. Polypeptide multilayer films surface scanning tests are done in tapping mode using Q-scope TM 250 scanning probe microscope

(Quesant Instrument Corp., USA). Scanning rate was 2 Hz, and resolution 500 pixels (20 $\mu\text{m} \times 20 \mu\text{m}$ images) or 1000 pixels (1 $\mu\text{m} \times 1 \mu\text{m}$ images). 2-D section or 3-D surface profiles can be provided by AFM.

CHAPTER FOUR

FINE TUNING OF PHYSICAL PROPERTIES OF DESIGNED
POLYPEPTIDE MULTILAYER FILMS
BY CONTROL OF PH

4.1 Introduction

The material properties of a LBL film can be manipulated in different ways. Variables include choice of substrate, solution conditions, method of post-fabrication functionalization, and PE structure. The mean charge per unit length of a "weak" PE varies gradually with pH. Polypeptides are considered weak PEs. Experimental multilayer film studies involving "conventional" weak PEs, for instance, poly(allylamine hydrochloride) (PAH) and poly(acrylic acid) (PAA), have revealed that various film properties can depend strongly on the pH of the polyelectrolyte assembly solution. Examples include surface friction, roughness, film morphology, and dielectric properties [37,40, 95-98]. pH can be used to "tune" film thickness [95,99-101], polymer interpenetration and surface wettability [37], film stability and morphology [28,36,40,96], and permeability [102,103] when PEs are weak. The effect of solution pH on weak PE multilayer film assembly has also been studied theoretically [104].

In this chapter, the role of solution pH in LBL self-assembly of designed 32 mer polypeptides has been investigated in detail using a combination of physical techniques.

Change of pH can alter the three-dimensional structure of a peptide in solution by changing the distribution of charge. Here we show that pH can influence adsorbed mass of polypeptide, film thickness, and surface morphology over a range of little more than 1 pH unit. Smooth and dense or rough and loose-packed peptide nanofilms have been fabricated by adjusting solution pH. As expected, film thickness depended on number of layers, as with conventional polyelectrolytes. Film density and morphology, however, varied more with pH than did thickness. Results of this work provide new insights into LBL and suggest that peptides are a promising class of polymers for the creation of designer thin film structures for novel application in biomaterials and other areas.

4.2 Experiments

Two peptides P1 and N1 were designed to be positively charged or negatively charged at neutral pH. The average net charge of P1 and N1 has been computed as a function of pH and plotted in Figure 4-1.

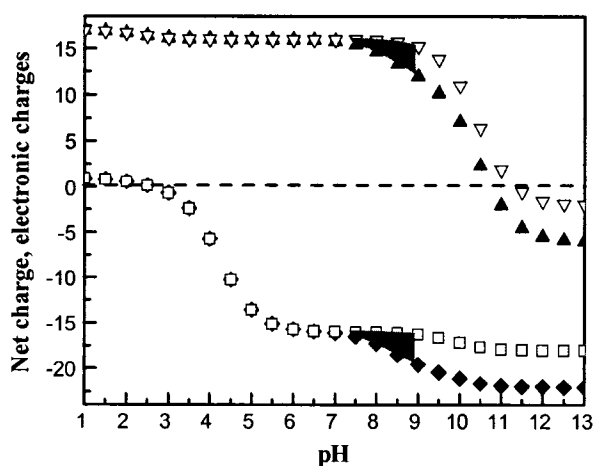


Figure 4-1. Calculated net charge *versus* pH. Shaded region indicates range of values discussed here. Solid symbols: Triangles: P1. Squares: N1. Solid symbols: as studied here. Open symbols: P1 and N1 with Cys replaced by serine.

In the present study, we investigated the role of solution pH on deposition of the designed peptides and the physical properties of the resulting films. The peptide concentration was 2 mg/mL in 10 mM Tris-HCl buffer, 20 mM NaCl. The pH was 7.4, 7.8, or 8.9. Tris buffers throughout the range pH 7.1 - 8.9 and was used in all experiments to minimize variables. The rinsing solution was 10 mM Tris-HCl (pH 7.4) for samples prepared on QCM resonators or quartz microscope slides, and D.I. H₂O for <100> Si wafers, used for ellipsometry, surface profilometry, and AFM experiments. The average value of at least three measurements was obtained in QCM, ellipsometry, and profilometry experiments. Error bars represent standard deviations.

4.3 Results

P1 and N1 are weak PEs. The degree of ionization, however, is high in the range pH 7.4 - 8.9 (Figure 4-1), since the pK_as of Lys and Glu are 10.5 and 4.3, respectively. Deprotonation of thiol results in the net charge of P1 decreasing on pH increase, and that of N1 increasing. A single P1 molecule therefore will have both positively-charged and negatively-charged residues at pH 8.9, giving increased odds of intramolecular self bridge formation and oligomerization. In N1, the side chains of Glu will repel those of Cys when the latter become ionized; otherwise the side chain of Cys is neutral. The absolute value of the net charge of P1 and N1 is matched at pH 7.4 but becomes increasingly different with increasing pH; the net charge is less watched at pH 8.9 than 7.4 (Figure 4-1 inset).

Figure 4-2a shows the variation in UV absorbance with the adsorption step. The increase implies that peptide was deposited during each step. UVS, CD, and QCM experiments at pH 7.4, 7.8, and 8.9 have revealed remarkable assembly behavior. As pH

increased, UV absorbance (Figure 4-2b) and QCM frequency shift (Figure 4-2c) decreased dramatically per adsorption step. By contrast, no obvious dependence on pH was observed for 32 mer poly-(lysine) and poly-(glutamic acid) peptides, or larger versions of these peptides in this pH range (see supporting information).

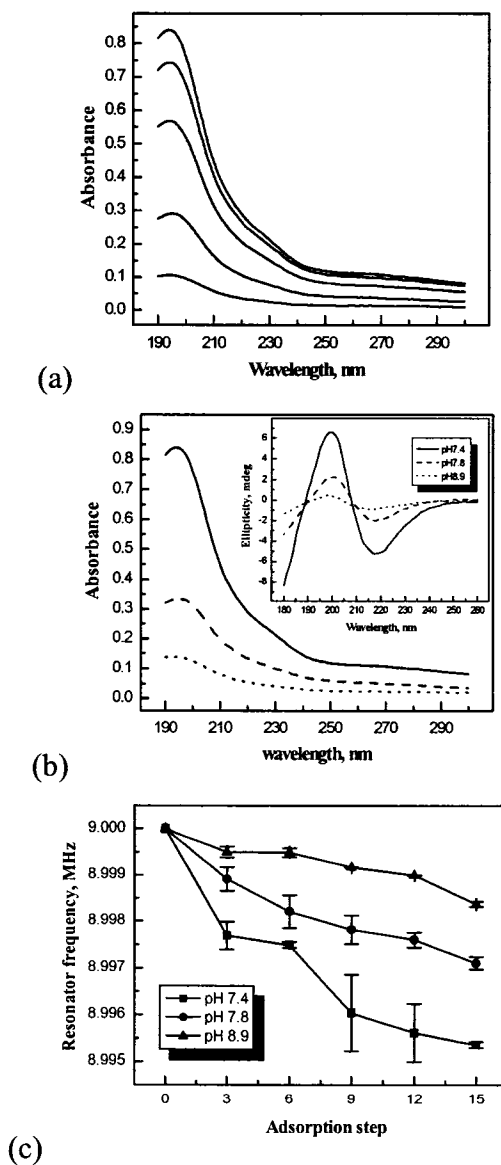


Figure 4-2. pH dependence of peptide multilayer film preparation. (a) UV-vis. The numbers of layers are 3, 6, 9, 12, and 15, respectively, as the absorbance increases. (b) Comparison of UV-vis and CD (inset) for 15-layer films. (c) QCM.

CD experiments show that the multilayer peptide films were dominated by β sheet structure (Figure 4-2b inset), as one can see from the negative $\pi - \pi^*$ transition at *c.* 216 nm, and the positive $n - \pi^*$ transition at *c.* 197 nm. There were small conformational changes in the films as the solution pH changed. Ellipticity indicates that substantially less material adsorbed at pH 8.9 than 7.4.

As expected, film thickness increased with the number of adsorption steps, according to ellipsometry (Figure 4-3a). Surprisingly, however, the thickness of films deposited at pH 8.9 was the same as or even slightly greater than at pH 7.4, despite the difference in deposited mass (Figure 4-2c). Surface profilometry experiments (Figure 4-3b) confirmed the ellipsometry results (Table 4-1).

Table 4-1 Thickness in nm, measured by surface profilometry and ellipsometry, of 20- and 40-layer peptide films produced at different pH values.

pH	20 layers		40 layers	
	Surface profilometry	Ellipsometry	Surface profilometry	Ellipsometry
7.4	19.8 ± 0.3	22.6 ± 0.3	49.4 ± 0.3	53.7 ± 0.2
7.8	18.3 ± 0.6	23.8 ± 0.2	54.2 ± 1.8	56.8 ± 0.1
8.9	21.3 ± 0.4	23.6 ± 0.9	59.2 ± 0.8	62.5 ± 0.6

Ellipsometry also showed that RI varied with the adsorption step. RI was higher for samples deposited at pH 7.4 than 8.9, though by a small amount (Figure 4-3c). This difference decreased with increasing number of layers.

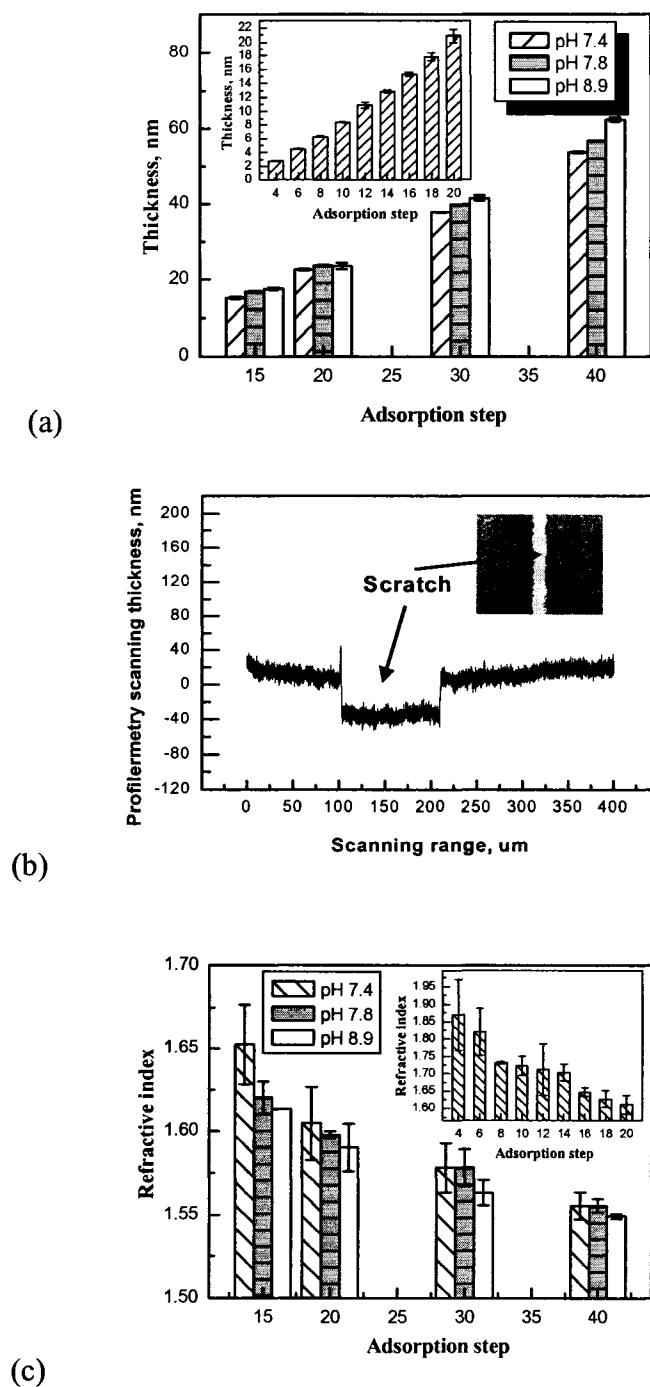


Figure 4-3. Bulk film properties. (a) Film thickness versus adsorption step, measured by ellipsometry. (b) Typical surface profilometry scanning profile over a gently prepared scratch on a peptide sample. The thickness measurements were performed on at least three sections for each scratch. The inset shows the scratch on the film. (c) RI of peptide multilayer films determined by ellipsometry.

Figure 4-4 displays AFM micrographs of surface morphology of 40-layer films fabricated in a narrow pH range. Evidently the wafer production process left a residue on the surface (Figure 4-4d). Films produced at pH 7.4 were very smooth and densely-packed, and the “nanopores”, similar to those observed in LBL multilayer films by Rubner *et al.* [40], were small in size but large in number (Figure 4-4c). Films fabricated at pH 8.9 were comparatively rough and loose-packed (Figure 4-4a), and fewer “nanopores” of large size were evident. The surface morphology of films fabricated at pH 7.8 was intermediate to those of pH 7.4 and 8.9 (Figure 4-4b). Effectively the same result was obtained with 20-layer films prepared independently (see supporting information).

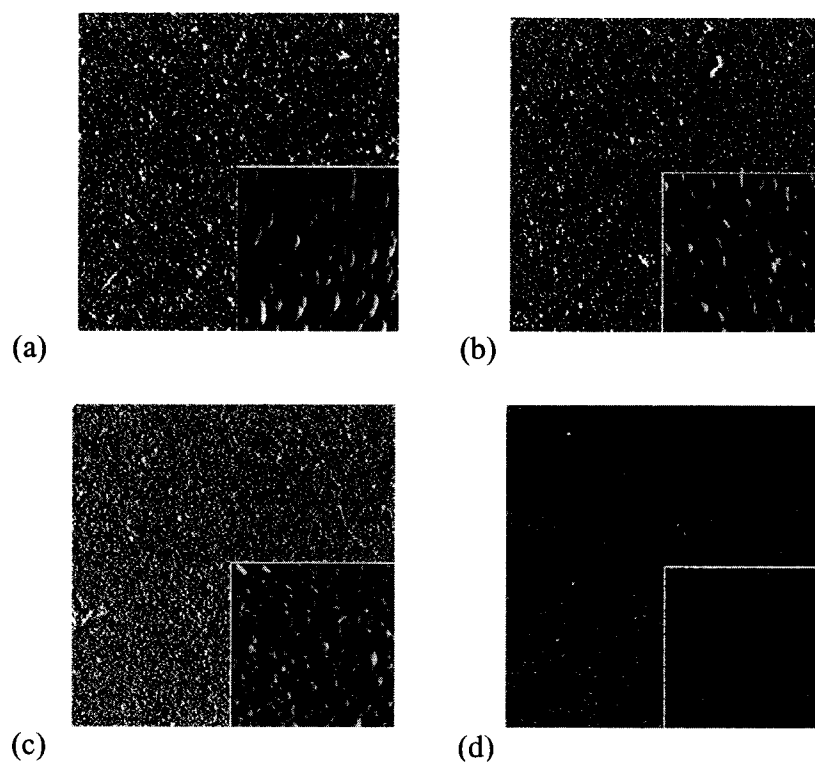


Figure 4-4. AFM micrographs of 40-layer peptide films deposited at different pH values, $20\ \mu\text{m} \times 20\ \mu\text{m}$ and $1\ \mu\text{m} \times 1\ \mu\text{m}$ (insets). (a) pH 8.9, (b) pH 7.8, (c) pH 7.4, and (d) Si wafer. Vertical scales, for $20\ \mu\text{m} \times 20\ \mu\text{m}$, are 194 nm, 150 nm, 84 nm, 36 nm, respectively; and for $1\ \mu\text{m} \times 1\ \mu\text{m}$, are 34 nm, 29 nm, 27 nm, 15 nm, respectively.

4.4 Discussion

The designed 32 mer peptides discussed here exhibit excellent LBL adsorption from the point of mass deposition, despite their low molecular mass [30]. As in Haynie *et al.* [4], the present study has demonstrated that solution pH can have a great impact on the assembly behavior of peptides. This work, however, also has shown that solution pH can have a correspondingly large effect on the physical properties of the resulting polypeptide films.

Figure 4-2a shows that with increasing adsorption step, resonator frequency decreased and UV absorbance increased. In general, at pH 7.4 a considerable amount of material was deposited in comparison with higher pH values: frequency shift was ~310 Hz/layer near 9 MHz (Figure 4-2c), absorbance ~0.056 AU/layer at 194 nm (Figure 4-2b). Increasing the pH of solution led to decreased adsorption according to spectrophotometry (Figure 4-2b) and QCM (Figure 4-2c). CD data show that the multilayer peptide films were dominated by β sheet structure (Figure 4-2b).

At pH 7.4, the absolute value of the net charge of the peptides is matched, and the linear charge density is about the same (Figure 4-1). It seems plausible that under such circumstances, the polyions could form rather tight complexes, every charge being compensated in a dense mass of peptide film. Moreover, because the peptides are short and the charge density is high neutral pH, they are expected to behave as relatively rigid rods (Figure 4-5a). On the contrary, the polypeptides with irregular structures tend to form loose and uneven films (Figure 4-5b).

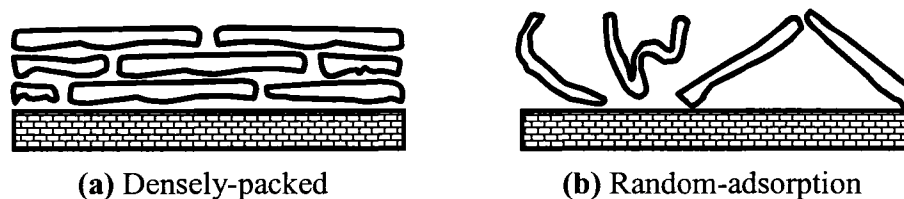


Figure 4-5. Schematic representation of the adsorbed layer at (a) pH 7.4 and (b) pH 8.9. The heterogeneity and surface roughness is much higher for pH 8.9 than 7.4, while the density for pH 8.9 is much smaller than for pH 7.4.

Cys deprotonates when the pH increases from neutral to near its pK_a (\sim pH 8.4). At pH 8.9, then, the negative peptide is more ionized and thus has a higher net charge than at pH 7.4, while the positive one is partially neutralized. The pH-based mismatch in charge (Figure 4-1 inset) will influence peptide assembly. The cooperative association of peptides could depend on charge matching, as could the rate and extent of diffusion of molecules in a film. At pH 8.9 P1 has both positively-charged Lys and negatively-charged Cys residues. The oppositely-charged residues could attract each other, biasing the conformation of this peptide in solution and in a film. The increase in net charge of N1, though modest, could also lead to conformational change, as the like-charged side chains of Glu and Cys will repel each other. That is, thiolate may significantly contribute to the electrostatic potential of the peptides and thus influence their solution structure, tendency to adsorb, and mechanisms of intermolecular interaction during and after adsorption. Random sequential adsorption of peptides at pH 8.9 thus results in a loose structure of rough surface (Figure 4-5b).

The dependence of assembly behavior on pH is supported by AFM and ellipsometry results. Figure 4-3a shows that although deposited mass depended significantly on pH, the thickness at pH 8.9 was about the same as at pH 7.4. This can be

explained as follows. At pH 8.9 peptides are hypothesized to be randomly packed (Figure 4-5b); a small amount of material might occupy the same volume as a large amount of densely-packed material (pH 7.4, Figure 4-5a). Surface profilometry experiments have confirmed that film thickness was about the same at pH 8.9 and 7.4 (Table 4-1), despite the difference in adsorbed mass. The apparent reason why thickness by surface profilometry is a few percent smaller than by ellipsometry is that contact mode was used, requiring a certain stylus force, and ellipsometry is a non-contact mode method. By QCM, however, the mass deposited, calculated using the Sauerbrey equation [14,73], was about three times higher at pH 7.4 than 8.9 for a 15-layer peptide film (Figure 4-2c). Thus, film density was much higher at pH 7.4 than 8.9. Our results appear to indicate that a larger mass deposition does not necessarily imply a larger film thickness. This is usually assumed to be the case in conventional PEs.

AFM shows that at pH 7.4 the films had a very smooth surface, consistent with dense packing (Figure 4-4c). Since the peptides were spread over an essentially flat substrate, “homogeneous” layers were formed; the film surface was correspondingly smooth. “Nanopores” may have been present in the film, as discussed in related research [96,97]. By contrast, at pH 8.9 the peptides appear to have extended away from the surface and may have formed loops, leading to heterogeneity of conformation, increased surface roughness, and larger “nanopores” . In any case, the AFM data demonstrate that adjusting pH in a narrow range can induce significant change in peptide LBL film morphology.

Solution pH is known to be able to have a dramatic influence on weak polyion adsorption behavior over a very narrow pH range. Control of pH has been used to tune

layer thickness. For instance, a remarkable thickness transition, from 45 to 3 Å layer⁻¹, has been reported over a pH range of only 0.5 units in the PAA/PAH system. In separate work, a pH shift from pH 7.4 to 5.0 had a great impact on materials adsorbed. The quantity of human serum albumin adsorbed depended on whether the outer layer was PAA or poly(ethyleneimine) as pH shifted from 7.4 to 5.0 [105].

By contrast, in the present study no significant change in thickness was observed on adjustment of solution pH in the range 7.4-8.9. At the same time, however, a dramatic difference in the amount of material adsorbed was observed. The reason for the difference from the results of Rubner and colleagues [37] could be that the polymers used here are relatively short, monodisperse heteropolymers, while those of the Rubner group were much longer, polydisperse, and homopolymers. Thus, solution pH can have a remarkable effect on surface morphology and density of polypeptide films. Films of smooth surface and high density or of rough surface and loose-packed material can be fabricated by fine-tuning of solution pH. This could be useful for membrane-based separations, as discussed by Schlenoff and co-workers [103].

pH has also successfully been used to tune RI in the development of anti-reflective coatings [40]. Here, as pH increased from 7.4 to 8.9 surface roughness increased, giving a slight decrease in RI. This is because increased roughness (formation of nanopores) will decrease RI. The “pores” are smaller than the wavelength of light, and light scattering by the pores leads to lower RI. In other words, RI can reflect the number of molecules per unit volume. With an increased number of layers, the “pore structure” is further enlarged and RI further decreases. Here, the change in RI can be directly related to the amount of peptide present in the adsorbed layer; it is well known that RI increases

with concentration of protein in solution [85]. Therefore, RI data also indicate that the fully formed film had higher density at pH 7.4 than 8.9.

The RI of adsorbed protein layers has been reported to vary between 1.35 and 1.6 [106,107], and from 1.53 to 1.66 for 20-layer PAH/poly(styrenesulfonate) [95]. In this work, RI was between 1.55 and 1.65 for films of 15 to 40 layers. A decrease in the number of layers increased RI to 1.87, in which case the substrate surface may have influenced parameter determination. The change in RI with film thickness may need to be considered when attempting to infer structural information such as layer thickness from optical measurements using an assumed RI.

4.5 Conclusion

The effect of pH of peptide solutions and number of adsorbed layers on surface morphology, mass deposition, film thickness, and RI of peptide films has been investigated. It has been shown that thickness and RI of the adsorbed peptide layer can depend substantially on solution pH. Thickness, RI, and surface morphology of films made of designed 32 mer peptides were measured using a combination of several label-free techniques, including QCM, UVS, CD, ellipsometry, surface profilometry, and AFM. These methods are particularly useful for studying different aspects of the adsorption of peptides on a solid support. It has been found that film density and RI can depend substantially on pH. The designed peptides formed more compact layers with a higher density and higher RI at pH 7.4 than 8.9. It would appear that the ionization state of Cys side chains plays a key role in the observed adsorption behavior and film preparation. Therefore, fine-tuning solution pH thus enables substantial control bulk and surface composition, density, and surface roughness of multilayer films. The approach

outlined here can be used to create “molecularly” smooth or relatively rough polypeptide films. Such films could be used as artificial membranes or for biomaterial surface modification.

4.6 Supplementary Information

Figure 4-S1 provides the complementary information that the Cys residue is the crucial factor that influences LBL behavior from pH 7.4 to pH 8.9, since the existence of lysine and glutamic acid residues in polypeptide chain cannot affect assembly too much in this pH range.

Figure 4-S2 shows large-scale AFM images of polypeptide films with vertical roughness, when compared with Figure 4-4.

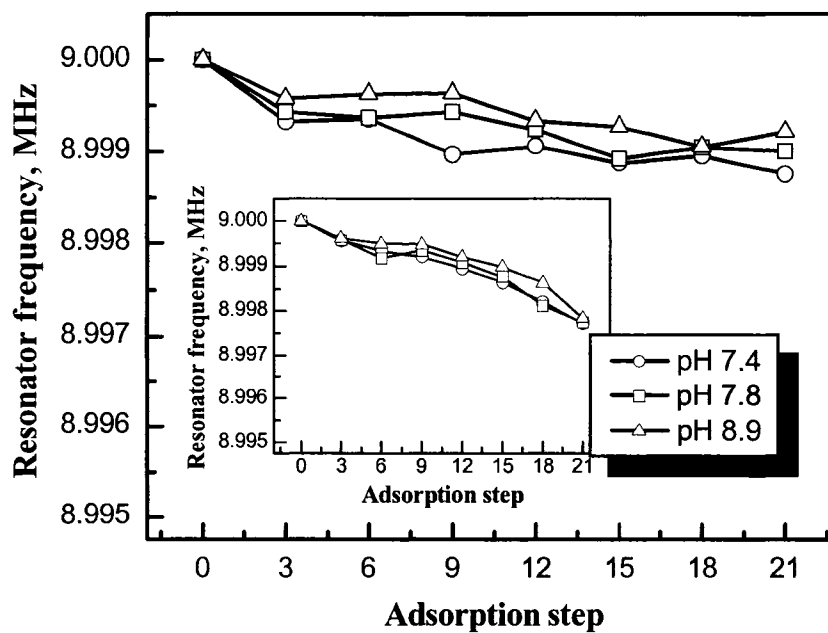


Figure 4-S1. Film deposition, monitored by QCM, at various pH values for two 32 mer peptides (sequences as follows). The inset is the LBL of polylysine (MW 13.6 kDa) and polyglutamic acid (MW 14.6 kDa). In both cases, no obvious influence of pH on assembly behavior was observed.

- (i) KKKK/KKKK/KKKK/KKKK/KKKK/KKKK/KKKK/KKKY
- (ii) EEEE/EEEE/EEEE/EEEE/EEEE/EEEE/EEEE/EEEE

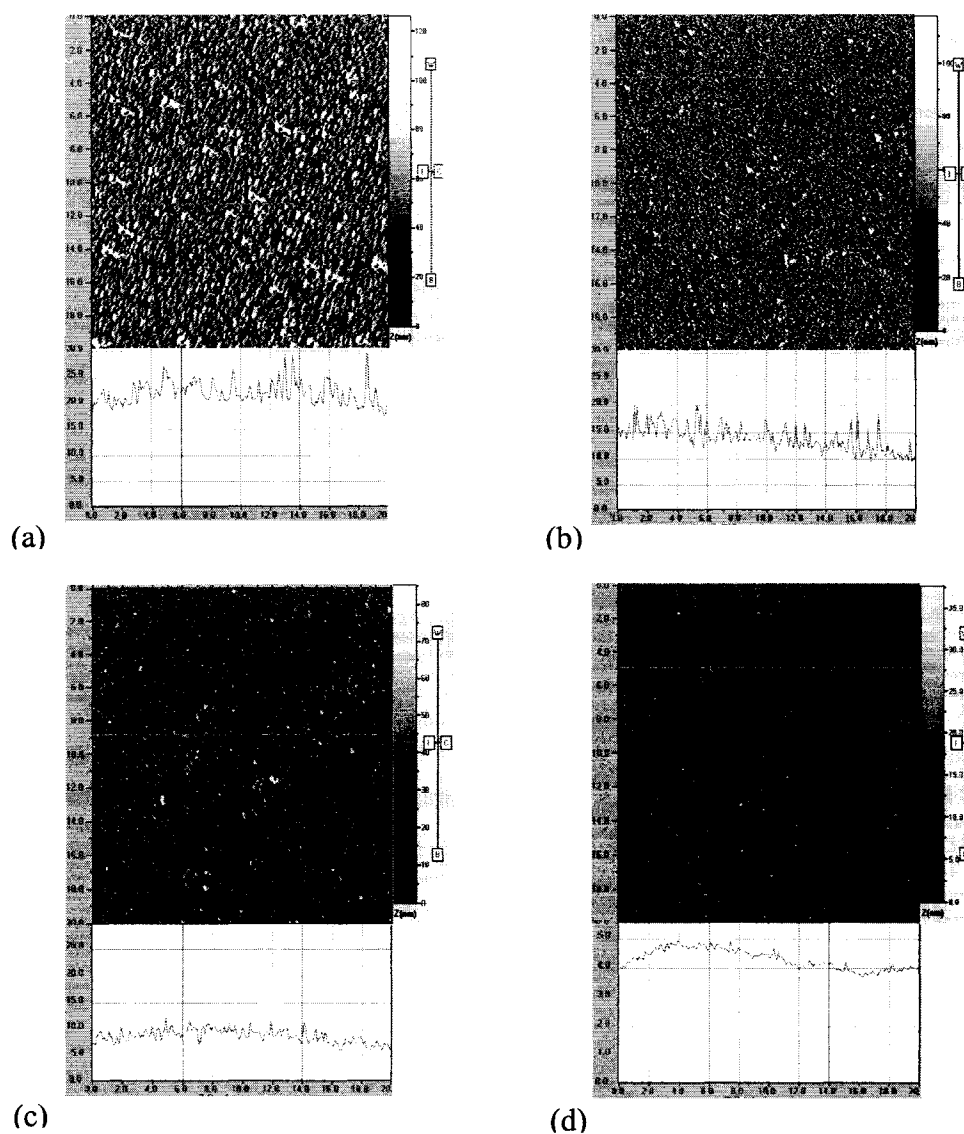


Figure 4-S2. The AFM micrographs, $20\ \mu\text{m} \times 20\ \mu\text{m}$, and roughness profiles, of 20-layer peptide films deposited at different pH values. (a) pH 8.9, (b) pH 7.8, (c) pH 7.4, and (d) Si wafer. It is clear that films prepared at higher pH have rougher surface than those at lower pH in the range of pH 7.4 to 8.9.

CHAPTER FIVE

CONTROL OF STABILITY OF POLYPEPTIDE MULTILAYER
NANOFILMS BY QUANTITATIVE CONTROL
OF DISULFIDE BOND FORMATION

5.1 Introduction

The crosslinking of polymers in a polymeric material, for example, a polyelectrolyte multilayer nanofilm (PEM), will alter mechanical properties of the material. Control over mechanical properties of PEMs could be useful for applications of the technology in medicine and other areas. Disulfide bonds are “natural” polypeptide crosslinks found widely in wild type proteins. Here, we have designed and synthesized three pairs of oppositely charged 32 mer polypeptide to have 0, 4, or 8 Cys residues per molecule, and we have characterized properties of the peptides in a PEM context. The average linear density of free thiol in the designed peptides was 0, 0.125, or 0.25 per amino acid residue. The peptides were used to make 10-bilayer PEMs by electrostatic LBL. Cys was included in the peptides to study specific effects of disulfide bond formation on PEM properties. Features of film assembly have been founded to depend on amino acid sequence, as in protein folding. Following polypeptide self-assembly into multilayer films, Cys residues were disulfide-crosslinked under mild oxidizing conditions. The stability of the crosslinked films at acidic pH has been found to depend on the

number of Cys residues per peptide for a given crosslinking procedure. Crosslinked and non-crosslinked films have been analyzed by UVS, ellipsometry, and AFM to characterize film assembly, surface morphology, and disassembly. A selective etching model of the disassembly process at acidic pH is proposed on the basis of the experimental data. In this model, regions of film in which the disulfide bond density is low are etched at a higher rate than regions where the density is high.

5.2 Experiments

Polypeptides. Three pairs of designed peptides, P0, N0, P1, N1, P2 and N2, were prepared by F-moc chemistry. Design principles of the peptides are described elsewhere [29]. The synthesis products were analyzed by mass spectrometry (Louisiana State University, Baton Rouge) and used without further purification. Designed polypeptides P0 and N0, P1 and N1, and P2 and N2 contain 0, 4, and 8 Cys residues each, respectively. The pK_a s of the Lys and Glu side chains are *c.* 10.5 and *c.* 4.3, respectively. P0, P1 and P2 will have about the same positive net charge in aqueous solution at pH 7.4, as well as N0, N1 and N2 will have about the same negative net charge at pH 7.4 (Figure 5-1). 4,000 Da PLL and 5,000 Da PLGA, from Sigma (USA), were used in control experiments.

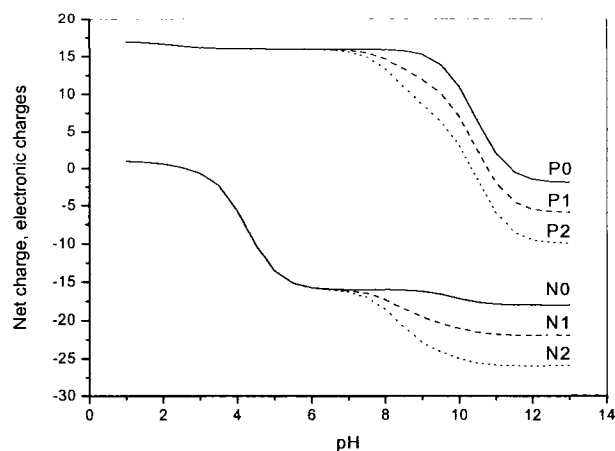


Figure 5-1. Estimated peptide net charge *versus* pH [1]. Peptides P0, P1, P2, N0, N1, and N2 all have about the same linear charge density at pH 7.4.

Multilayer film assembly, oxidization, and disassembly. Lyophilized peptides were reconstituted in 10 mM Tris, 50 mM NaCl, 0.1% NaN₃, pH 7.4, bubbled with nitrogen for 0.5 h. Final peptide concentration was 1 mg/mL. PEMs were assembled on quartz microscope slides (Electron Microscopy Sciences, USA) or N-type <100> silicon wafers (Montco Silicon Technologies Inc., USA). The substrate cleaning process is described elsewhere [28]. The substrates were immersed alternately in a solution of P0, P1, P2, or PLL, and in a solution of N0, N1, N2, or PLGA for 15 min per polymer adsorption step. The substrate was rinsed thrice in separate baths of deionized water for 2, 1, and 1 min after each peptide adsorption step and dried with nitrogen gas.

PEMs with 10 bilayers were oxidized in 10 mM Tris, 50 mM NaCl, 0.1 % NaN₃, 1 μ M MnCl₂, pH 7.4 and 40 % (v/v) dimethylsulfoxide (DMSO). Films were immersed in oxidizing solution for *c.* 48 h, rinsed with deionized. water, dried with an air gun, and left in air *c.* 40 h. This mild oxidization treatment promoted disulfide bond formation between cysteine residues [30] in P1/N1, P2/N2, P1/PLGA, and PLL/N1 films. After

oxidation, the PEMs were immersed in acidic pH solution to test film stability. The film disassembly solution was 10 mM KCl, 50 mM NaCl, 0.1 % NaN₃, pH 2.0 or 10 mM glycine, 50 mM NaCl, 0.1 % NaN₃, pH 3.0, bubbled with air for 0.5 h. At acidic pH non-crosslinked polypeptide PEMs disassemble due to deionization of acidic side chains and electrostatic repulsion between polycations [4,28,30]. The efficiency of covalent crosslinking in multilayers was assessed by determining film thickness at defined time points after initiation of disassembly. The amount of peptide retained on the substrate was estimated by UVS absorbance at 190 nm. Films were rinsed with deionized water and dried with an air gun after each disassembly step.

5.3 Results

PEM assembly. The absolute value of the net charge of P0, P1, and P2 and of N0, N1, and N2 is about the same at pH 7.4. Figure 5-2 shows that P1/N1 (4 Cys residues per peptide) and P2/N2 (8 Cys residues per peptide) show about the same UV absorbance increment per peptide deposition step. By contrast, P0/N0 (0 Cys residue per peptide but a comparatively large number of valine residues) has an absorbance increment about twice that of P1/N1 and P2/N2. Nevertheless, growth of P0/N0 with adsorption step, like that of P1/N1 and of P2/N2, is approximately linear. The inset of Figure 5-2 shows the corresponding ellipsometry data; the results are consistent: P0/N0 is thicker than P1/N1 or P2/N2. The absorbance and therefore thickness of P0/N0 is twice as large as that of P1/N1 and P2/N2, according to UVS and CD data (Figure 5-2). This reflects the more limited deposition of P1 and N1 and P2 and N2. Generally, a high linear density of charge will give a greater extent of intra-layer charge repulsion and therefore thinner layers. Cysteine, however, titrates in the mildly basic pH range, giving a combination of

positive and negative charges and slightly reducing the linear charge density in peptides P1 and P2.

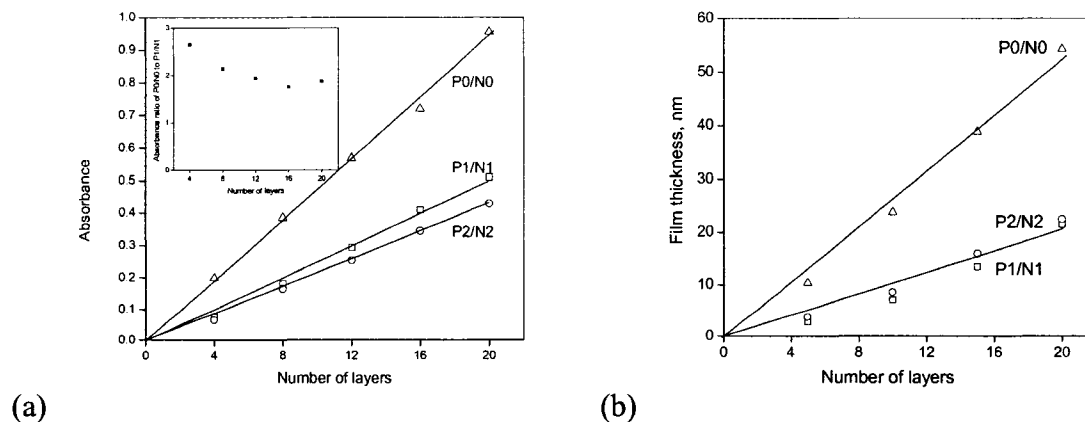


Figure 5-2. Film thickness. (a) Peptide bond absorbance at 190 nm during the assembly process. The inset shows the ratio of absorbance P0/N0 to absorbance of P1/N1. The ratio is approximately 2 for 0-10 layers. The molecular weights of P0, N0, P1 and N1 are 3719, 3733, 3567 and 3581 Da, respectively. The ratio of molecular weights of P0/N0 and P1/N1 is 2.1. (b) Ellipsometric film thickness during the assembly process. P1/N1 and P2/N2 behave similarly with regard to absorbance and thickness.

There are other differences in assembly behavior. For example, Cotton effect amplitudes vary as $P0/N0 > P1/N1 > P2/N2$ (Figure 5-3). Deconvolution of the CD spectra suggest that these films have the following respective secondary structure content: β sheet, 53.5 %, 27.1 %, and 43.4 %; β turn, 20.3 %, 26.4 % and 21.7 %; random coil, 26.2 %, 43.8 % and 30.9 %, and α helix, 0 %, 2.7 %, 3.9 %. The β sheet is predominant in P0/N0, while random coil is more abundant in P1/N1 and P2/N2. All these films show substantially more β structure than α helix. According to CD deconvolution, more than half of all residues in P0/N0 are in a β strand conformation. A β sheet can be stabilized by hydrogen bonds formed between different regions of the same molecule or different molecules.

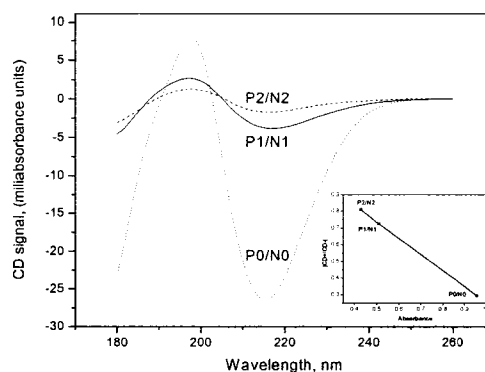


Figure 5-3. CD spectra of 10-bilayer films. The amplitudes of CD spectra follow the trend: $P0/N0 > P1/N1 > P2/N2$. In $P0/N0$ the negative Cotton effect amplitude is about 240 % larger than the positive one. On the contrary, the asymmetry of the positive and negative Cotton effect amplitudes of $P1/N1$ and $P2/N2$ is much smaller, with the negative amplitudes 39 % and 25 % larger than positive ones, respectively. The inset illustrates the correlation between CD and UVS data for $P0/N0$, $P1/N1$ and $P2/N2$. $|CD+/CD-|$ is the absolute ratio of the positive Cotton effect amplitude to negative Cotton effect amplitude for 10-bilayer films. Absorbance was at 190 nm. CD spectra are sensitive to the secondary structure of the films, which will depend on different amino acid sequences of designed polypeptides.

Further analysis of the CD and UVS spectra for $P0/N0$, $P1/N1$ and $P2/N2$ films is shown in the inset of Figure 5-3. $|CD+/CD-|$ represents the absolute value of the ratio of positive Cotton effect to negative one after baseline subtraction. Differences in this ratio are indicative of differences in internal structure of the polypeptide PEMs. UVS absorbance was measured at 190 nm. Low absorbance correlates with high $|CD+/CD-|$: extent of peptide deposition is related to film structural properties for the peptides studied here. The ratio of UV absorbance to $|CD+/CD-|$ ratio shows the trend $P0/N0 > P1/N1 > P2/N2$.

Surface morphology of $P1/N1$ and of $P2/N2$ is about the same (Supplemental information), in terms of the similar roughness and grain size. The number of cysteine residues had relatively little effect on peptides assembly. It should be noted that the

situation could be different at a higher pH value, where the probability of ionization of cysteine is greater [6].

PEM disassembly. Experiments were done to test polypeptide PEM stability following film oxidization and formation of disulfide crosslinks. Figure 5-4a shows UVS absorbance of P0/N0, P1/N1, and P2/N2 during disassembly at pH 2. P0/N0 loses nearly all its material within 0.5 h, whereas P1/N1 retains 50 % of its material after 2 h and P2/N2 shows effectively no change. There is a clear correlation between retention of material and number of Cys residue per peptide.

Figure 5-4b shows ellipsometric thickness of peptide films. Film P0/N0 loses all of its material within 15 min. Film P1/N1 loses 30 % of its thickness after 4.5 h of disassembly while P2/N2 retains nearly all of its thickness in the same time interval. The ellipsometry data are broadly consistent with the UVS results shown in Figure 5-4a. The results are consistent with the hypothesis that the number of disulfide bonds actually formed in the film is related to the number Cys residues in the film [30].

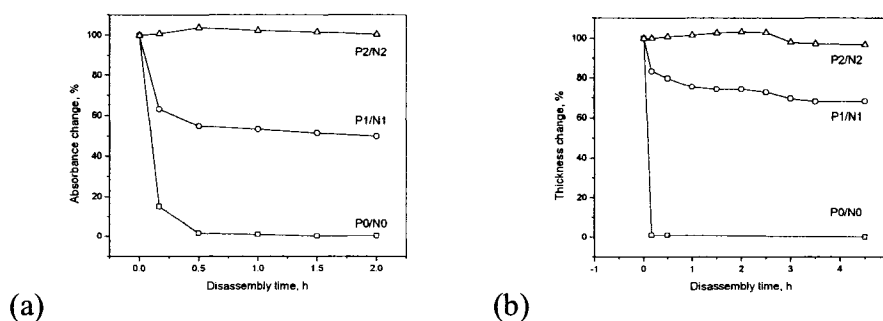


Figure 5-4. Polypeptide film disassembly in pH 2.0 KCl buffer. (a) Absorbance at 190 nm during film disassembly. Film P0/N0 loses almost all of its absorbance within 0.5 h, P1/N1 loses about 45 % of its absorbance within 0.5 h but only an additional 5 % within 2 h. P2/N2 loses practically no material on the same time scale. (b) Ellipsometric thickness during film disassembly. After 4.5 h of disassembly, P2/N2 has retained almost all its thickness and P1/N1 has lost 30 % of its thickness. P0/N0 loses all its thickness in 15 min.

Control experiments were done with 10-bilayer PEMs made of P1, N1, PLL, and PLGA. Figure 5-5 presents the assembly and disassembly behavior of these films. As shown in the inset, P1/N1 deposits the most material after 20 layers, PLL/PLGA the least. Peptide assembly is driven primarily by coulombic attraction but also hydrophobic interactions, and it is limited primarily by coulombic repulsion. Lysine and glutamic acid side chains are charged at pH 7.4; the absolute charge density of PLL or PLGA is much higher than that of P1 or N1. P1/N1, P1/PLGA, PLL/N1 and PLL/PLGA were disassembled in pH 3.0 glycine-HCl buffer. P1/N1 is the most stable film at pH 3.0. Very little mass is lost over 40 min. P1/PLGA loses 5 % of its mass while PLL/N1 loses about 10 % in 40 min. PLL/PLGA loses 45 % of its mass in the first 5 min of disassembly, and after 40 min, it loses about 55 % of its mass.

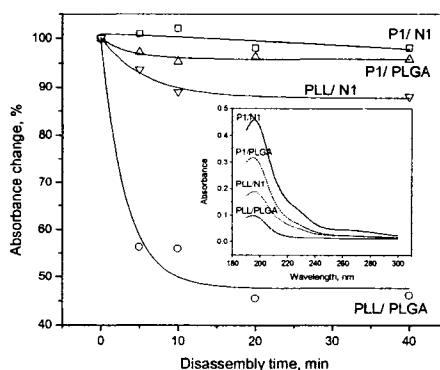


Figure 5-5. Film disassembly in pH 3.0 glycine-HCl buffer. After 40 min of disassembly, P1/N1 has almost the same mass; P1/PLGA has lost 5 % of its mass while PLL/N1 has lost about 10 %. PLL/PLGA has lost 45 % of its mass within the first 5 min of disassembly, and after 40 min, it has lost about 55 %. Time constants of film disassembly were determined by fitting the data with a first-order exponential decay model. P1/PLGA, PLL/N1 and PLL/PLGA have time constants of 5.8 min, 3.7 min, and 3.2 min, respectively. The inset shows the assembly behavior of the same four pairs of peptides. P1/N1 assembles the most material; PLL/PLGA, the least.

Disassembly of P1/N1 at pH 2.0 has also been monitored by AFM. Representative surface images and vertical scan profiles which represent surface roughness are shown in Figure 5-6. Apparent graininess decreases from *c.* 100 nm to *c.* 50 nm in “granule” diameter on film oxidization. Roughness was on the order of 6 nm. After 30 min of disassembly (Figure 5-6c), the film surface is smoother than before disassembly and graininess is less obvious. After 1 h of disassembly (Figure 5-6d), the film has a roughness on the order of 10 nm, greater than the roughness after 30 min of disassembly (Figure 5-6c, about 7 nm).

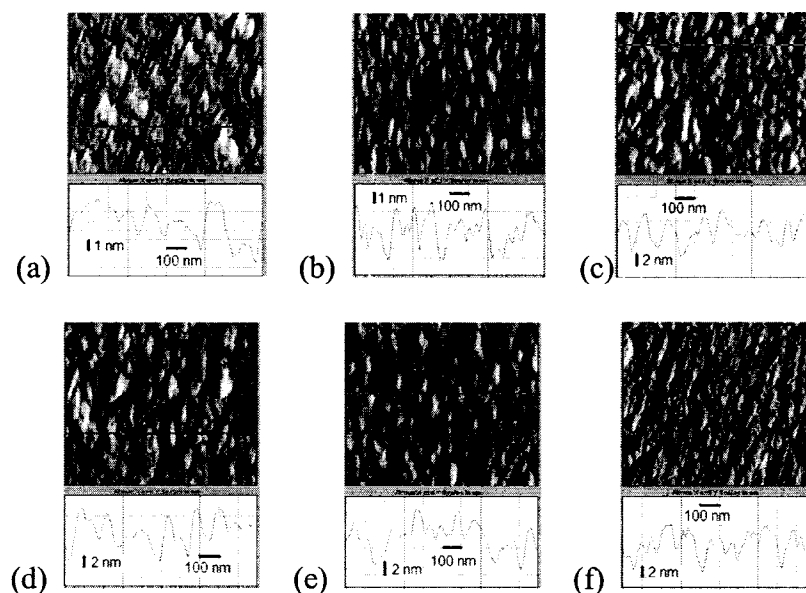


Figure 5-6. AFM images of P1/N1 during disassembly at pH 2.0. (a) After assembly, (b) After oxidation, (c) After 30 min disassembly, (d) After 1 h disassembly, (e) After 2 h disassembly, (f) After 3 h disassembly. Image dimensions are $1 \times 1 \mu\text{m}^2$, and the z-axis scales for (a)–(f) are all 24 nm. Surface roughness (from section profiles) is about 6 nm, 6 nm, 7 nm, 10 nm, 6 nm, and 8 nm, respectively.

5.4 Discussion

Films based on biopolymers or polypeptides are hydrogels; they are "soft" and sensitive materials [43,48,108,109]. Common polymers in LBL are organic homopolyelectrolytes of high water solubility but low biocompatibility [3]. Polypeptides are a type of weak polyelectrolyte with inherent biocompatibility. Polypeptides biodegrade into amino acids, essential for protein synthesis. We have used designed polypeptides to prepare LBL films [5,6,11,29,30,47]. Amino acid composition and sequence has been found to influence LBL film assembly and disassembly, providing both an explanation for observed film assembly behavior but also a foundation for the development of applications of the polypeptide PEM technology.

Effects of crossing poly(allylamine hydrochloride)/poly(acrylic acid) films by heat-induced amidation has been investigated in considerable depth by Bruening [8]. Such crosslinking provides advantages in maintaining film physical and/or chemical properties but not biofunctionality. Crosslinking can also be achieved with photo-reactive diazo-resin and sulfonate groups under UV irradiation [8]. These methods, though useful, are not as convenient as disulfide bond formation. Moreover, they are irreversible.

In previous work we have studied the stabilization of PEMs by formation of disulfide bonds [6,30,47,54]. S-S bonds are important for the stability of some native protein structures. The reversibility of S-S bond formation has been shown for peptide films [6,30,47] and microcapsules [54]. Such reversibility is potentially useful for the preparation of environemennally-responsive PEMs and microcapsules on change of redox potential. The stability of disulfide crosslinked films has been tested in various harsh physical and chemical conditions [11].

The purpose of the present study was to assess control over PEM stability by control over peptide structure and S-S bond formation. The data show that amino acid composition and sequence influence film assembly, and that the number of S-S bonds per peptide influences rate and extent of disassembly.

Film assembly. Normally, accessible surface area (ASA) can be the sum of main-chain ASA and side-chain ASA. And side-chain ASA can be the sum of nonpolar (hydrophobic) and polar (hydrophilic) side-chain ASA. The hydrophobicity/hydrophilicity of amino acids used in this experiment are shown in Table 5-1. From Table 5-1b, the hydrophobicities of designed peptides pairs follow this rule: P0/N0 > P1/N1 > P2/N2. The interactions of the peptides with water will influence assembly behavior. The more hydrophobic the polypeptide is, the less soluble it will be in a polar solvent. The side chain of valine is hydrophobic. P0 and N0, P1 and N1, and P2 and N2 have 15, 7, and 3 valine residues per molecule, respectively. The percentage of valine in P0/N0 is large enough to influence polypeptide assembly; not only the electrostatic force but also hydrophobic interactions are relevant to film formation. Two layers of peptide will form in each deposition step, as shown in Figure 5-7. This is consistent with UVS, CD, and ellipsometry showing that twice as much P0/N0 assembles as P1/N1 or P2/N2.

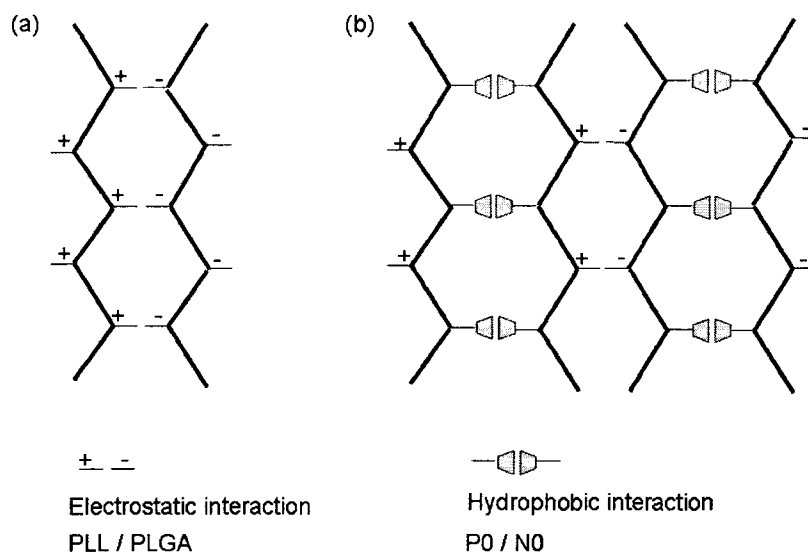


Figure 5-7. LBL assembly mechanism. (a) The main driving force in LBL is coulombic attraction, and effectively one peptide layer only is formed during each adsorption step. (b) Assembly of peptide molecules with alternating charged and hydrophobic side chains. In aqueous solvent, two peptide layers will form in each deposition step [62].

Table 5-1 Hydrophobicity/hydrophilicity* of polypeptides.

(a)

Accessible surface area and hydropathy of amino acid residues [29]						
Amino acid residue	Total (\AA^2)	Main-chain atoms (\AA^2)	Side-chain atoms (\AA^2)			Hydropathy index
			Total	Nonpolar	Polar	
Cys (C)	140	36	104	35	69	2.5
Glu (E)	183	45	138	61	77	-3.5
Gly (G)	85	85	-	-	-	-0.4
Lys (K)	211	44	167	119	48	-3.9
Tyr (Y)	229	42	187	144	43	-1.3
Val (V)	160	43	117	117	-	4.2

(b)

Polypeptide	Average surface area of side chains (\AA^2)	Fraction nonpolar	Average hydropathy	Average thiol density per residue
P0	144	0.83	-0.02	0
N0	130	0.69	0.18	0
P1	128	0.73	-0.8	0.125
N1	113	0.57	-0.6	0.125
P2	126	0.66	-1.0	0.25
N2	112	0.49	-0.8	0.25

* The hydrophilicity of the polypeptides is indicated by their average hydropathy [29].

Possibly more important, neither P0 nor N0 comprises glycine residues, whereas P1, N1, P2 and N2 have four glycine residues each. This is relevant because the peptide backbone is very flexible in the vicinity of glycine residues. During assembly process, then, the adsorption of P1, N1, P2 and N2 is less favored than that of P0 and N0 from the point of view of chain entropy. This view is consistent with early work on peptide structure in solution by Flory and colleagues [110].

Film oxidation. DMSO promotes oxidation of thiols to disulfides, the rate depending on DMSO concentration at a given temperature, and increasing DMSO in the oxidizing solution at pH 7.5 increases film stability [47]. A simpler oxidation process for S-S bond formation depends merely on the presence of atmospheric oxygen. Here, PEMs were oxidized for 40 h oxidation in 40 % DMSO at pH 7.4, and 48 h in air.

Designed polypeptides P1 and N1 have 4 Cys residues in the polypeptide chain, P2 and N2 have 8 Cys residues, and P0 and N0 have none. Presumably, during oxidization more disulfide bonds can form in P2/N2 than P1/N1, judging by the approximately equal number of molecules deposited per adsorption step and greater number of Cys residues in P2 and N2 than in P1 and N1, and no disulfide bonds can form in P0/N0. The formation of disulfide bonds is not detected directly by CD in the absence of polymer modification, but it is tested indirectly in PEM disassembly experiments, since crosslinks increase film stability and retard disintegration.

Disassembly behavior. In pH 2.0 KCl buffer, P0/N0 loses almost all of its mass and thickness after 15-30 min. The physical cause of disassembly in P0/N0 is presumably protonation of carboxylate groups in the negatively-charged peptide and electrostatic repulsion between the positively-charged peptides, leading to the disintegration of the

deposited multilayer film in the absence of crosslinking [47]. By contrast, oxidized P1/N1 (containing 4 cysteine residues) retains about 50 % more mass and 70 % thickness, and P2/N2 (containing 8 cysteine residues) retains about 100 % both of its mass and thickness under the same conditions for the same duration. S-S bonds stabilize LBL peptide films despite charge repulsion. Treatment of the film in an oxidizing solution promoted the formation of S-S bonds from free sulfhydryl groups, presumably crosslinking intralayer like-charged peptides as well as interlayer oppositely-charged peptides. [47]. When the crosslinked P1/N1 film is treated with reducing reagent and as the result the S-S bonds get broken, the film will totally disassemble within two hours [30]. By control the number of Cys residues in peptide chain, it is possible to control S-S bond formation in peptide films and film stability at acidic pH. Controlled film destruction in response to environmental pH or reducing potential may be useful in drug release and other applications in medicine.

Comparison of disassembly behavior of P1/N1, P1/PLGA, PLL/N1, and PLL/PLGA showed adjustable stability depending on extent of crosslinking. During oxidization under mild conditions, P1/N1 forms S-S bonds in 3 dimensions: with layers and between layers. P1/PLGA and PLL/N1 form S-S bonds within layers; PLL/PLGA forms no crosslinks. The stability of the peptide films followed the rule: P1/N1 > P1/PLGA \approx PLL/N1 > PLL/PLGA. The results provide further indirect evidence for the existence of disulfide bonds in the PEMs and indicate the influence on form of S-S crosslinking on film stability.

The disassembly process monitored by AFM clarifies the role of disulfide bonds in film stability. Figure 5-6 shows “smooth \rightarrow rough \rightarrow smooth \rightarrow rough” changing

procedure of P1/N1 film surface morphology, which can be expressed schematically in Figure 5-8. When a polypeptide PEM is immersed in acidic disassembly solution at pH 2.0, protuberant parts on the surface are the first to be etched away. As a result, film roughness decreases. At the same time, regions of film not connect to surrounding regions by a sufficient number of S-S bonds are etched, leaving the surface rougher. Grain size, however, decreases in this process. P2/N2 will disassemble in the same way. There is less overall change, however, in P2/N2 than P1/N1. If the crosslinked films are used in making capsules, it will retain the drug release. We can control the number of crosslinkers by design polypeptides, which will be very promising in pharmacy area.

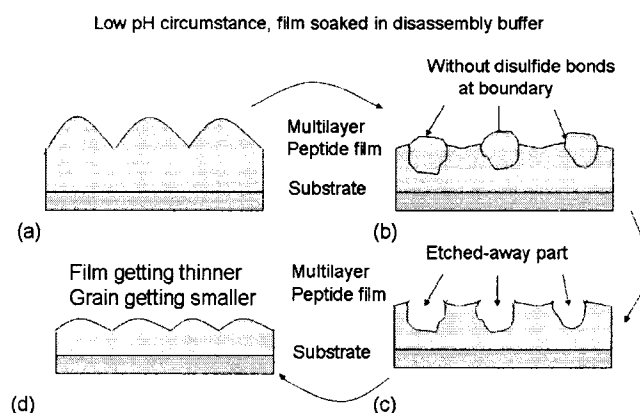


Figure 5-8. Model of disassembly Cys containing peptide PEMs. (a) LBL multilayer peptide film assembled on substrate. After oxidation, disulfide bonds form between and inside layers. (b) Film is immersed in acidic solution. The solution etches the film, firstly protuberant parts. The film becomes smoother. (c) Regions with few or no disulfide bonds are etched away. The film surface becomes rougher, but the grains become smaller as compared to (a). (d) Acidic disassembly solution etches the protuberant parts. The surface becomes smooth again.

5.5 Conclusion

Designed 32 mer polypeptides were used to fabricate LBL multilayer films, and disulfide bonds formed to strength the film stability under strong acidic circumstance.

Different amino acid components in polypeptide chain influenced the driving interaction of assembly. Both electrostatics force and hydrophobic interactions influenced a lot on the designed peptide film formation. The introduction of different number of cysteine residues in peptide chain followed by different disulfide formation mechanism (2-D or 3-D) provided a quantitative control on the film stability under strong acidic circumstance, which will have promising application in medicine usage. The crosslinked film disassembly behavior is also quite sensible to the change of pH or reducing potential.

5.6 Supplementary Information

Figure 5-S1 shows the AFM images of polypeptide films, silicon wafer substrate, and quartz slide substrate with different scanning sizes.

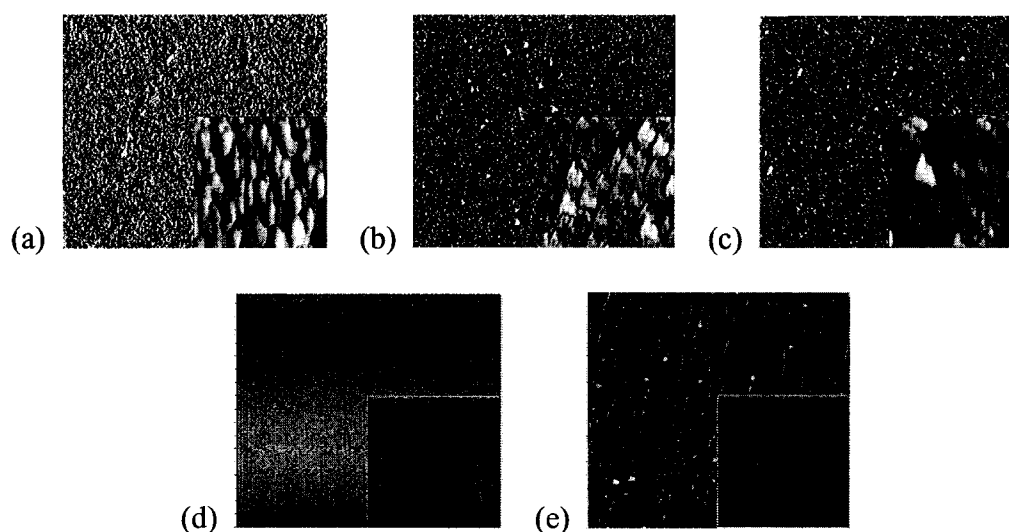


Figure 5-S1. AFM images for 20-layer polypeptide films. (a)-(c) marked with $20 \times 20 \mu\text{m}^2$ AFM images for 20-layer P0/N0, P1/N1, P2/N2 peptide films on wafer substrate with vertical scale 50 nm, 110 nm, 100 nm respectively. The insets are $1 \times 1 \mu\text{m}^2$ images with vertical scale 18 nm, 15 nm, 16 nm respectively. (d) is $20 \times 20 \mu\text{m}^2$ AFM image for clean wafer substrate with vertical scale 25 nm. The inset is $1 \times 1 \mu\text{m}^2$ image with vertical scale 7 nm. (e) is $20 \times 20 \mu\text{m}^2$ AFM image for clean quartz slide with vertical scale 30 nm. The inset is $1 \times 1 \mu\text{m}^2$ image with vertical scale 10 nm.

CHAPTER SIX

CONTROLLED LOADING AND RELEASE OF
A MODEL DRUG FROM POLYPEPTIDE
MULTILAYER NANOFILMS

6.1 Introduction

When the main driving force in LBL for adsorption of species from solution is electrostatic interaction (combined with a gain in entropy on release of counterions to solution), the accessibility of ionic groups on the film surface will be crucial for film buildup. Hydrogen bonds and hydrophobic interactions too can influence LBL multilayer film assembly [27,111,112]. Polymers in adjacent layers of a polyelectrolyte multilayer film interpenetrate [113,114]. Various physical properties of these films are potentially useful for drug loading and release [55].

The amino acid subunits are joined by peptide bonds. Essentially planar and less flexible than an ordinary covalent bond, the peptide unit has both a hydrogen bond donor and an acceptor, contributing to secondary structure formation both in aqueous solution and in the condensed state. Structural properties of polypeptides also provide possibilities for encapsulation and controlled release of chemical compounds in biological or medical applications; for example, linear charge density, immunogenicity [29], susceptibility to enzymatic digestion, antimicrobial activity [115], and film density, surface morphology,

stability, and susceptibility to environmental perturbation [5] can be influenced by peptide design [3]. Polyelectrolyte multilayer films can be modified to have microporous or nanoporous structure by treatment in a harsh environment, for instance, immersion in a strong acid or base or subjection to high temperature, increasing the duration of release of large molecular weight drugs (e.g., ketoprofen and cytochalasin D) from hours to days [116].

The model encapsulant MB, a monovalent cation of 373.9 Da molecular weight, is known as a useful mediator of electrocatalysis/electron-transfer [117,118]. Important for the present work, MB is highly soluble and it has an absorption peak in the visible range. MB has been used to model drug loading in and release from polypeptide multilayer films prepared by LBL under different conditions. Loading and release behavior of MB and film surface morphology have been characterized [119].

6.2 Experiments

Materials. Poly(L-lysine) (“PLL”) with molecular weight 84.0 kDa (vis) , 97.8 kDa (vis) poly(L-glutamic acid) (“PLGA”), 4.0 kDa (vis) poly(L-lysine) (“PLL-S”) and 5.0 kDa (vis) poly(L-glutamic acid) (“PLGA-S”) were from Sigma (USA) and used without further purification. The polypeptides (KVKGKCKV)₃KVKGKCKY (“P1”), (EVEGECEV)₃ EVEGECEY (“N1”), (KV)₁₁KY (“P3”), and (EV)₁₁EY (“N3”) were prepared by solid-phase synthesis. The synthesis products were analyzed by mass spectrometry (Louisiana State University, Baton Rouge) and used without further purification. The linear charge density of PLL-S or PLGA-S was considerably larger than that of P1 or N1 at pH 4.0, pH 5.5 or pH 7.4 (Figure 6-1).

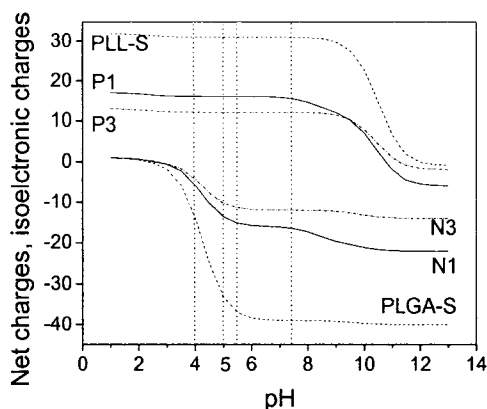


Figure 6-1. Comparison of calculated net charge of polypeptides in solution. The net charge of PLL-S and of PLGA-S is comparatively large at pH 4.0, 5.0, 5.5 and 7.4. The charge density will be somewhat different in a multilayer film: the increased presence of oppositely charged groups results in a shift of pKa.

Film assembly. Lyophilized polypeptides were dissolved in assembly buffer (10 mM Tris, 10 mM sodium acetate, 130 mM NaCl, 0.1 % NaN₃, pH 4.0, pH 5.0, pH 5.5, or pH 7.4). The final peptide concentration was 2 mg/mL. Polypeptide multilayer films were assembled on quartz microscope slides (Electron Microscopy Sciences, USA) by LBL [3,12,28]. Substrates were immersed alternately in a solution of PLL, PLL-S, P1, or P3 followed by a solution of PLGA, PLGA-S, N1, or N3, for 15 min per polypeptide adsorption step. After each peptide deposition step, the film was rinsed thrice in separate baths of deionized water for 2 min, 1 min, and 1 min and dried with nitrogen gas. 10.5-bilayer polypeptide films of PLL/PLGA were assembled at pH 4.0, 5.5, or 7.4. In some cases, (PLL/PLGA)_{*n*} capping layers were assembled at pH 7.4 on (PLL/PLGA)_{5.5} 5.5-bilayer films assembled at pH 4.0, where *n* is 0, 0.5, 2.5, or 4.5. 10.5-bilayer PLL-S/PLGA-S films were assembled at pH 4.0; 10.5-bilayer P1/N1 films were assembled at pH 5.5; 10.5-bilayer P3/N3 films and P3/PLGA-S films were assembled at pH 5.0. The surface area of each film was about 2 cm².

MB loading and release. MB (Sigma) was dissolved in 50 % (v/v) assembly buffer and ultrapure water, and the pH was adjusted to 7.4. The final concentration of MB was 10^{-3} M. Films were immersed in MB solution for 15 min for small molecule loading [55]. Then films were rinsed and dried as described for film assembly. Release of MB was tested by immersion of a loaded film in 40 mL assembly buffer at pH 7.4, pH 5.5, or pH 4.0, or in 40 mL deionized water at pH 7.4 or pH 5.5. Films loaded with MB were immersed in release medium, and the medium was stirred with a 10 mm magnetic stirring bar at 60 rpm. The release medium was replaced every 2 h to ensure efficiency of MB release.

Film characterization. Polypeptide multilayer film absorbance spectra were recorded with a Shimadzu UV-1650 PC UV-Vis (UVS) spectrophotometer (Japan) in the range 190-800 nm. MB in films has an absorbance peak in the range 560-610 nm; a shoulder is evident around 665 nm. MB absorbance spectra in release media were recorded in range 500-800 nm. The path length was 1 cm. The concentration of MB in solution ranged between 10^{-6} and 10^{-5} M and was quantified by the Beer-Lambert law with an extinction coefficient of $7850 \text{ M}^{-1} \text{ mm}^{-1}$ at 665 nm [55]. AFM was used to characterize film surface morphology and roughness at the nanometer scale. Surface scanning was done in tapping mode with a Q-scope TM 250 scanning probe microscope (Quesant Instrument Corp., USA).

6.3 Results

Influence of pH on film assembly. PLL/PLGA films were assembled at pH 4.0, pH 5.5 or pH 7.4. Optical thickness of the films followed the trend: pH 7.4 > pH 5.5 > pH 4.0 (Figure 6-3). PLL and PLGA have the same linear charge density as PLL-S and PLGA-S under given conditions. PLGA titrates at acidic pH: the pKa of the Glu side chain is *c.* 4.3, while that of the Lys side chain is *c.* 10.5 [1]. At pH 4.0, PLGA (or PLGA-S) is partially charged and PLL (or PLL-S) is fully charged. At pH 7.4, both PLL-S and PLGA-S are approximately fully charged. The charge density of PLGA-S increases by over 100 % as the pH increases from 4 to 7.4, whereas the net charge of PLL-S is approximately constant in the same range (Figure 6-1).

Kinetics of MB loading. PLL/PLGA assembled at pH 4.0 was used to assess the kinetics of MB loading. The absorbance peak at 572 nm of MB in the film increased with loading time. After *c.* 15 min, MB loading reached saturation (Figure 6-2). The saturation time for MB loading will scale with PEM thickness [55]. The defined MB loading time, 15 min, was apparently sufficient for (PLL/PLGA)_{5,5} films to reach capacity for loading MB.

Influence of pH on MB loading. pH had a marked influence on MB loading efficiency. An MB absorbance peak was detected in the pH 4.0 PLL/PLGA film but not in the pH 7.4 film or the pH 5.5 film (inset of Figure 6-3). When compared with Figure 6-2, film thickness was least when the polypeptide charge density during assembly was highest (Figure 6-3). PLGA was partially charged at pH 4.0 but nearly fully charged at pH 5.5 and pH 7.4 (Figure 6-1). Free carboxylic acid groups will bind positively charged MB molecules [55]. There are almost no carboxylic acid groups in pH 5.5 and pH 7.4 films,

except ones due to thermal fluctuations, and therefore practically no MB binding sites.

There are numerous carboxylic acid groups in the pH 4.0 films.

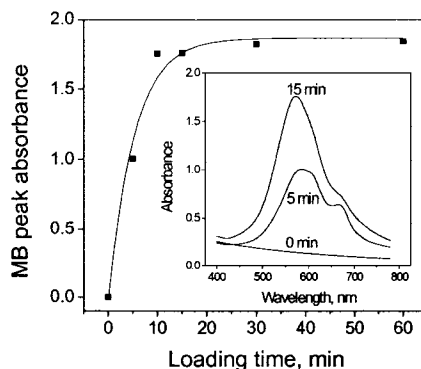


Figure 6-2. Loading with MB at pH 7.4 of PLL/PLGA assembled at pH 4.0. Inset, UVS spectra of PLL/PLGA during loading process. The peak at 572 nm is attributable to MB. The film is loaded to 90 % of capacity within 15 min. MB loading is saturated by 30 min. The time constant for MB loading at ambient temperature, 5.3 ± 1.0 , was determined by fitting experimental data with a first order exponential decay model.

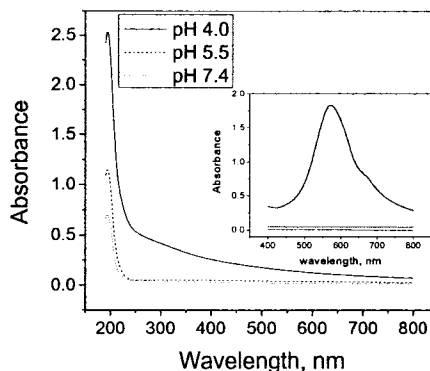


Figure 6-3. Absorbance spectra of PLL/PLGA before loading with MB. PLL/PLGA assembled at pH 4.0, pH 5.5, and pH 7.4, respectively. Absorbance at 190 nm follows the trend: pH 4.0 > pH 5.5 > pH 7.4. Inset, absorbance spectra of the films after MB loading. A typical MB absorbance peak is visible at about 570 nm in the pH 4.0 film. By contrast, the films assembled at pH 5.5 and pH 7.4 show no MB peak.

Influence of film composition on MB loading. Figure 6-4 shows absorbance spectra of the assembly and loading behavior of 10.5-bilayer films fabricated from PLL,

PLL-S, PLGA, PLGA-S, P1, N1, P3, and N3. MB absorbance peak magnitudes are tabulated in Table 6-1. MB absorbance at 572 nm varied as PLL/PLGA > P3/PLGA-S > PLL-S/PLGA-S > P3/N3 > P1/N1. The peak at 190 nm, due to peptide bond absorbance, followed the trend: P3/PLGA > PLL/PLGA > P1/N1 > P3/N3 > PLL-S/PLGA-S. Loading efficiency, calculated as the ratio of absorbance value at 572 nm to that at 190 nm, varied as: PLL/PLGA > PLL-S/PLGA-S > P3/PLGA-S > P3/N3 > P1/N1.

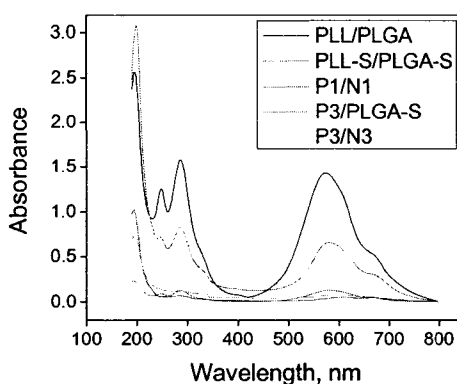


Figure 6-4. Absorbance spectra of 10.5-bilayer films of PLL/PLGA, PLL-S/PLGA-S, P1/N1, P3/N3 and P3/PLGA after loading of MB. See Table 1 for pH of assembly. The absorbance peak at 572 nm indicates the amount of MB loaded, while absorbance at 190 nm indicates the amount of polypeptide deposited. Table 6-1 presents details of the spectra.

Table 6-1 Assembly and loading comparison of polypeptide multilayer films.

	PLL/PLGA	PLL-S/PLGA-S	P1/N1	P3/N3	P3/PLGA-S
Assembly pH	4.0	4.0	5.5	5.0	5.0
Peptide bond absorbance (A_{190})	2.38	0.22	0.97	0.67	2.46
MB peak absorbance (A_{572})	1.42	0.12	0.05	0.07	0.64
A_{572} / A_{190}	0.60	0.55	0.05	0.10	0.26

The PLL/PLGA film assembled at pH 4.0 was rougher than ones assembled at pH 5.5 or pH 7.4 (Figure 6-5a~5c). The average feature size of structures on the surface of PLL-S/PLGA-S at pH 4.0 was about 50 nm (Figure 6-5d), while that of PLL/PLGA was about 150 nm (Figure 6-5a). The surface roughness of PLL-S/PLGA-S was approximately 6 nm, more than 3-fold smaller than that of PLL/PLGA. The polyelectrolyte chains in PLL/PLGA are relatively long; they might cluster together and form globular structures on the film surface. The molecular weight of the polymers in PLL-S/PLGA-S was only 5 % of those in PLL/PLGA. The PLL-S or PLGA-S molecules might prefer to adopt a regular conformation in the film, consistent with a previous study of polypeptides having a low degree of polymerization [29]. P1/N1 also had a very smooth surface (Figure 6-5e). The designed peptides P1 and N1 seemed to stick to each other and form a uniform surface during assembly. Disulfide bonds will form between polymers in this film under oxidizing conditions (for example, exposure to air), and this could influence grain size. MB is small in comparison to PLL, PLGA, P1 and N1 molecules, only 373.9 Da. Surface roughness per se is not likely to affect MB binding, because MB molecules are small enough to pass through defects in the multilayer films, but a large surface roughness could represent a large film surface area and therefore a large number of MB binding sites.

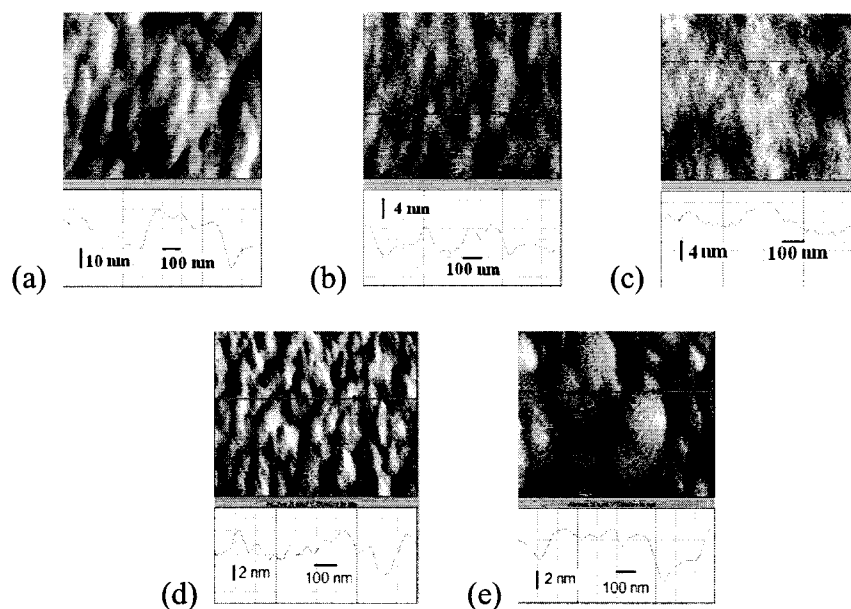


Figure 6-5. AFM images of 10.5-bilayer polypeptide films. (a) PLL/PLGA assembled at pH 4.0. (b) PLL/PLGA assembled at pH 5.5. (c) PLL/PLGA assembled at pH 7.4. (d) PLL-S/PLGA-S assembled at pH 4.0. (e) P1/N1 assembled at pH 5.5. Surface roughness (from section profiles) from (a) ~ (e) is about 20 nm, 12 nm, 8 nm, 6 nm, and 4 nm, respectively.

Influence of capping on film and MB loading. Capping films of $(\text{PLL/PLGA})_n$ (where n represents 0, 0.5, 2.5, or 4.5) were assembled at pH 7.4 on top of $(\text{PLL/PLGA})_{5.5}$ films assembled at pH 4.0. Figure 6-6a shows that an increase in number of capping layers in a limited range contributed to an increase in optical thickness. For 4.5 capping bilayers, the absorbance was smaller than for 2.5 capping bilayers. The reason might be that in the elementary films, the PLGA layers are partially charged, but after immersed in pH 7.4 solution, PLGA becomes deprotonated, leading to structural reorganization of molecules in the film and a change in optical properties. PLGA molecules will repel each other more strongly at pH 7.4 than at pH 4.0 due to the increase of linear charge density. As a result, some peptide molecules are lost in solution, giving a thinner film and reduced optical thickness.

Loading time was increased to 1 h to test the loading of MB into films with capping layers. The absorbance peak at 572 nm in a (PLL/PLGA)_{5.5} film shows that MB was present (Figure 6-6b). By contrast, no MB absorbance peak is seen in the spectra curves of capped films (PLL/PLGA)_{5.5}+PLL, (PLL/PLGA)_{5.5} +(PLL/PLGA)_{2.5} and (PLL/PLGA)_{5.5} + (PLL/PLGA)_{4.5} (Figure 6-6b). That is to say, addition of capping layers following the procedure outlined here reduced the ability to load MB, either by blocking entry of MB or by changing the properties of the basic films in the process of depositing the capping layers.

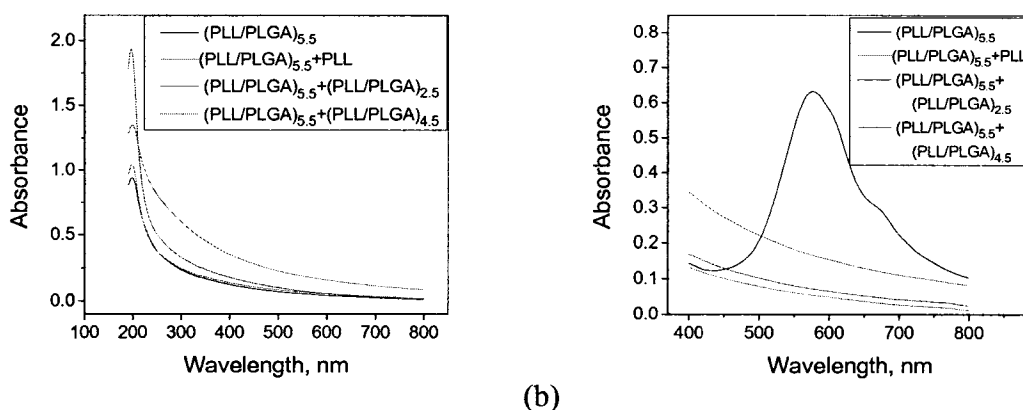


Figure 6-6. Absorbance spectra of polypeptide films with different numbers of capping layers. (a) Absorbance spectra before loading. (b) Absorbance spectra after 1 h of MB loading. (PLL/PLGA)_{5.5} represents a 5.5-bilayer base film assembled at pH 4.0. All capping layers were assembled at pH 7.4. +PLL represents one PLL capping layer. +(PLL/PLGA)_{2.5} and +(PLL/PLGA)_{4.5} represent 2.5 and 4.5 capping bilayers, respectively.

MB release. PLL/PLGA films assembled at pH 4.0 were loaded with MB at pH 7.4. When a PLL/PLGA film was immersed in deionized water at pH 5.5, MB particles gradually diffused out of the film, leading to an increase in absorbance of the surrounding medium in the visible range (Figure 6-7a). The primary absorbance peak of MB in aqueous solution is close to 665 nm; there is a shoulder at ~605 nm (Figure 6-7b)

[55,120]. The amount of MB in release solution was quantified. After 5 h, the amount of MB in the release medium had reached saturation. The time constants for MB loss in the film and MB increase in pH 5.5 deionized water, determined by fitting experimental data with a first-order exponential decay model, were 0.80 ± 0.10 h and 0.71 ± 0.02 h, respectively (Figure 6-7).

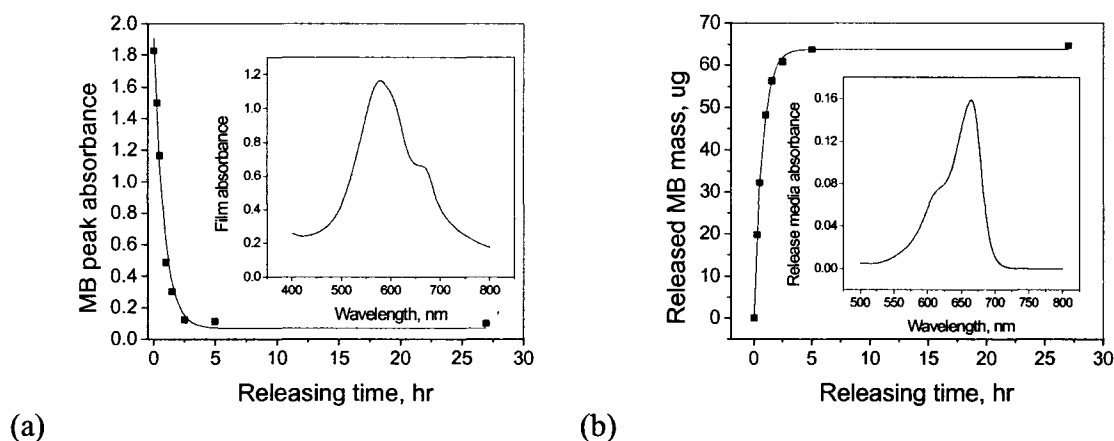


Figure 6-7. MB release in pH 5.5 deionized water from PLL/PLGA assembled at pH 4.0. (a) MB in film as a function of time. (b) Kinetics of release of MB into pH 5.5 deionized water. Insets, spectra of film and release medium after 30 min of release, respectively. The time constants for MB loss from film and MB increase in pH 5.5 deionized water were 0.80 ± 0.10 h and 0.71 ± 0.02 h, respectively, as determined by fitting experimental data with a first-order exponential decay model. Agreement is good. The difference in MB spectra may reflect differences in electronic environment between film and aqueous solution.

Controlled MB release. The fitted time constants for MB release from PLL/PLGA films in pH 4.0, pH 5.5 and pH 7.4 buffer, were 0.41 ± 0.11 , 0.88 ± 0.06 , and 1.63 ± 0.05 min, respectively (Figure 6-8a). The time constants for MB release for PLL/PLGA films in pH 5.5 and pH 7.4 deionized water were 0.89 ± 0.12 , and 8.6 ± 2.5 h, respectively (Figure 6-8b). MB release in buffer was much faster than in deionized water; lower pH too will increase the release rate.

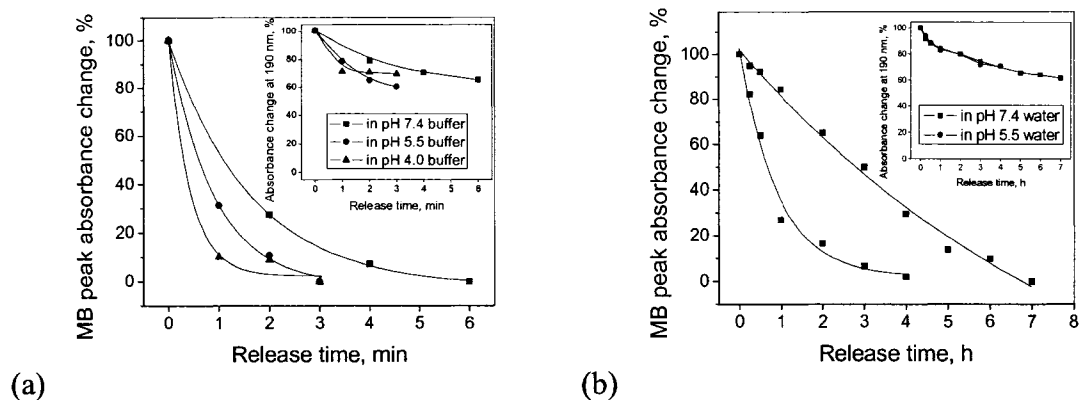


Figure 6-8. Release of MB into different media from PLL/PLGA assembled at pH 4.0. (a) Release into pH 4.0, pH 5.5 and pH 7.4 assembly buffer (timescale of min). The release rate follows the trend: pH 4.0 buffer > pH 5.5 buffer > pH 7.4 buffer. The time constants are 0.41 ± 0.11 min, 0.88 ± 0.06 min, and 1.63 ± 0.05 min, respectively. (b) Release into pH 5.5 and pH 7.4 deionized water (timescale of h). The time constants are 0.89 ± 0.12 h and 8.63 ± 2.52 h, respectively. Insets, apparent disassembly of film during MB release process as assessed by absorbance at 190 nm.

Measurement of film absorbance at 190 nm provided complementary information on film disassembly during the MB release process. The inset of Figure 6-8a shows that when MB release was complete, after 3 min in pH 4.0 or pH 5.5 buffer and after 6 min in pH 7.4 buffer, film mass was about 70 %, 60 %, and 65 % of the value before release, respectively, as assessed by the change in optical thickness of the films at 190 nm. The inset of Figure 6-8b shows that after depletion of MB from the films, 4 h in pH 5.5 water and 7 h in pH 7.4 water, the films retained 70 % and 62 % of their mass, respectively. The immersion of a film into release medium and the release of MB influenced film stability. For films assembled at pH 4.0 and MB molecules loaded at pH 7.4, when the films were immersed in release medium at different pH values, especially 4.0 and 5.5, MB gradually diffused into the surrounding liquid. This contributed to breakage of electrostatic interactions between MB and the carboxylic acid groups of PLGA. Intermolecular

interactions in the films reorganized throughout the film on the increase in density of negative charges. It would appear that some film disassembly occurs in the process.

Peptide and MB binding competition. Apparently, no MB remained in the film following the capping process (Figure 6-9). When a film loaded with MB was immersed into the peptide assembly solution for capping, MB quickly diffused into the surrounding medium, similar to the release of MB in pH 7.4 buffer (Figure 6-8a). Even when the assembly solution for capping was changed by increasing the MB concentration from 0 mM to 20 mM and decreasing NaCl concentration from 130 mM to 10 mM, MB molecules were still depleted from the film within 15 min during cap assembly. Figure 6-9 shows that although no MB remained in the film after capping, the absorbance at 193 nm increased from 1.58 to 1.72. This implies that PLL adsorbed onto the film surface in capping process. PLL was absorbed first in the capping process, because PLGA is negatively charged and will draw positively charged MB out of film.

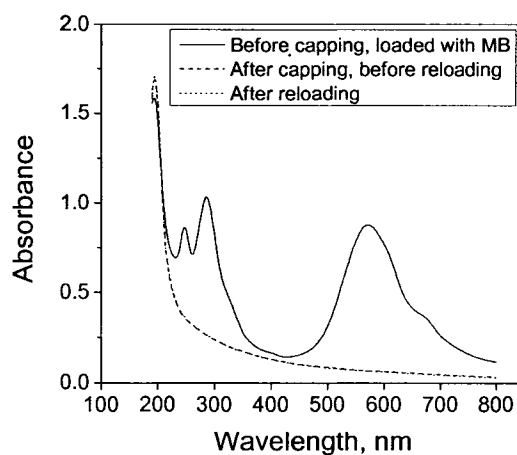


Figure 6-9. PLL/PLGA spectra before and after capping. “After reloading” represents the same film after capping and after attempted reloading with MB. The last two spectra are virtually identical.

Figure 6-9 also shows that the film spectra for before and after MB “reloading” were practically identical. In the capping process, there is a competition for binding sites between large PLL molecules and small MB molecules. Each PLL molecule has many more binding sites than a single MB molecule, so PLL will bind greater affinity than MB. In the capping process, PLL will replace MB and occupy many of its binding sites. As a result, MB molecules are released into solution. Once a PLL molecule has adsorbed onto the film surface, it will be difficult to release it. In the subsequent MB reloading process, MB didn’t bind because there were essentially no free carboxylate groups.

6.4 Discussion

Rubner and colleagues have done extensive research on the LBL assembly of conventional weak electrolytes, e.g., PAA and PAH [37,55,116,121]. The linear charge density of a weak polyelectrolyte will be sensitive to the pH of the environment. The pK_a of ionizable groups too will change with the local electronic environment, for example, aqueous solution versus film [103]. Polypeptides are weak polyelectrolytes [3]. Some designs of polypeptide are suitable for LBL [29]. One can control multilayer film thickness, surface morphology, secondary structure, covalent bond density (e.g., disulfide bonds), etc, by control over peptide design [4-6,30]. Polypeptide multilayer films have not only the properties of other weak electrolyte but also unique properties [3]. The design of polypeptides for LBL enables control over the physical and chemical properties of multilayer nanofilms. One application of such films is drug release in a biomedical context. The present work examined the loading and release of a model drug, MB, from polypeptide multilayer films.

Influence of polypeptide structure on film assembly. Film assembly can be controlled by design of polypeptides [27,62]. Polymer linear charge density can be controlled by design of peptide structure, which will influence not only the driving force for multilayer film assembly but also the number of model drug binding sites. The mass of peptide deposited on the film was $P3/PLGA > PLL/PLGA > P1/N1 > P3/N3 > PLL-S/PLGA-S$, according to absorbance at 190 nm (Figure 6-4). The linear charge density of P1, N1, P3 or N3 was less than one half that of PLL-S or PLGA-S (Figure 6-1). The electrostatic force repelled molecules of the same sign of charge, limiting the amount of polymer deposited per layer. P1/N1 and P3/N3 deposited more mass than PLL-S/PLGA-S. At the same time, 10-fold more material was deposited for PLL/PLGA than PLL-S/PLGA-S. The PLL and PLGA molecules were more than 20 times more massive than the PLL-S and PLGA-S molecules. Not only linear surface charge density but also chain length will affect polypeptide assembly behavior in an LBL context [3,4]. The longer a polypeptide molecule, the easier for it to attract oppositely charged polypeptides, form a complex with oppositely charged peptides on the film instead of returning to the solution, form a structure of irregular conformation, and increase surface roughness, especially when the linear charge density is high. Similar reasoning helps to explain why P1/N1 assembled 45 % more mass than P3/N3. P3/N3 with 24 mer length were shorter than 32 mer P1/N1, resulting in a poorer assembly behavior. Furthermore, glycine residues in P1/N1 increase the flexibility of peptide chain and decrease the odds of adsorption from the point of view of entropy. P3/PLGA, which deposited the most mass on the substrate, is an exception: P3 aggregates in solution, as close to 50 % of the residues are valine residues; the hydrophobic side chains of valine residues drive the P3

molecules together, sequestering hydrophobic groups from the polar solvent [122], as well as keeping the hydrophilic groups of other residues pointing outside to the environment.

Influence of polypeptide architecture on MB loading. Positively charged MB molecules can penetrate into a polyelectrolyte multilayer film and bind carboxyl groups of polypeptides by coulombic attraction. The pH value of peptide deposition has a strong influence on MB loading. Design of peptide sequence and careful choice of experimental conditions, e.g., ionic strength, pH value, enable control over multilayer film optical thickness and other properties [4,6,28]. Such experimental data provide clues on how to achieve precise control over the amount of drug loaded.

The amount of MB loaded in a film based on absorbance at 572 nm followed the trend: PLL/PLGA > P3/PLGA-S > PLL-S/PLGA-S > P3/N3 > P1/N1. The ratio of absorbance at 572 nm to at 190 nm followed the trend: PLL/PLGA > PLL-S/PLGA-S > P3/PLGA-S > P3/N3 > P1/N1, providing a sense of MB loading efficiency. PLL/PLGA and PLL-S/PLGA-S showed about the same loading efficiency, 59.7 % and 54.5 %, respectively. PLGA and PLGA-S have about the same linear charge density at pH 4.0 and, therefore, about the same binding site percentage for MB. The binding efficiencies of P1/N1 and P3/N3 were 5.1 % and 10.4 %, respectively—much smaller than for PLL/PLGA or PLL-S/PLGA-S. The linear charge density of N1 and of N3 was less than one half that of PLGA in the present work. Most of the charged side chains in P1/N1 or P3/N3 (K or E) will have contributed to LBL assembly, leaving few free binding sites for MB loading. The MB loading efficiency of P3/PLGA-S was 26 %, about one half that of PLL-S/PLGA-S. The linear charge density of P3 was about 1/3 that of PLL-S (Figure

6-1). The net film charge will be neutral after each deposition step by the condition of electroneutrality. In order to balance the charge of PLGA-S deposited in a previous layer, P3 will deposit about twice as much mass as PLL-S. As a result, the percentage of PLGA-S in P3/PLGA-S was about one half that in PLL-S/PLGA-S, and therefore the MB loading efficiencies were different (26 % in P3/PLGA-S and 54 % in PLL-S/PLGA-S).

Capping layers. Chung and Rubner (2002) have studied capping layers of PAA/PAH assembled at pH 6.5 on a 10.5-bilayer PAA/PAH multilayer film assembled at pH 2.5. It was found that one capping layer could permit some amount of MB to load into the underlying film. In present work, the capping layers $(\text{PLL/PLGA})_n$ were assembled at pH 7.4 on $(\text{PLL/PLGA})_{5.5}$ films assembled at pH 4.0, where n was 0, 0.5, 2.5, or 4.5. When PLL was the outermost layer of basic film at pH 4.0, it was necessary to start the capping process at pH 7.4 with a layer of PLL [55,121]. One layer only of PLL ($n=0.5$) could effectively blocked the loading of MB into the base film (Figure 6-6) in a 1 h loading period. PAA, PAH, PLL and PLGA are different weak polyelectrolytes; the linear charge density shows a marked dependence on pH. PLL and PLGA are polypeptides, which can be metabolized into amino acids, the essential precursors of protein synthesis. PLL and PLGA can form secondary structure in a multilayer polypeptide film [123].

Controlled release. The rate of MB release increased with decreasing pH, apparently due to changes in electrostatic interactions (Figure 6-8). Electrostatic interactions between MB and the carboxylate groups of PLGA were broken with decreasing pH, as carboxylate groups converted to carboxylic acid groups. Free positively charged MB molecules will repel each other and diffuse out of a multilayer film. The

release rate of MB was greater in buffered solution than in water (Figure 6-8). Ions within the buffered solution shielded charges within PLL/PLGA, weakening electrostatic interactions between MB molecules and carboxylate groups and allowing the MB molecules to freely diffuse from the film. It is also possible that the charge shielding further swelled the film. Both effects will tend to increase the release rate of MB. There was little difference between our results and those of Chuang and Rubner (2002), suggesting that with regard to the small molecular weight of cationic MB molecules, film architecture has a relatively minor impact on release rate. Film architecture is likely to be a more important factor in drug release when the size of the encapsulant is comparable to the size of film pores. Nevertheless, polypeptide coatings present advantages over conventional polyelectrolyte coating with regard to biocompatibility and environmental benignity.

The stability of a polypeptide multilayer film with regard to temperature, pH, ionic strength, solvent, and so on, will influence drug release rate [3]. Drug release and film degradation has been investigated with poly(β -amino ester) and polysaccharides [124] or polyamine [59]. In the present work, MB release attached PLL/PLGA film structuring and degradation. The rate of film corrosion was much faster in buffer than in D.I. water (minute *versus* hour). A decrease in the pH of the release medium resulted in broken electrostatic interactions between MB and the carboxylate groups of PLGA, as well as conversion of carboxylate groups to carboxylic acid groups, resulting in diffusion of MB out of the film. The rearrangement of charged groups inside the film will influence film integrity. When the release occurs in buffer, ions and counter ions of the buffer solution will shield weakened electrostatic bonds between MB molecules and carboxylate

groups or, allowing the MB molecules to diffuse freely from the film. At the same time, the ions and counter ions will swell the film structure by making polypeptides more coiled, and they will also replace the positions of carboxylate group or MB frequently by thermodynamic movements. All the above factors contributed to the degradation of multilayer films. Once the films had degraded, the loaded drugs could not remain on the film. Film degradation thus influenced drug release rate.

6.5 Conclusion

Both commercial and designed polypeptides were used to fabricate multilayer films by LBL. MB, a cationic drug indicator, was loaded into the films. The amount of MB loaded and the rate of MB release were controlled by the choice of polypeptide film species, pH, number of capping layer and release medium. Lower pH and the existence of salt ions in release medium could accelerate the release of MB.

CHAPTER SEVEN

REDOX-STIMULATED RELEASE OF SMALL MOLECULES FROM POLYPEPTIDE MULTILAYER NANOCOATINGS

7.1 Introduction

LBL has been used for a variety of purposes in surface modification, including optical coatings, contact lens coatings, anti-microbial coatings, and cell culture coatings. A polypeptide multilayer coating is simply a multilayer coating made of polypeptides [3,123]. Key features of such coatings are biodegradability, biocompatibility, and environmental benignity. The physical, chemical, and biological properties of a polypeptide multilayer coating can be controlled by polypeptide design, coating architecture, coating fabrication method, and post-fabrication processing. For example, Cys residues can be introduced into a polypeptide chain by amino acid sequence design, and following multilayer coating fabrication by LBL, intra- and inter- layer disulfide bonds will be formed between Cys residues on exposure of the coating to an oxidizing agent, increasing coating stability [6,11,12,30,47]. Other physical properties of polypeptide multilayer coatings, e.g., thickness, refractive index, and surface morphology, can be controlled by degree of polymerization, salt concentration, and pH [4,5,28].

It has been proposed that multilayer coatings could be useful for drug delivery, for example, from implant devices such as stents [125,126]. In one approach, model drugs are loaded into the coating after fabrication, and the compound is released by diffusion [55,116]. In another approach, model drug microcrystals are encapsulated within a multilayer coating for subsequent release [58,127,128]. Here, the small DTNB molecules have been conjugated to Cys containing 32 mer polypeptides, the peptides have been incorporated into a multilayer film by LBL, and TNB molecules have been released from the polypeptide multilayer film by a change in redox potential. DTNB, also known as Ellman's reagent [63], is commonly used to quantify free sulfhydryl groups and disulfides in peptides and proteins [64-67]. In previous work we used Ellman's reagent to show that disulfide bonds are formed in multilayer films made of Cys containing peptides under oxidizing conditions [30]. Here, we have tested whether Cys containing 32 mer polypeptides might be suitable for disulfide-based "loading" of small molecules, multilayer film assembly, and release of small molecules in response to an environmental stimulus.

7.2 Experiments

Materials. Cys containing 32 mer polypeptides (KVKGKCKV)₃ KVKGKCKY ("P1") and (EVEGECEV)₃ EVEGECEY ("N1") were prepared by GenScript, Inc. (USA). 4-15 kDa poly(L-lysine) ("PLL"), 13 kDa poly(L-glutamic acid) ("PLGA"), and DTNB were from Sigma (USA). DL-dithiothreitol (DTT), a reducing agent, was from Gold Biotechnology, Inc. (USA). All the other reagents were from Sigma. P1, N1, PLL and PLGA were dissolved in TA buffer (10 mM tris, 10 mM sodium acetate, 20 mM NaCl, 0.1 % NaN₃, pH 7.4) to a final concentration of 1 mg/mL.

Labeling of N1 with DTNB. A DTNB molecule can react with a free thiol group under oxidizing conditions (Figure 7-1a). Peptides P1 and N1 contain Cys residues. The TNB dianion will form a disulfide bond with a Cys side chain, releasing TNB to the surroundings. An aqueous solution of free TNB is yellow and has an absorbance peak at 412 nm at mildly basic pH [129,130]. The extinction coefficient of TNB ranges from 11,400 to 14,150 $M^{-1} cm^{-1}$ [129], depending on conditions. Here, 11,400 $M^{-1} cm^{-1}$ was used to estimate TNB concentration.

Lyophilized N1 was prepared for loading by dissolution in “reducing TA buffer” (TA buffer, 10 mM DTT, pH 8.1) and incubation at ambient temperature for 24 h. 2 mL N1 solution was introduced into 1000 MWCO dialysis tubing (SpectroPor 7, Spectrum Laboratories, Inc., USA) and dialyzed against 200 mL “DTNB solution” (TA buffer, 10 mM DTNB, pH 8.1) with continuous stirring. DTNB solution was changed after 1, 2, 4, and 17 h. After labeling of N1, the same dialysis bag was immersed in pH 7.4 TA buffer to remove excess DTNB and adjust the pH from 8.1 to 7.4. TA buffer was changed after 1, 2, 4, and 17 h. The final concentration of labeled N1 (LN1) was adjusted to 1 mg/mL with pH 7.4 TA buffer. UV absorbance spectra of LN1 before and after treatment with DTT, are shown in Figure 7-1b.

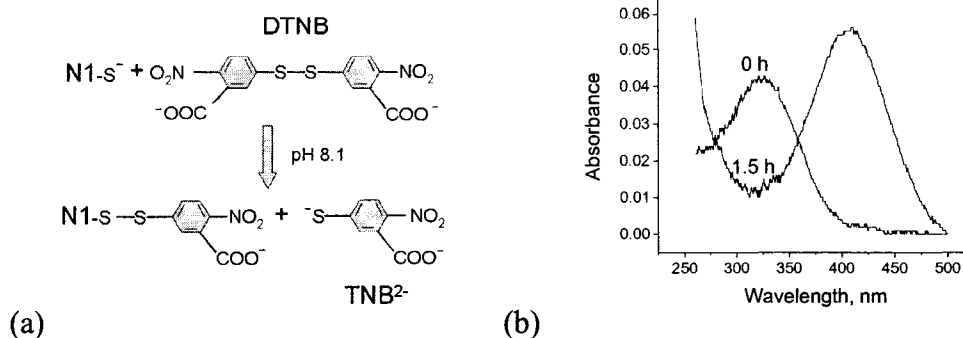


Figure 7-1. Loading of the model drug onto peptide N1 for subsequent multilayer film assembly. (a) DTNB reacts with Cys side chains in N1. A TNB group becomes attached to a peptide thiol group by formation of a disulfide bond. (b) Absorbance spectrum of LN1 solution after extensive dialysis to remove unreacted DTNB but before (0 h) and 1.5 h after adding DTT: The peak at 412 nm in the 1.5 h spectrum is due to TNB dianions, while that at 328 nm (0 h) is due to TNB-thiol mixed disulfide [131]. The sharp increase in absorbance below 300 nm is due to DTT. The shoulder evident around 275 nm in later time points (not shown) is due to oxidized DTT.

Polypeptide multilayer nanocoating assembly. Polypeptide multilayer coatings were assembled on quartz microscope slides (Electron Microscopy Sciences, USA) subsequent to carrying out the substrate cleaning process described in [28]. The substrate was repetitively immersed in a positively charged polypeptide solution (P1 or PLL) and in a negatively charged polypeptide solution (N1, LN1, or PLGA) for 15 min. Each peptide adsorption step was followed by rinsing of the coated slide in separate deionized water baths for 2 min, 1 min, and 1 min. Polypeptide films with 30 layers were assembled. P1/N1, P1/LN1, P1/PLGA, PLL/N1, and PLL/PLGA coatings were prepared in the same way. In some cases, as indicated below, two “capping” bilayers of P1 and N1, (P1/N1)₂, were assembled on top of 30-layer P1/LN1 coatings.

TNB release from LN1 nanocoatings. pH 7.4 LN1 solution was diluted 4-fold with deionized water and DTT was added to a final concentration of 2 mM (Figure 7-1b). The mixture was agitated gently throughout the release process on a rocking platform.

Solution absorbance spectra were recorded with a Shimadzu UV mini 1240 UV-Vis spectrophotometer (Japan). The surface area of a polypeptide film on the quartz substrate was about 2 cm². To bring the absorbance peak of TNB into the detectable range, ten P1/LN1 polypeptide films were immersed sequentially in 3 mL release medium (pH 7.4 TA buffer diluted 4-fold with deionized water; 0, 0.1, or 1 mM DTT), and the absorbance of the release medium was recorded by scanning spectroscopy at different time points. Each film was immersed for 5 min for the first absorbance measurement and 15 min for subsequent measurements. The tube containing the film sample and release medium was rocked throughout the release process.

7.3 Results and Discussion

Polyelectrolyte multilayer nanocoatings are promising for numerous areas of technology development, for instance, surface modification and device fabrication. Small molecule model drugs, for example, methylene blue [55], rhodamine B [56], and carboxyfluorescein [57], have been loaded into coatings after film fabrication. The polyanions DNA and RNA have also been used to fabricate multilayer films for subsequent release [59-61,132]. Redox-sensitive multilayer films have been made from poly(anilineboronic acid) (PABA) and RNA by the formation of boronate ester, boron-nitrogen dative bond, and electrostatic interactions [61]. When the covalent bonds between PABA and RNA are broken, RNA is released.

Disulfide bonds play an important role in maintaining the structure and function of secreted proteins, for instance, immunoglobulin G, insulin, and lysozyme. In previous work we have studied the role of reversible disulfide bond formation on the stability of polypeptide multilayer coatings and capsules [6,11,12,30,54]. Recently, Zelikin et al.

[133] and Blacklock et al. [132] have studied disulfide bond stabilization on other kinds of polyelectrolyte multilayer films. Here, TNB was “loaded” onto Cys containing polypeptides by forming disulfide bonds. Then the loaded peptides were incorporated into multilayer coatings by LBL. Release of the model drug was stimulated by a change in redox potential of the surrounding environment of the coating.

TNB loading onto N1. DTT can maintain monothiols completely in the reduced state and reduce disulfides quantitatively [134]. Polypeptide N1 was treated with DTT to break possible inter- and intramolecular disulfide bonds and to protect the free thiol groups of Cys residue side chains. The resulting N1 molecules, which have several free thiol groups, were used for TNB loading in mildly basic solution (Figure 7-1a). The absorbance peak at 328 nm in Figure 7-1b, due to TNB and thiol mixed disulfides [131], shows that N1 molecules were successfully loaded with TNB. Tyrosine absorbance at 275 nm is more than 10-fold smaller than that of TNB in the near UV [76,129].

Polypeptide multilayer assembly. P1/N1, P1/LN1, P1/PLGA, PLL/N1, and PLL/PLGA coatings with 30 layers were assembled on quartz slides by LBL. Figure 7-2 shows the build up in film thickness as a function of the number of absorption steps.

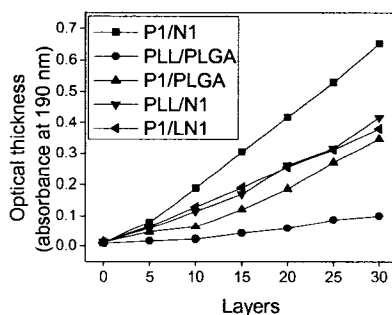


Figure 7-2. Multilayer film absorbance at 190 nm *versus* number of layers. Assembly behavior falls into three categories: P1/N1; PLL/N1, P1/LN1, and P1/PLGA; and PLL/PLGA.

P1/N1 showed the largest amount of material deposited for 30 adsorption steps. The difference in optical mass between P1/N1 and PLL/PLGA suggests the importance of linear charge density, amino acid sequence, and degree of polymerization in multilayer film buildup, consistent with previous reports [4,6,27,29]. Strong Coulombic forces both attract oppositely-charged species and repel like-charged ones, limiting film thickness [27,135]. The assembly behavior of P1/LN1 resembles that of PLL/N1 and P1/PLGA. Each bound TNB increased peptide hydrophobicity and added a single negative charge under the conditions of the experiments. Both electrostatic forces and hydrophobic interactions influence peptide assembly behavior and film stability [27,62]. The difference in assembly behavior between P1/LN1 and P1/N1 is indirect evidence of labeling of N1, consistent with the data in Figure 7-1b.

Polypeptide design plays an important role in the approach to drug loading and release described here. DTNB molecules could be loaded onto P1 and hen egg white lysozyme (HEWL), and TNB could be released from the labeled molecules in solution on addition of DTT (data not shown). Neither loaded P1 molecules nor loaded HEWL molecules, however, were useful for multilayer film assembly by LBL. P1 and HEWL are positively charged at pH 7.4, while TNB groups are negatively charged. The combination of different signs of charged groups in a single molecule will decrease average linear charge density and thereby reduced suitability for electrostatic LBL. Charge distribution in HEWL is complex, and many of the hydrophobic groups present form the hydrophobic core in the intact native enzyme. LN1, by contrast, proved useful for fabricating multilayer films by electrostatic LBL. Moreover, TNB was released from films containing LN1 by a change of redox potential.

Controlled TNB release. Similar to its behavior in solution (Figure 7-1b), TNB attached to N1 in multilayer nanocoatings was released on immersion of the coating in an aqueous reducing environment (Figure 7-3a). The absorbance peak at 412 nm (Figure 7-3b) shows how TNB concentration changed as a function of coating incubation time in 0.1 mM DTT solution. Figure 7-3c compares the kinetics of TNB release from coatings with or without capping layers. The first-order time constant for 0.1 mM DTT was 8 min. The higher the DTT concentration, the higher the probability of a collision of DTT with TNB in the coating for a given amount of time, and the faster the release of TNB from the films. TNB was not released to a detectable level under mild oxidizing conditions (0 mM DTT). The concentration of TNB in 0.1 mM DTT solution after 60 min was 2.2 μM , or 1.3 μg in 3 mL release medium.

Capping bilayers (P1/N1)₂ reduced the rate of release of TNB from P1/LN1 films. The time constant for capped films was 19 min (Figure 7-3d), about twice as large as for non-capped films. The capping layers contained no TNB; they could block or inhibit inward diffusion of DTT and outward diffusion of TNB, and bond with TNB and DTT (Figure 7-3b).

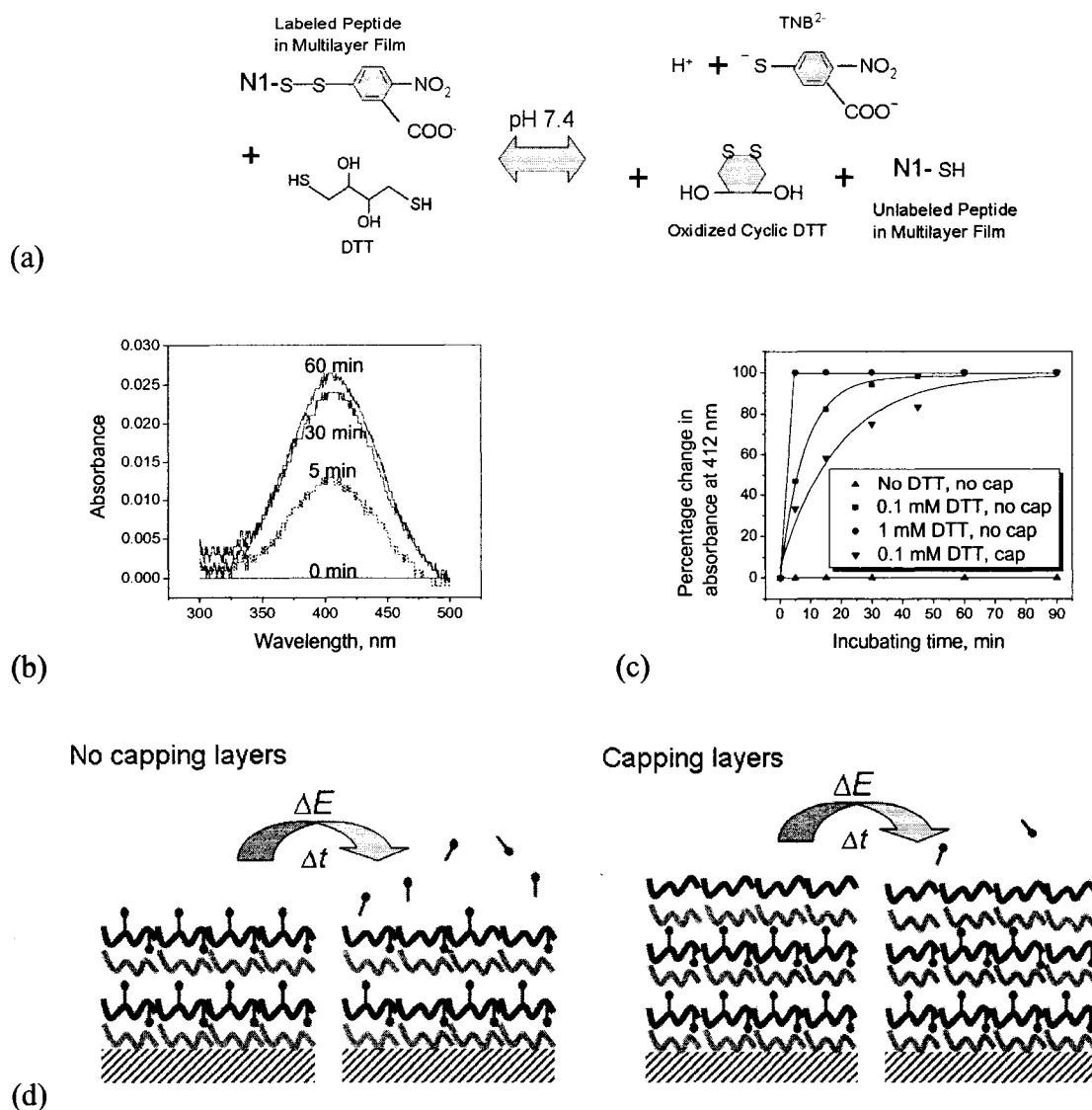


Figure 7-3. Release of TNB from multilayer nanocoatings. (a) TNB dissociates from peptide LN1 on the inward diffusion of DTT. (b) Absorbance spectra of liquid medium surrounding of 10 P1/LN1 nanocoatings, recorded 0, 5, 30, or 60 min after immersion in 0.1 mM DTT solution. TNB absorbance increases with time. (c) Absorbance at 412 nm of release media for 10 P1/LN1 films *v.* incubation time. “Capped” films had (P1/N1)₂ on the outer surface (see panel d). TNB release kinetics depends on redox potential and the physical behavior presented by the capping layers. (d) Schematic diagram of redox-stimulated release of TNB from polypeptide multilayer nanocoatings. DTT molecules are omitted for simplicity. ΔE signifies the change in reducing potential, Δt is time.

7.4 Conclusion

The small molecule DTNB has been conjugated to designed, negatively-charged, Cys containing 32 mer polypeptides. The labeled polypeptides have been used to assemble multilayer coatings by LBL. The change in redox potential has been used to stimulate release of TNB from the coatings. The approach differs substantially from loading the drug after film fabrication and is likely to be substantially more efficient. Redox potential change and capping are two methods to control drug release from the polypeptide multilayer films. Redox-based model drug release has a marked dependence on the stability of disulfide bonds, which might be durable under a change of pH or salt concentration but sensitive to a substantial change of redox potential. This demonstration of covalent loading of a model drug onto polyelectrolyte molecules prior to film fabrication represents a new strategy for drug delivery.

CHAPTER EIGHT

CONCLUSIONS

8.1 Conclusions

Polypeptide multilayer nanofilms are important biomaterial which has promising application in nanotechnology and biotechnology. This research on polypeptide multilayer nanofilms not only provides crucial knowledge on polypeptide and protein, but also explores their possible usage in surface modification, cell culture, encapsulation, and drug delivery areas.

This dissertation work conducted fundamental research on the investigation of properties and stabilities of polypeptide multilayer nanofilms, especially the Cys containing polypeptides, and their application in drug loading and release based on two mechanisms: electrostatic interaction combining with concentration gradient driving diffusion and redox-stimulation.

The crucial driving forces of LBL—intermolecular interactions, e.g., electrostatic interaction, hydrophobic/hydrophilic interaction and hydrogen bond, can be quantitatively controlled by including different number of various amino acid residues into polypeptide chain. For example, electrostatic interaction can be introduced in LBL by including lysine and glutamic acid with polar side chains into amino acid sequences. The hydrophobic interaction can be introduced in LBL by including valine with nonpolar

side chain into amino acid sequence. The design of architecture of polypeptide chains can influence its LBL behavior by the amount of polypeptide deposited at every deposition step, the thickness and density of thin layers, and the surface morphology of polypeptide nanofilms, etc.

The LBL behavior of polypeptide films can also be influenced by the pH value. The side chain of amino acid residue has distinct pK_a affected by its electronic environment, which contributes to different charged status of amino acid under certain pH. As a result, the linear charge density of polypeptide will vary together with the pH of its environment. This dissertation work demonstrated that when the pH changes from 7.4 to 8.9, the deprotonation of thiol groups in Cys residues influenced the LBL behavior and the properties of polypeptide multilayer nanofilms. At pH 8.9, the stronger electrostatic repulsion between N1 molecules and the coexistence of positive and negative charges in P1 molecules, which were caused by deprotonation of Cys residues, resulted in a thicker but loosely packed multilayer nanofilm than at pH 7.4.

The post-fabrication treatment can also change the properties of polypeptide multilayer nanofilms. Crosslinking is an effective method to strengthen the multilayer film stability. It is widely used in polymer, polyelectrolyte and hydrogel films. This dissertation work designed 32 mer polypeptides with different number of Cys residues in their peptide chains, and controlled the number of covalent bonds between Cys residues to form 2-D or 3-D disulfide crosslinking after nanofilm fabrication, in order to fortify film stability at different extents. The disulfide crosslinkings also changed the surface morphology of the polypeptide nanofilms. According to the disassembly of crosslinked polypeptide nanofilms under strong acidic conditions, the AFM images and following

schematic modeling analysis also gave the proof that disulfide bonds could stabilize the multilayer films.

In recent years, concentrated research efforts have been carried out to gain further knowledge for the application of PEMs in drug loading and release. This dissertation work used two drug models—cationic MB and DTNB with free thiol groups—to investigate the loading and release behaviors of the polypeptide multilayer nanofilms. Positively charged MB bound onto carboxyl group of glutamic acid side chain after the fabrication of polypeptide films, and the release of MB was based on the change of internal electrostatic environment and the diffusion driven by MB concentration gradient. The binding and release of DTNB from Cys side chains were determined by the formation and breakage of disulfide bond, under the change of redox potential. Different from MB, DTNB was loaded onto polypeptide before nanofilm LBL fabrication, which explored a new drug delivery method—the coating material of capsules could be modified to have therapeutic effects. Furthermore, the redox-stimulated drug loading and release also simulate the real drug delivery mechanism in organisms. By design of peptide sequence and architecture of polypeptide multilayer nanofilms, different drug loading and release mechanisms can be included, for example, electrostatic force, covalent bonding, redox potential change, etc., which provide insight to the promising targeted drug delivery.

8.2 Future Work

The understanding of protein is still very limited within our knowledge nowadays. So many research works can be done in this field, such as, the physics basis investigation of polypeptide multilayer film assembly, the control over the secondary and/or higher

protein structures, the modification of protein biofunctions, the human implant design based on proteins, etc. Proteins not only compose organism, but also executes functions of lives. Investigation on protein is an important clue to seek mystery of life.

Polypeptide multilayer nanofilms can be used to encapsulate active drugs inside to perform targeted delivery. According to customized design, biofunctional or bioactive groups can be included in polypeptide molecules and then to modify the characteristics of capsule coating in order to make the drug more therapeutically effective. The biocompatibility and biodegradability of polypeptide is another advantage over other materials for its usage in medicine field.

This dissertation work tested the redox-stimulated model drug loading and release onto polypeptide molecules before the nanofilm or capsule fabricated. If real drugs can be modified to have free thiol groups, they can bind to polypeptide molecules covalently by disulfide bond formation. Therapeutic coating can be made from these labeled polypeptides. The bound drug may release into *in vivo* circumstance through the breakage of disulfide bonds.

REFERENCES

- [1] Creighton, T. E., *Proteins: Structures and Molecular Properties*, 2nd ed. (New York: Freeman, 1993).
- [2] Online:
<http://home.comcast.net/~john.kimball1/BiologyPages/P/PrimaryStructure.html>,
<http://home.comcast.net/~john.kimball1/BiologyPages/S/SecondaryStructure.html>,
<http://web.mit.edu/esgbio/www/lm/proteins/structure/structure>, (last accessed: December 08, 2006).
- [3] Haynie, D. T., Zhang, L., Rudra, J. S., Zhao, W., Zhong, Y., and Palath, N., "Polypeptide Multilayer Films," *Biomacromolecules* 6 (2005): 2895-2913.
- [4] Haynie, D. T., Balkundi, S., Palath, N., Chakravarthula, K., and Dave, K., "Polypeptide Multilayer Films: Role of Molecular Structure and Charge," *Langmuir* 20 (2004): 4540-4547.
- [5] Zhang, L., Li, B., Zhi, Z., and Haynie, D. T., "Perturbation of Nanoscale Structure of Polypeptide Multilayer Thin Films," *Langmuir* 21 (2005): 5439-5445.
- [6] Zhong, Y., Li, B., and Haynie, D. T., "Fine Tuning of Physical Properties of Designed Polypeptide Multilayer Films by Control of pH," *Biotechnology Progress* 22 (2006): 126-132.
- [7] Iler, R. K., "Multilayers of Colloidal Particles," *Journal of Colloid and Interface Science* 21 (1966): 569-594.
- [8] Decher, G., and Schlenoff, J. B., Ed., *Multilayer Thin Films: Sequential Assembly of Nanocomposite Materials* (Weinheim, Germany: Wiley-VCH, 2003).
- [9] Tripathy, S. K., Kumar, J., and Nalwa, H. S., *Handbook of Polyelectrolytes and Their Applications. Volume 1: Polyelectrolyte-Based Multilayers, Self-Assemblies and Nanostructures* (Stevenson Ranch, CA: American Scientific Publishers, 2002).
- [10] Lvov, Y., and Caruso, F., "Biocolloids with Ordered Urease Multilayer Shells as Enzymatic Reactors," *Analytic Chemistry* 73 (2001): 4212-4217.

- [11] Li, B., Rozas, J., and Haynie, D. T., "Structural Stability of Polypeptide Nanofilms under Extreme Conditions," *Biotechnology Progress* 22 (2006): 111-117.
- [12] Zhong, Y., Li, B., and Haynie, D. T., "Control of Stability of Polypeptide Multilayer Nanofilms by Quantitative Control of Disulfide Bond Formation," *Nanotechnology*, in press.
- [13] Zhong, Y., Whittington, C. F., and Haynie, D. T., "Redox-Stimulated Release of Small Molecules from Polypeptide Multilayer Nanocoatings," *Chemical Communications*, accepted.
- [14] Lvov, Y., Ariga, K., and Kunitake, T., "Layer-by-Layer Assembly of Alternate Protein/Polyion Ultrathin Films," *Chemistry Letters* 23 (1994): 2323-2326.
- [15] Lvov, Y., Ariga, K., Ichinose, I., and Kunitake, T., "Assembly of Multicomponent Protein Films by Means of Electrostatic Layer-by-Layer Adsorption," *Journal of the American Chemical Society* 117 (1995): 6117-6123.
- [16] Caruso, F., Furlong, D. N., Ariga, K., Ichinose, I., and Kunitake, T., "Characterization of Polyelectrolyte-Protein Multilayer Films by Atomic Force Microscopy, Scanning Electron Microscopy, and Fourier Transform Infrared Reflection-Absorption Spectroscopy," *Langmuir* 14 (1998): 4559-4565.
- [17] Mrksich, M., and Whitesides, G. M., "Using Self-Assembled Monolayers to Understand the Interactions of Man-Made Surfaces with Proteins and Cells," *Annual Review of Biophysics and Biomolecular Structure* 25 (1996): 55-78.
- [18] Zhang, S., "Fabrication of Novel Biomaterials through Molecular Self-Assembly," *Nature Biotechnology* 21 (2003): 1171-1178.
- [19] Eckle, M., and Decher, G., "Tuning the Performance of Layer-by-Layer Assembled Organic Light Emitting Diodes by Controlling the Position of Isolating Clay Barrier Sheets," *Nano Letters* 1 (2001): 45-49.
- [20] Liu, X., and Bruening, M. L., "Size-Selective Transport of Uncharged Solutes through Multilayer Polyelectrolyte Membranes," *Chemistry of Materials* 16 (2004): 351-357.
- [21] Laurent, D., and Schlenoff, J. B., "Multilayer Assemblies of Redox Polyelectrolytes," *Langmuir* 13 (1997): 1552-1557.
- [22] Shchukin, D. G., Shutava, T., Shchukina, E., Sukhorukov, G. B., and Lvov, Y., "Modified Polyelectrolyte Microcapsules as Smart Defense Systems," *Chemistry of Materials* 16 (2004): 3446-3451.

- [23] Rubner, M. F., in *Multilayer Thin Films: Sequential Assembly of Nanocomposite Materials*, Decher, G., and Schlenoff, J. B., Eds. (Weinheim Germany: Wiley-VCH, 2003).
- [24] Park, S. Y., Barrett, C. J., Rubner, M. F., and Mayes, A. M., "Anomalous Adsorption of Polyelectrolyte Layers," *Macromolecules* 34 (2001): 3384-3388.
- [25] Lavalle, Ph., Gergely, C., Cuisinier, F. J. G., Decher, G., Schaaf, P., Voegel, J. C., and Picart, C., "Comparison of the Structure of Polyelectrolyte Multilayer Films Exhibiting a Linear and an Exponential Growth Regime: an In Situ Atomic Force Microscopy study," *Macromolecules* 35 (2002): 4458-4465.
- [26] Elbert, D. L., Herbert, C. B., and Hubbell, J. A., "Thin Polymer Layers Formed by Polyelectrolyte Multilayer Techniques on Biological Surfaces," *Langmuir* 15 (1999): 5355-5362.
- [27] Haynie, D. T., Zhang, L., Zhao, W., and Smith, J. M., "Quantal Self-Assembly of Polymer Layers in Polypeptide Multilayer Nanofilms," *Biomacromolecules* 7 (2006): 2264-2268.
- [28] Zhi, Z., and Haynie, D. T., "Direct Evidence of Controlled Structure Reorganization in a Nanoorganized Polypeptide Multilayer Thin Film," *Macromolecules* 37 (2004): 8668-8675.
- [29] Zheng, B., Haynie, D. T., Zhong, H., Sabnis, K., Surpuriya, V., Pargaonkar, N., Sharma, G., and Vistakula, K., "Design of Peptides for Thin Films, Coatings and Microcapsules for Applications in Biotechnology," *Journal of Biomaterials Science, Polymer Edition* 16 (2005): 285-299.
- [30] Li, B., and Haynie, D. T., "Multilayer Biomimetics: Reversible Covalent Stabilization of a Nanostructured Biofilm," *Biomacromolecules* 5 (2004): 1667-1670.
- [31] Turko, I. V., Yurkevich, I. S., and Chashchin, V. L., "Langmuir-Blodgett Films of Immunoglobulin G for Immunosensors," *Thin Solid Films* 205 (1991): 113-116.
- [32] Dubrovsky, T., Vakula, S., Nicolini, C., "Preparation and Immobilization of Langmuir-Blodgett Films of Antibodies Conjugated to Enzymes for Potentiometric Sensor Application," *Sensors and Actuators B* 22 (1994): 69-73.
- [33] Avnir, D., Braun, S., Lev, O., and Ottolenghi, M., "Enzymes and Other Proteins Entrapped in Sol-Gel Materials", *Chemistry of Materials* 6 (1994): 1605-1614.
- [34] Leggett, G. J., Roberts, C. J., Williams, P. M., Davies, M. C., Jackson, D. E., and Tendler, S. J. B., "Approaches to the Immobilization of Proteins at Surfaces for Analysis by Scanning Tunneling Microscopy," *Langmuir* 9 (1993): 2356-2362.

- [35] Lin, J. N., Drake, B., Lea, A. S., Hansma, P. K., and Andrade, J. D., "Direct Observation of Immunoglobulin Adsorption Dynamics Using the Atomic Force Microscope," *Langmuir* 6 (1990): 509-511.
- [36] Dubas, S. T., and Schlenoff, J. B., "Polyelectrolyte Multilayers Containing a Weak Polyacid: Construction and Deconstruction," *Macromolecules* 34 (2001): 3736-3740.
- [37] Yoo, D., Shiratori, S. S., and Rubner, M. F., "Controlling Bilayer Composition and Surface Wettability of Sequentially Adsorbed Multilayers of Weak Polyelectrolytes," *Macromolecules* 31 (1998): 4309-4318.
- [38] Steitz, R., Jaeger, W., and Klitzing, R. v., "Influence of Charge Density and Ionic Strength on the Multilayer Formation of Strong Polyelectrolytes," *Langmuir* 17 (2001): 4471-4474.
- [39] Tan, H. L., McMurdo, M. J., Pan, G., and Van Patten, P. G., "Temperature Dependence of Polyelectrolyte Multilayer Assembly," *Langmuir* 19 (2003): 9311-9314.
- [40] Hiller, J., and Rubner, M. F., "Reversible Molecular Memory and pH-Switchable Swelling Transitions in Polyelectrolyte Multilayers," *Macromolecules* 36 (2003): 4078-4083.
- [41] Kotov, N. A., Magonov, S., and Tropsha, E., "Layer-by-layer Self-Assembly of Aluminosilicate-Polyelectrolyte Composites: Mechanism of Deposition, Crack Resistance, and Perspectives for Novel Membrane Materials," *Chemistry of Materials* 10 (1998): 886-895.
- [42] Mao, G. Z., Tsao, Y. H., Tirrell, M., Davis, H. T., Hessel, V., and Ringsdorf, H., "Interactions, Structure, and Stability of Photoreactive Bolaform Amphiphile Multilayers," *Langmuir* 11 (1995): 942-952.
- [43] Richert, L., Boulmedais, F., Lavalle, P., Mutterer, J., Ferreux, E., Decher, G., Schaaf, P., Voegel, J. C., and Picart, C., "Improvement of Stability and Cell Adhesion Properties of Polyelectrolyte Multilayer Films by Chemical Cross-Linking," *Biomacromolecules* 5 (2004): 284-294.
- [44] Sun, J., Wu, T., Sun, Y., Wang, Z., Xi, Z., Shen, J., and Cao, W., "Fabrication of a Covalently Attached Multilayer via Photolysis of Layer-by-Layer Self-Assembled Films Containing Diazo-Resins," *Chemical Communications (Cambridge)* 17 (1998): 1853-1854.
- [45] Welsh, E. R., Schauer, C. L., Santos, J. P., and Price, R. R., "In Situ Cross-Linking of Alternating Polyelectrolyte Multilayer Films," *Langmuir* 20 (2004): 1807-1811.

- [46] Yang, S. Y., and Rubner, M. F., "Micropatterning of Polymer Thin Films with pH-Sensitive and Cross-Linkable Hydrogen-Bonded Polyelectrolyte Multilayers," *Journal of the American Chemistry Society* 124 (2002): 2100-2101.
- [47] Li, B., Haynie, D. T., Palath, N.; and Janisch, D., "Nanoscale Biomimetics: Fabrication and Optimization of Stability of Peptide-Based Thin Films," *Journal of Nanoscience Nanotechnology*, 5 (2005): 2042-2049.
- [48] Richert, L., Engler, A. J., Discher, D. E., and Picart, C., "Elasticity of Native and Cross-Linked Polyelectrolyte Multilayer Films," *Biomacromolecules* 5 (2004): 1908-1916.
- [49] Park, M. K., Xia, C., Advincula, R. C., Schutz, P., and Caruso, F., "Cross-Linked, Luminescent Spherical Colloidal and Hollow-Shell Particles," *Langmuir* 17 (2001): 7670-7674.
- [50] Dai, J., Jensen, A. W., Mohanty, D. K., Erndt, J., and Bruening, M. L., "Controlling the Permeability of Multilayered Polyelectrolyte Films through Derivatization, Cross-Linking, and Hydrolysis," *Langmuir* 17 (2001): 931-937.
- [51] Balachandra, A. M., Dai, J., and Bruening, M. L., "Enhancing the Anion-Transport Selectivity of Multilayer Polyelectrolyte Membranes by Templating with Cu^{2+} ," *Macromolecules* 35 (2002): 3171-3178.
- [52] Online: <http://www.proscitech.com.au/catalogue/msds/c001.pdf>, (last accessed: December 08, 2006).
- [53] McKenzie, H. A., and White, F., "Lysozyme and Alpha-Lactalbumin: Structure, Function, and Interrelationships," *Advances in Protein Chemistry* 41 (1991): 173-315.
- [54] Haynie, D. T., Palath, N., Liu, Y., Li, B., and Pargaonkar, N., "Biomimetic Nanostructured Materials: Inherent Reversible Stabilization of Polypeptide Microcapsules," *Langmuir* 21 (2005): 1136-1138.
- [55] Chung, A. J., and Rubner, M. F., "Methods of Loading and Releasing Low Molecular Weight Cationic Molecules in Weak Polyelectrolyte Multilayer Films," *Langmuir* 18 (2002): 1176-1183.
- [56] Quinn, J. F., and Caruso, F., "Facile Tailoring of Film Morphology and Release Properties using Layer-by-Layer Assembly of Thermoresponsive Materials," *Langmuir* 20 (2004): 20-22.
- [57] Khopade, A. J., and Caruso, F., "Electrostatically Assembled Polyelectrolyte/Dendrimer Multilayer Films as Ultrathin Nanoreservoirs," *Nano Letters* 2 (2002): 415-418.

- [58] Ma, N., Zhang, H., Song, B., Wang, Z., and Zhang, Z., "Polymer Micelles as Building Blocks for Layer-by-Layer Assembly: an Approach for Incorporation and Controlled Release of Water-Insoluble Dyes," *Chemistry of Materials* 17 (2005): 5065-5069.
- [59] Zhang, J., Chua L. S., and Lynn, D. M., "Multilayered Thin Films that Sustain the Release of Functional DNA under Physiological Conditions," *Langmuir* 20 (2004): 8015-8021.
- [60] Ren, K., Ji, J., and Shen, J., "Tunable DNA Release from Crosslinked Ultrathin DNA/PLL Multilayered Films," *Bioconjugate Chemistry* 17 (2006): 77-83.
- [61] Recksiedler, C. L., Deore, B. A., and Freund, M. S., "A Novel Layer-by-Layer Approach for the Fabrication of Conducting Polymer/RNA Multilayer Films for Controlled Release," *Langmuir* 22 (2006): 2811-2815.
- [62] Haynie, D. T., Zhang, L., Zhao, W., "Polypeptide Multilayer Films: Experiments, Simulations, Implications," *Polymeric Materials Science and Engineering* 93 (2005): 94-97.
- [63] Ellman, G. L., "A Calorimetric Method for Determining Low Concentrations of Mercaptans," *Archives of Biochemistry and Biophysics* 74 (1958): 443-450.
- [64] Ellman, G. L., "Tissue Sulfhydryl Groups," *Archives of Biochemistry and Biophysics* 82 (1959): 70-77.
- [65] Gething, M. J. H., and Davidson, B. E., "The Molar Adsorption Coefficient of Reduced Ellman's Reagent: 3-Carboxylato-4-Nitro-Thiophenolate," *European Journal of Biochemistry* 30 (1972): 352-353.
- [66] Anderson, W. L., "A New Method for Disulfide Analysis of Peptides," *Analytical Biochemistry* 67 (1975): 493-502.
- [67] Ramachandran, S., and Udgaonkar, J. B., "Stabilization of Barstar by Chemical Modification of the Buried Cysteines," *Biochemistry* 35 (1996): 8776-8785.
- [68] Feynman, R., "There's Plenty of Room at the Bottom," *Caltech's Engineering and Science* (February 1960).
- [69] Feynman, R., "Infinitesimal Machinery," *Journal of Microelectromechanical Systems* 2 (1993): 4-14.
- [70] Jelinek, R., and Kolusheva, S., "Carbohydrate Biosensors," *Chemical Reviews* 104 (2004): 5987-6016.

- [71] Mohammed, J. S., DeCoster, M. A., and McShane, M. J., "Micropatterning of Nanoengineered Surfaces to Study Neuronal Cell Attachment in Vitro," *Biomacromolecules* 5 (2004): 1745-1755.
- [72] Njue, C. K., and Rusling, J. F., "Controlling Catalytic Activity of A Polyion Scaffold on an Electrode via Microemulsion Composition," *Journal of the American Chemical Society* 122 (2000): 6459-6463.
- [73] Sauerbrey, G. Z., "Use of Quartz Crystal Vibrator for Weighting Thin Films on a Microbalance" *Physics* 155 (1959): 206-222.
- [74] Frauenfelder, H., in *Physics of Proteins* (Springer Verlag, 2003), Chan, S., and Austin, R. Eds.
- [75] Online: http://en.wikipedia.org/wiki/UV/VIS_spectroscopy, (last accessed: December 08, 2006).
- [76] Gill, S. C., and Von Hippel, P. H., "Calculation of Protein Extinction Coefficients from Amino Acid Sequence Data," *Analytical biochemistry* 182 (1989): 319-326.
- [77] Zhu, G., "Study of Protein Secondary Structure Using Spectroscopies," Online: http://mercury.chem.pitt.edu/~rob/chem2810/present281/guangyu_zhu.ppt, (last accessed: December 16, 2006).
- [78] Parac, T. N., and Kostic, N. M., "Regioselective Cleavage by A Palladium(II) Aqua Complex of A Polypeptide in Different Overall Conformations," *Inorganic Chemistry* 37 (1998): 2141-2144.
- [79] Woody, R. W., in *The Peptides: Analysis, Synthesis, Biology* (Orlando, FL: Academic, 1985), V. J. Hruby, Ed.
- [80] Arnold, P. A., Benson, D. R., Brink, D. J., Hendrich, M. P., Jas, G. S., Kennedy, M. L., Petasis, D. T., and Wang, M., "Helix Induction and Springboard Strain in Peptide-Sandwiched Mesohemes," *Inorganic Chemistry* 36 (1997): 5306-5315.
- [81] Kelly, S. M., Jess, T. J., and Price, N. C., "How to Study Proteins by Circular Dichroism," *Biochimica et Biophysica Acta* 1751 (2005): 119-139.
- [82] Online: <http://www.gaertnerscientific.com/ellipsometers/introduction.htm>, (last accessed: December 16, 2006).
- [83] Lvov, Y., Ariga, K., Onda, M., Ichinose, I., and Kunitake, T., "Alternate Assembly of Ordered Multilayers of SiO₂ and Other Nanoparticles and Polyions," *Langmuir* 13 (1997): 6195-6203.

- [84] Online: <http://ece-www.colorado.edu/~bart/book/ellipsom.htm>, (last accessed: December 16, 2006).
- [85] De Feijter, J. A., Benjamins, J., and Veer, F. A., "Ellipsometry as a Tool to Study the Adsorption Behavior of Synthetic and Biopolymers at the Air-Water Interface," *Biopolymers* 17 (1978): 1759-1772.
- [86] Ramsden, J. J., "Experimental Methods for Investigating Protein Adsorption Kinetics at Surfaces," *Quarterly Reviews of Biophysics* 27 (1993): 41-105.
- [87] Stalgren, J. J. R., Eriksson, J., and Boschkova, K., "A Comparative Study of Surfactant Adsorption on Model Surfaces Using the Quartz Crystal Microbalance and the Ellipsometer," *Journal of Colloid and Interface Science* 253 (2002): 190-195.
- [88] Azzam, R. M. A., and Bashara, N. M., *Ellipsometry and Polarized Light* (Amsterdam: North-Holland Elsevier, 1989).
- [89] Cuypers, P. A., Corsel, J. W., Janssen, M. P., Kop, J. M. M., Hermens, W. T., and Hemker, H. C., "The Adsorption of Prothrombin to Phosphatidylserine Multilayers Quantitated by Ellipsometry," *Journal of Biological Chemistry* 258 (1983): 2426-2431.
- [90] Mermut, O., Lefebvre, J., Gray, D. G.; and Barrett, C. J., "Structural and Mechanical Properties of Polyelectrolyte Multilayer Films Studied by AFM," *Macromolecules* 36 (2003): 8819-8824.
- [91] Fa, K., Nguyen, A. V., and Miller, J. D., "Hydrophobic Attraction as Revealed by AFM Force Measurements and Molecular Dynamics Simulation," *Journal of Physical Chemistry B* 109 (2005): 13112-13118.
- [92] Wenzler, L. A., Moyes, G. L., Olson, L. G., Harris, J. M., and Beebe Jr., T. P., "Single-Molecule Bond-Rupture Force Analysis of Interactions Between AFM Tips and Substrates Modified with Organosilanes," *Analytic Chemistry* 69 (1997): 2855-2861.
- [93] Mukhopadhyay, R., "The AFM Goes Mainstream," *Analytic Chemistry A-Pages* 77 (2005): 469A-474A.
- [94] Online: http://en.wikipedia.org/wiki/Image:Atomic_force_microscope_block_diagram, (last accessed: December 16, 2006).
- [95] Harris, J. J., and Bruening, M. L., "Electrochemical and In Situ Ellipsometric Investigation of the Permeability and Stability of Layered Polyelectrolyte Films," *Langmuir* 16 (2000): 2006-2013.

- [96] Mendelsohn, J. D., Barrett, C. J., Chan, V. V., Pal, A. J., Mayes, A. M., and Rubner, M. F., "Fabrication of Microporous Thin Films from Polyelectrolyte Multilayers," *Langmuir* 16 (2000): 5017-5023.
- [97] Fery, A., Scholer, B., Cassagneau, T., and Caruso, F., "Nanoporous Thin Films Formed by Salt-Induced Structural Changes in Multilayers of Poly(Acrylic Acid) and Poly(Allylamine)," *Langmuir* 17 (2001): 3779-3783.
- [98] Burke, S. E., and Barrett, C. J., "pH-Responsive Properties of Multilayered Poly(L-lysine)/Hyaluronic Acid Surfaces," *Biomacromolecules* 4 (2003): 1773-1783.
- [99] Kim, B. Y., and Bruening, M. L., "pH-Dependent Growth and Morphology of Multilayer Dendrimer/Poly(Acrylic Acid) Films," *Langmuir* 19 (2003): 94-99.
- [100] Sun, J., Wu, T., Liu, F., Wang, Z., Zhang, X., and Shen, J., "Covalently Attached Multilayer Assemblies by Sequential Adsorption of Polycationic Siazos-Resins and Polyanionic Poly(Acrylic Acid)," *Langmuir* 16 (2000): 4620-4624
- [101] Schoeler, B., Poptoshev, E., and Caruso, F., "Growth of Multilayer Films of Fixed and Variable Charge Density Polyelectrolytes: Effect of Mutual Charge and Secondary Interactions," *Macromolecules* 36 (2003): 5258-5264.
- [102] Sukhorukov, G. B., Antipov, A. A., Voigt, A., Donath, E., and Mohwald, H., "pH-Controlled Macromolecule Encapsulation in and Release from Polyelectrolyte Multilayer Nanocapsules," *Macromolecular Rapid Communications* 22 (2001): 44-46.
- [103] Rmaile, H. H., Farhat, T. R., and Schlenoff, J. B., "pH-Gated Permeability of Variably Charged Species through Polyelectrolyte Multilayer Membranes," *Journal of Physical Chemistry B* 107 (2003): 14401-14406.
- [104] Bohmer, M. R., Evers, O. A., and Scheutjens, J. M. H. M., "Weak Polyelectrolytes between two Surfaces: Adsorption and Stabilization," *Macromolecules* 23 (1990): 2288-2301.
- [105] Müller, M., Rieser, T., Dubin, P. L., and Lunkwitz, K., "Selective Interaction between Proteins and The Outermost Surface of Polyelectrolyte Multilayers: Influence of the Polyanion Type, pH and Salt," *Macromolecular Rapid Communications* 22 (2001): 390-395.
- [106] Benesch, J., Askendal, A., and Tengvall, P., "The Determination of Thickness and Surface Mass Density of Mesothick Immunoprecipitate Layers by Null Ellipsometry and Protein (125) Iodine Labeling," *Journal of Colloid and Interface Science* 249 (2002): 84-90.

- [107] Vörös, J., "The Density and Refractive Index of Adsorbing Protein Layers," *Biophysical Journal* 87 (2004): 553-561.
- [108] Glinel, K., Prevot, M., Krustev, R., Sukhorukov, G. B., Jonas, A. M., and Mohwald, H., "Control of The Water Permeability of Polyelectrolyte Multilayers by Deposition of Charged Paraffin Particles," *Langmuir* 20 (2004): 4898-4902.
- [109] Azzaroni, O., Moya, S., Farhan, T., Brown, A. A., and Huck, W. T. S., "Switching the Properties of Polyelectrolyte Brushes via 'Hydrophobic Collapse,'" *Macromolecules* 38 (2005): 10192-10199.
- [110] Miller, W. G., Brant, D. A., and Flory, P. J., "Random Coil Configurations of Polypeptide Copolymers," *Journal of Molecular Biology* 23 (1967): 67-80.
- [111] Wang, L., Fu, Y., Wang, Z., Fan, Y., Zhang, X., "Investigation into an Alternating Multilayer Film of Poly(4-Vinylpyridine) and Poly(acrylic acid) Based on Hydrogen Bonding," *Langmuir* 15 (1999): 1360-1363.
- [112] Sukhishvili, S. A., Granick, S., "Layered, Erasable Polymer Multilayers Formed by Hydrogen-Bonded Sequential Self-Assembly," *Macromolecules* 35 (2002): 301-310.
- [113] Schmitt, J., Grünewald, T., Decher, G., Pershan, P. S., Kjaer, K., Lösche, M., "Internal Structure of Layer-by-layer Adsorbed Polyelectrolyte Films: a Neutron and X-Ray Reflectivity Study," *Macromolecules* 26 (1993): 7058-7063.
- [114] Decher, G., Lvov, Y., Schmitt, J., "Proof of Multilayer Structural Organization in Self-Assembled Polyanion-Polycation Molecular Films," *Thin Solid Films* 244 (1994): 772-777.
- [115] Rudra, J. S., Dave, K., Haynie, D. T., "Antimicrobial Polypeptide Multilayer Nanocoatings," *Journal of Biomaterial Science, Polymer Edition* 17 (2006): 1301-1315.
- [116] Berg, M. C., Zhai, L., Cohen, R. E., and Rubner, M. F., "Controlled Drug Release from Porous Polyelectrolyte Multilayers," *Biomacromolecules* 7 (2006): 357-364.
- [117] Khoo, S. B., and Chen, F., "Studies of Sol-gel Ceramic Film Incorporating Methylene Blue on Glassy Carbon: an Electrocatalytic System for the Simultaneous Determination of Ascorbic and Uric Acids," *Analytical Chemistry* 74 (2002): 5734-5741.
- [118] Wang, B., Li, B., Wang, Z., Xu, G., Wang, Q., and Dong, S., "Sol-gel Thin-film Immobilized Soybean Peroxidase Biosensor for the Amperometric Determination of Hydrogen Peroxide in Acid Medium," *Analytical Chemistry* 71 (1999): 1935-1939.

- [119] Zhong, Y., Whittington, C. F., Zhang, L., and Haynie, D. T., "Controlled Loading and Release of a Model Drug from Polypeptide multilayer nanofilms," *Nanomedicine*, submitted.
- [120] Bujdak, J., Komadel, P., "Interaction of Methylene Blue with Reduced Charge Montmorillonite," *Journal of Physical Chemistry B* 101 (1997): 9065-9068.
- [121] Shiratori, S. S., and Rubner, M. F., "pH-dependent Thickness Behavior of Sequentially Adsorbed Layers of Weak Polyelectrolytes," *Macromolecules* 33 (2000): 4213-4219.
- [122] Brack, A., and Orgel, L. E., "Beta-structures of Alternating Polypeptides and Their Possible Prebiotic Significance," *Nature* 256 (1975): 383-387.
- [123] Haynie, D. T., "Physics of Polypeptide Multilayer Films," *Journal of Biomedical Materials Research Part B: Applied Biomaterials* 78 (2006): 243-252.
- [124] Wood, K. C., Boedicker, J. Q., Lynn, D. M., and Hammond, P. T., "Tunable Drug Release from Hydrolytically Degradable Layer-by-Layer Thin Films," *Langmuir* 21 (2005): 1603-1609.
- [125] Jewell, C. M., Zhang, J., Fredin, N. J., Wolff, M. R., Hacker, T. A., Lynn, D. M., "Release of Plasmid DNA from Intravascular Stents Coated with Ultrathin Multilayered Polyelectrolyte Films," *Biomacromolecules* 7 (2006): 2483-2491.
- [126] Patel, H. J., Su, S. H., Patterson, C., Nguyen, K. T., "A Combined Strategy to Reduce Restenosis for Vascular Tissue Engineering Applications," *Biotechnology Progress* 22 (2006): 38-44.
- [127] Ai, H., Jones, S. A., de Villiers, M. M., Lvov, Y., "Nano-Encapsulation of Furosemide Microcrystals for Controlled Drug Release," *Journal of Controlled Release* 86 (2003): 59-68.
- [128] Qiu, X., Leporatti, S., Donath, E., Mohwald, H., "Studies on the Drug Release Properties of Polysaccharide Multilayers Encapsulated Ibuprofen Microparticles," *Langmuir* 17 (2001): 5375-5380.
- [129] Online:
<http://www.sigmaaldrich.com/sigma/product%20information%20sheet/d8130pis.pdf>, (last accessed: December 16, 2006).
- [130] Robyt, J. F., and White, B. J., *Biochemical Techniques, Theory and Practice* (Waveland Press Inc., 1987).

- [131] Sliwowski, M. X. , and Levine, R. L., "Labeling of Cysteine-Containing Peptides with 2-Nitro-5-Thiobenzoic Acid," *Analytical Biochemistry* 147 (1985): 369-373.
- [132] Blacklock, J., Handa, H., Manickam, D. S., Mao, G., Mukhopadhyay, A., Oupický, D., "Disassembly of Layer-by-Layer Films of Plasmid DNA and Reducible TAT Polypeptide," *Biomaterials*, in press.
- [133] Zelikin, A. N., Quinn, J. F., Caruso, F., "Disulfide Cross-linked Polymer Capsules: En Route to Biodeconstructible Systems," *Biomacromolecules* 7 (2006): 27-30.
- [134] Cleland, W. W., "Dithiothreitol, a New Protective Reagent for SH Groups," *Biochemistry* 3 (1964): 480-482.
- [135] Decher, G., "Fuzzy Nanoassemblies: Toward Layered Polymeric Multicomposites," *Science* 277 (1997): 1232-1237.